# THE SYNTHESIS, CHARACTERIZATION, AND EVALUATION OF A POLYPYRROLE/ALUMINUM FLAKE COMPOSITE PIGMENT

A Thesis
Submitted to the Graduate Faculty
of the
North Dakota State University
of Agriculture and Applied Science

By

Christopher Alan Vetter

In Partial Fulfillment of the Requirements
for the Degree of
MASTER OF SCIENCE

Major Department:
Coatings and Polymeric Materials

August 2010

Fargo, North Dakota

# North Dakota State University
## Graduate School

**Title**

The Synthesis, Characterization, and Evaluation of a Polypyrrole/Aluminum Flake Composite Pigment

**By**

Christopher Alan Vetter

The Supervisory Committee certifies that this ***disquisition*** complies with North Dakota State University's regulations and meets the accepted standards for the degree of

**MASTER OF SCIENCE**

## ABSTRACT

Vetter, Christopher Alan, M.S., Department of Coatings and Polymeric Materials, College of Science and Mathematics, North Dakota State University, August 2010. The Synthesis, Characterization, and Evaluation of a Polypyrrole/Aluminum Flake Composite Pigment. Major Professor: Dr. Victoria Johnston Gelling.

The goal of this study was to synthesize a polypyrrole/aluminum flake composite pigment to inhibit corrosion on aluminum alloy 2024 T3. This was done in order to remedy some of the problems associated with the application of pure polypyrrole as a coating. Namely these problems are insolubility in common solvents, brittleness, poor adhesion to metal substrates, and catastrophic failure in some conditions due to fast ion incorporation. By incorporating the polypyrrole composite pigment into an epoxy primer, the superior mechanical properties of the epoxy binder can be combined with the corrosion inhibiting properties of the polypyrrole.

Results indicated that the dopant of the polypyrrole played a large role in the corrosion inhibition of the substrate. While the sulfate doped sample inhibited corrosion in areas underneath the coating, it did not inhibit corrosion in defect areas. The vanadate doped and molybdate doped pigments did inhibit corrosion in defect areas.

## ACKNOWLEDGEMENTS

I would like to acknowledge Dr. Victoria Gelling for all of her help and support during my graduate studies. I would also like to acknowledge Dr. Stuart Croll, Dr. Chad Ulven, and Dr. Andriy Voronov for serving on my committee. Dr. Maocheng Yan performed the SVET and coupling current measurements and helped me greatly with his advice and insight. I would also like to acknowledge Scott Payne and the rest of the NDSU electron microscopy lab for their work obtaining scanning electron microscope images of my samples. I would also like to acknowledge Heidi Docktor for obtaining the conductive AFM images of my samples. Finally I would like to acknowledge the rest of the department of coatings and polymeric materials and the United States Army for funding this work.

## DEDICATIONS

I would like to dedicate this thesis first and foremost to my wife Patti who has been an unwavering source of love, support, encouragement, and motivation throughout my graduate studies. I would also like to dedicate this thesis to my parents and the rest of my family who taught me the value of hard work and education and supported me throughout my life. Finally, I would like to dedicate this thesis to my mother and father in-law who always supported me and reminded me that you have to enjoy life now because tomorrow may not come.

## TABLE OF CONTENTS

## LIST OF TABLES

## LIST OF FIGURES

# CHAPTER 1.

# IMPROVING THE PROCESSABILITY AND APPLICABILITY OF POLYPYRROLE

## 1.1. Abstract

While being very effective at inhibiting corrosion on aluminum and its various alloys, hexavalent chromates are known to be highly carcinogenic. Because of this, chromates are being gradually fazed out of use and soon will be banned by legislation.[1] As of yet, an environmentally friendly alternative that performs as well as chromates has not been found. Therefore, a massive effort is underway to find a suitable replacement. One option that is being explored is the use of electroactive conducting polymers such as polypyrrole. Polypyrrole, however, has its own set of problems associated with it. PPY is insoluble in common solvents which creates processing problems. It also has poor mechanical properties and does not adhere well to substrates. Because of these problems, there is a body of work dedicated to solving these issues. There are currently three strategies being investigated. One such technique is chemically altering the polypyrrole by copolymerization or grafting soluble groups onto the pyrrole monomer. A second technique involves forming useful composite materials with polypyrrole and other organic or inorganic compounds. The third technique uses the counterion present in oxidized polypyrrole to affect the properties of the polypyrrole. The work presented in this thesis falls into the second category of composite materials. This technique was chosen for a number of reasons. This technique allows the use chemical oxidants for a batch synthesis of materials which allows the synthesis to be easily scaled up for industrial use. The

aluminum flake that is used to form the composite pigment with polypyrrole can add some barrier properties to a coating in which they are incorporated by lengthening the diffusion pathway of species passing through a coating. Finally, the binder material used in the coating has the potential to impart mechanical properties that are far superior to those possible for pure polypyrrole, to the composite coating.

## 1.2. Introduction

Currently, to inhibit corrosion on aluminum and aluminum alloy structures such as airplanes, hexavalent chromates are being used with excellent results. Its performance is linked to its ability to be stored in a coating for many years, due to its low water solubility, and to simultaneously inhibit the cathodic reactions and heal anodic damage, thereby passivating the aluminum surface to corrosion.[2] Unfortunately, hexavalent chromates have been shown to be strongly carcinogenic. Coupled with their water solubility, they are very dangerous to work with and there are added expenses associated with safely disposing of hexavalent chromate containing waste. Therefore, an environmentally benign replacement is needed. One such material that has shown some promise is polypyrrole. The structure of neutral polypyrrole that hasn't been oxidized or reduced can be seen in Figure 1.1. It is important to note the conjugation along the polymer chain which is responsible for the observed conductivity of polypyrrole.

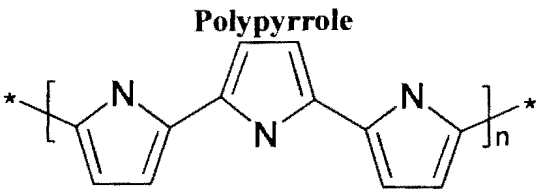


Figure 1.1. The structure of polypyrrole.

Polypyrrole is a member of a class of materials known as intrinsically conducting polymers (ICP's). The first work done producing conductive polypyrrole was by McNeil et al. in 1963 synthesizing iodine doped polypyrrole with a conductivity of approximately 1 S/cm.[3-5] While this is a somewhat modest conductivity, it was the first example of a conductive polymer. It was followed by the work of Shirakawa et al. in which doped polyacetylene with a conductivity of approximately $10^5$ S/cm was synthesized. This was remarkable in that it was the first example of a polymer with conductivities similar to many metals.[6] For this work Professor Alan J. Heeger, Professor Alan G. MacDiarmid, and Professor Hideki Shirakawa received the Nobel Prize in Chemistry in 2000.[7]

The key factor affecting the conductivity of polypyrrole and other conducting polymers is the presence of a conjugated polymer backbone and, therefore, a system of delocalized π-electrons. These electrons are more loosely bound to the carbon nuclei and are more free to move and be conducted through a chain. In polypyrrole however, the polymer must first be oxidized and doped with a counter-ion before the polypyrrole band gap is small enough for high conductivities (10-100 S/cm) to be observed.[8]

### 1.3. Chemical Structure Solutions

One of the methods by which researchers have been altering the solubility of polypyrrole has been to graft alkyl groups or polar groups onto the beta position of the pyrrole ring and then polymerizing the pyrrole into a soluble polymer. Walczak et al. has devised an interesting synthesis pathway to make Poly(3,4-alkylenedioxypyrrole)s which are soluble in a large array of organic solvents and processable.[9] The reaction mechanism can be seen in Figure 1.2.

Depending on which process is used, a polymer that is soluble in more polar or nonpolar solvents can be synthesized. For example, when monomer 7d is polymerized, it forms a water soluble polymer. Monomers 7c and 7a however, with their less polar substituents, form polymers that are soluble in nonpolar solvents. Melting point can also be controlled as the monomer precursors to 7a,c, and d were vitreous liquids while the monomer for 7b was a solid. This is very useful as the solubility of the monomer and polymer as well as the phase of the monomer can be tailored somewhat for a given application with other structures also being possible by this method. The polymerization of these monomers was discovered accidentally as these monomers will self initiate polymerization at room temperature but the process takes a week or more. With the addition of hydrazine, it was found that the polymerization is self doping as the iodine released from monomer 6 will oxidatively dope the polymerized product.

Most importantly, the polymers formed by this process retained their electroactive nature. As can be seen in Figure 1.3, polymers 7a,c, and d exhibit reversible or quasi-reversible redox processes at fairly low potentials. Polymer 7a exhibits two redox processes whose current decreases markedly with each subsequent potential cycle which is attributed to delamination from the platinum electrode. Polymers 7c and 7d exhibit stability as the current responses decreased very little even after 20 cycles. Looking at the potential side of the plots, the oxidation and reduction reactions of polymer 7d are remarkably reversible which would make it suitable for use in electrochromic devices or possibly battery application.[9]

Overall, this is a fairly flexible synthesis process that would tolerate the presence of functional groups much better than other processes which use stronger oxidizing agents,

and is capable of creating a large and varying array of polymers with tailored properties. It is, however, a seven step process and uses some highly dangerous chemicals such as hydrazine which would add great difficulty and expense to an industrial scale up. It does offer a water soluble alternative for processing conductive polypyrrole which is very favorable because of environmental concerns which, with current restrictions on volatile solvents and future restrictions which are surely coming, are and will continue to be a limiting factor in what chemistries can be used on an industrial scale.[9]

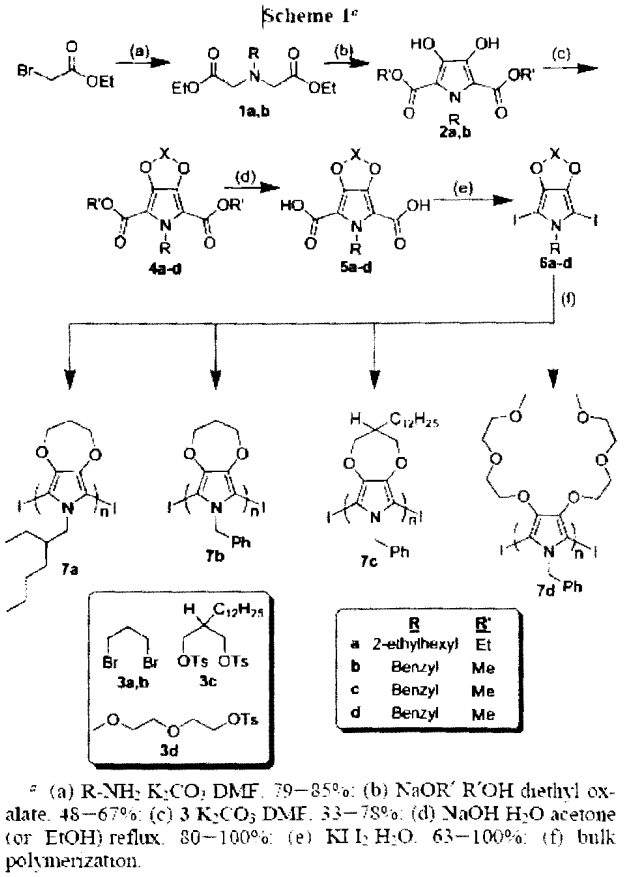


[a] (a) R-$NH_2$ $K_2CO_3$ DMF, 79−85%; (b) NaOR' R'OH diethyl oxalate, 48−67%; (c) 3 $K_2CO_3$ DMF, 33−78%; (d) NaOH $H_2O$ acetone (or EtOH) reflux, 80−100%; (e) KI $I_2$ $H_2O$, 63−100%; (f) bulk polymerization.

Figure 1.2. The synthetic route to several Poly(3,4-alkylenedioxypyrrole)s.[9]

*Reprinted with permission from Macromolecule. **41(3)** Walczak R., Leonard J., and Reynolds J., Processable, Electroactive, and Aqueous Compatible Poly (3, 4-alkylenedioxypyrrole) s through a Functionally Tolerant Deiodination Condensation Polymerization.: p. 691-700., 2008 American Chemical Society.*

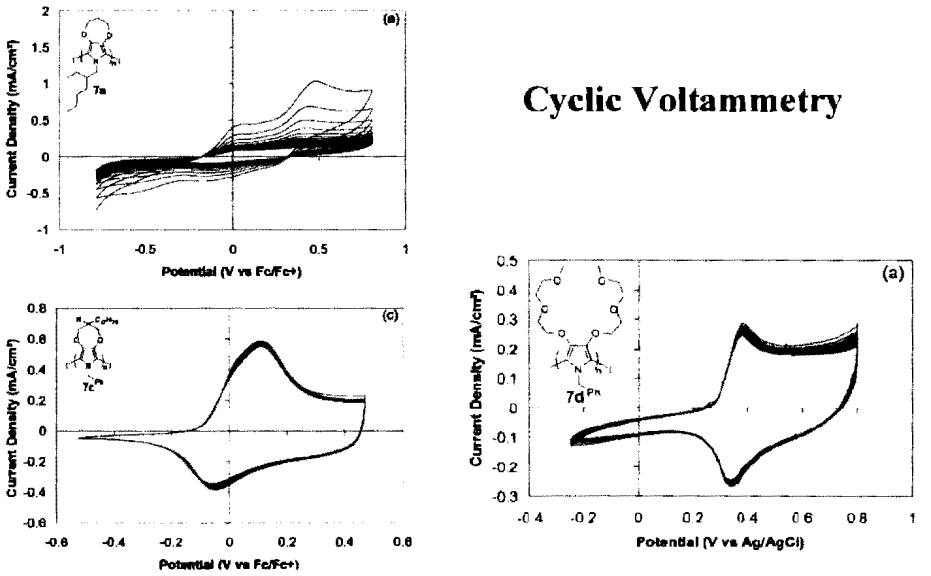


Figure 1.3. The cyclic voltammograms of polymers 7a,c, and d, cast onto platinum electrodes using toluene for 7a and 7c and water for 7d.[9]

*Reprinted with permission from Macromolecule. **41**(3) Walczak R., Leonard J., and Reynolds J., Processable, Electroactive, and Aqueous Compatible Poly (3, 4-alkylenedioxypyrrole) s through a Functionally Tolerant Deiodination Condensation Polymerization.: p. 691-700., 2008 American Chemical Society.*

Another interesting polymer was synthesized by Tian et al. who have synthesized an N-vinyl pyrrole. What is so interesting about this monomer is that when it is polymerized, it produces a polyethylene chain parallel to an alpha linked pyrrole chain. Also notable about this process is its simplicity. It uses common reactants and reactions that are straight out of any organic chemistry text book and is carried out at a fairly low temperature of 80° C which would make this a much cheaper and easily scaled up alternative to the method used by Walczak et al. Despite its simplicity however, it also could be used to make polymers with tunable properties. While it likely could not be used to make water soluble polymers, by using bromo-alkanes other than 1,2-dibromoethane such as a 1,3-dibromopropane or 1,4-dibromobutane, a polypropylene or polybutylene

chain could be connected to the pyrrole chain at the N position. This could introduce more flexibility or toughness to the normally brittle polypyrrole, especially if longer, higher molecular weight olefins are attached.[10] This synthesis can be seen if Figures 1.4 and 1.5.

**Vinyl Pyrrole Synthesis**

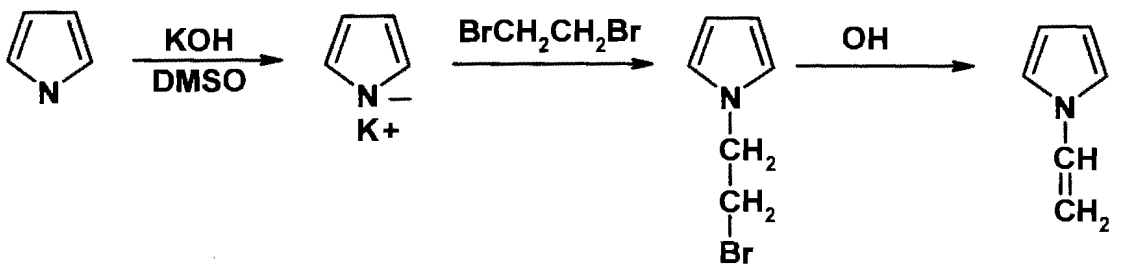


Figure 1.4. The synthesis of N-vinyl pyrrole reproduced from [10].

*Reprinted from Synthetic Metals, **158**(17-18), Wang W., Yu D., and Tian F., Synthesis and characterization of a new polypyrrole based on N-vinyl pyrrole.: p. 717-721. 2008 with permission from Elsevier.*

**Vinyl Pyrrole Polymerization**

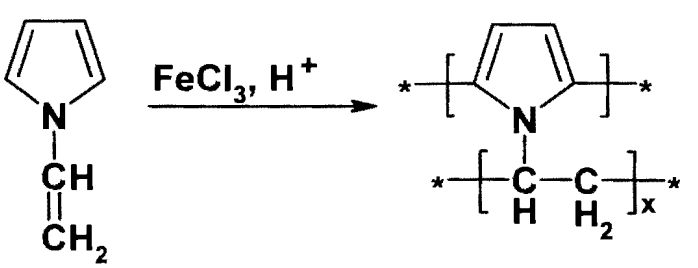


Figure 1.5. The polymerization of N-vinyl pyrrole reproduced from [10].

*Reprinted from Synthetic Metals, **158**(17-18), Wang W., Yu D., and Tian F., Synthesis and characterization of a new polypyrrole based on N-vinyl pyrrole.: p. 717-721. 2008 with permission from Elsevier.*

Another advantage to this method is the symmetry of the N-vinyl pyrrole it produces. Because of its symmetry, there is not a head or tail end as is seen in β-substituted pyrroles. Therefore, when it is polymerized, it results in a more ordered and

planar backbone which tends to decrease the band gap across the chain and, therefore, produces polymers with higher conductivities than the polymerization of β-substituted pyrroles.[10]

It was reported by the authors that the polymerized N-vinyl pyrrole was indeed soluble in DMSO, THF, $CHCl_3$ and $CH_2Cl_2$ with the most homogeneous films being cast using $CHCl_3$. This was confirmed by a morphology study performed using a scanning electron microscope (SEM) which can be seen in Figure 1.6.[10]

As can be seen in Figure 1.6, extremely smooth and homogenous films of the poly(N-vinyl pyrrole) could be cast using chloroform. The resolution of most SEM instruments is in the approximate range of 50-100 nm. Without surface profiles higher than this, it is difficult to obtain an image from the surface. In Figure 1.6 it is difficult to detect any features of the surface of the cast film leading to the conclusion that the surface profile is extremely smooth and is likely on the order of hundreds of nanometers.

An analog to the N-vinyl pyrrole is seen in pyrrole that is N-functional in poly methyl methacrylate. This is done in much the same way as with the N-vinyl pyrrole. The methyl methacrylate monomer is grafted onto the N position of the pyrrole monomer with subsequent polymerization possible for both of the grafted monomers. There are several papers exploring a methyl methacrylate backbone with a polypyrrole chain grafted to it through the nitrogen on the pyrrole rings in various conformations and copolymerized with other polymers such as thiophenes and styrene.[11-20] These materials are made in a slightly different manner in comparison to the N-vinyl pyrrole polymerization. What is typically done is the ω or γ form of the methyl methacrylate N-Pyrrole monomer is first synthesized.

**SEM Images**

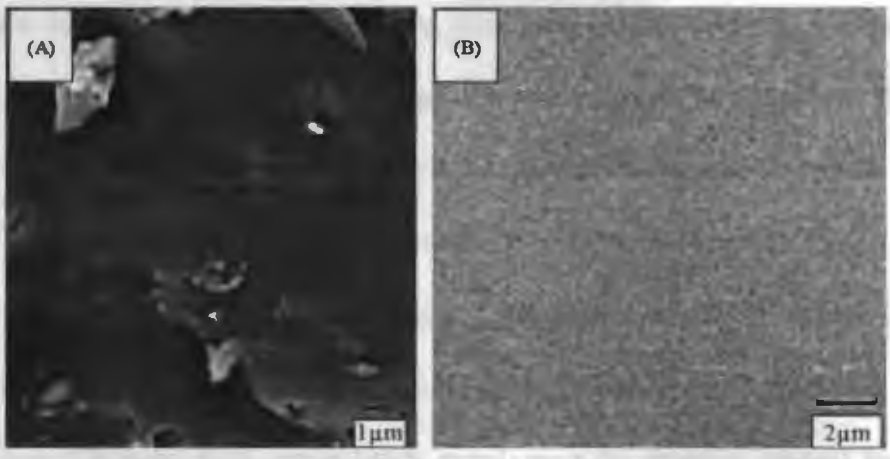


Figure 1.6. SEM images of bulk polymer (A) and a chloroform cast film (B).[10]

*Reprinted from Synthetic Metals, **158**(17-18), Wang W., Yu D., and Tian F., Synthesis and characterization of a new polypyrrole based on N-vinyl pyrrole.: p. 717-721. 2008 with permission from Elsevier.*

This monomer containing a pyrrole moiety is then polymerized in some ration with methyl methacrylate, styrene or any other monomer that is capable of undergoing free radical chain growth polymerization. This polymer backbone is then placed into a pyrrole solution and the pyrrole is polymerized via the addition of an oxidizing agent such as $FeCl_3$.[11-13, 17, 19] In this synthesis scheme, the pyrrole moieties covalently attached to the polymer backbone act as initiation points where a polypyrrole chain that is attached to the methyl methacrylate chain can grow. Once a polypyrrole chain has grown from these attached pyrrole rings it acts as a crosslink between the polypyrrole chain and the methyl methacrylate chain. Therefore, by controlling the ratio of methyl methacrylate N-pyrrole to methyl methacrylate in the first polymerization, the degree of connectedness between the poly methyl methacrylate and polypyrrole backbones can be controlled. This allows for tunable properties to some degree where the method used with vinyl pyrrole, with both chains being fully crosslinked, does not.

There is a similar process where a thiophene moiety is grafted onto a methyl methacrylate molecule through the β carbon on the thiophene ring.[14-16] This grafted monomer is used in two ways. The first is similar to the pyrrole monomer that is N-functional with methyl methacrylate where the pyrrole moiety is used as a cross link between a poly methyl methacrylate chain and a polypyrrole chain. Here the N-functional pyrrole moiety is simply replaced by a β-functional thiophene moiety.[14-15] The other way in which it is used is to create block copolymers by growing methyl methacrylate chains that are end capped with thiophene. The end caps can then be used to grow either polythiophene or polypyrrole chains off of the ends of the poly methyl methacrylate chain.[16]

The approaches used in grafting polypyrrole to polypropylene yielded films with conductivities ranging from 0.4 S/cm in the random thiophene functional copolymer case to 13 S/cm in the case of the thiophene functional block copolymer. The thiophene functional materials had glass transition temperatures between 70 and 106 °C. For the cases in which pyrrole was grafted onto methyl methacrylate, conductivities ranging from $10^{-4}$ to 0.2 S/cm were achieved with glass transition temperatures near 130° C. Because pristine polypyrrole under normal circumstance does not have a discernable glass transition temperature, being coupled to the poly methyl methacrylate produced a copolymer with a much lower glass transition temperature than that of pure polypyrrole. The mechanical properties of these copolymers were not examined in these studies, so it is unknown what effect the copolymerization had on the mechanical properties of the polypyrrole. It would stand to reason however, that the poly methyl methacrylate would impart some flexibility and possibly toughness into the copolymer.[11-13, 17-20]

A similar technique was also use to graft polypyrrole onto a polymer backbone consisting of a copolymer between acrylonitrile and vinyl acetate. This method produced a film with a glass transition temperature of approximately 90° C, a conductivity of 0.1 S/cm, a Young's Modulus of 1878 ± 20 MPa, a strain at break of 16.1 ± 0.1 %, and a stress at break measurement of 30.8 ± 0.2 MPa. This is a vast improvement over pure polypyrrole and is somewhat comparable to the mechanical properties of polypropylene.[21] Other polymer backbones that have been used in a similar fashion include polyamines, polyimines, ethyl acetate, ethyl stearate, caprolactones, and carboxylic acids.[22-25]

One of the earlier attempts at synthesizing a processable pyrrole that has been shown to inhibit corrosion comes from the collaborative work of Ashraf et al. and Gelling et al. In this work, a poly(β-octyl pyrrole) was synthesized by Ashraf et al. which was then cast into films and evaluated for its corrosion inhibiting properties by Gelling et al.[26-27] The synthesis of the alkyl pyrrole monomer can be seen in Figure 1.7. A separate route to β-octyl pyrrole was found by Masuda et. al through oxidative coupling.[28] The synthesis of 3-octadecyl and 3-docosylpolypyrrole was also investigated by Guernion et al. These products were soluble in chloroform and were easily coated onto microporous membranes to form sensors.[29] 3-ester pyrroles have also been investigated for a water soluble version of this technique.[30]

Here again, the monomer synthesis from Figure 1.7 is somewhat complicated. After the monomer synthesis, the polymerization was carried out through electrodeposition onto platinum electrodes in a $CH_2Cl_2$ solution. The polymer was then removed from the electrode which was flexible enough to form free standing films. For

other studies, polymer films were recast using xylenes. A cyclic voltammogram from is process can be seen in Figure 1.8.[26]

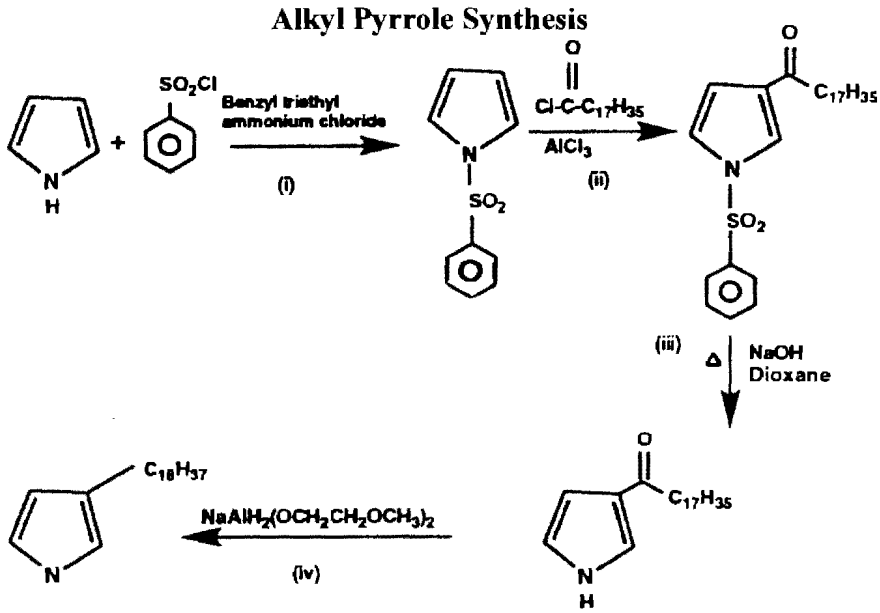


Figure 1.7. The synthesis of β-alkyl pyrrole.[26]

*Reprinted from Polymer, 37(13), Ashraf S., Chen F., Too C., and Wallace G., Bulk electropolymerization of alkylpyrroles.: p. 2811-2819. 1996 with permission from Elesevier.*

The increasing current for each subsequent potential sweep indicates that the poly(alkyl pyrrole) film is growing on the surface of the platinum electrode. This is due to the corresponding oxidation and reduction reactions of the poly(alkyl pyrrole) that has been deposited. This current is due to the flow of dopant anions into and out of the growing film. Oxidized polypyrrole has a net positive charge, and so to satisfy charge neutrality, it must incorporate negatively charged anions into its structure which are held fairly tightly by coulombic forces. This influx of ions accounts for current flow into the film. Once the polypyrrole is reduced back to a neutral state, the anions are no longer needed for charge neutrality and are expelled by the film resulting in current flowing out of the film.

Naturally, as more polypyrrole is deposited onto the electrode, this effect will be magnified as more anions flow into and out of the film.[26]

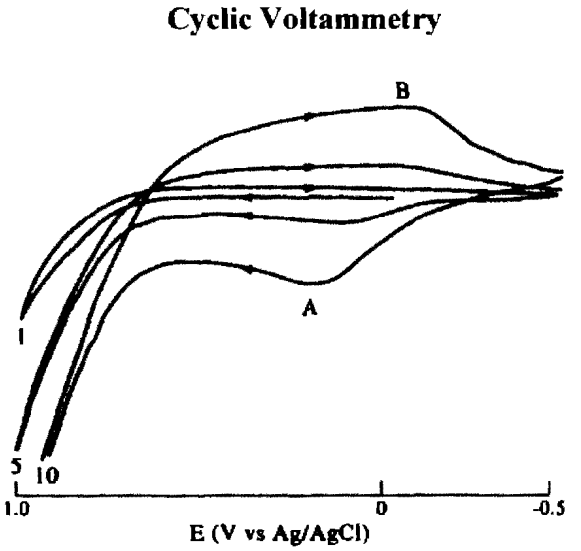


Figure 1.8. The first, fifth, and tenth cyclic voltammetry cycles from the alkyl pyrrole polymerization.[26]

*Reprinted from Polymer, 37(13), Ashraf S., Chen F., Too C., and Wallace G., Bulk electropolymerization of alkylpyrroles.: p. 2811-2819. 1996 with permission from Elesevier.*

The reported conductivity for the poly-octyl pyrrole was $2.4 \times 10^{-4} \pm 2 \times 10^{-5}$ S/cm when p-toluenesulfonic acid monohydrate was the dopant and $4.6 \times 10^{-3} \pm 2 \times 10^{-4}$ S/cm when $ClO_4^-$ was the dopant. These are very low conductivities for polypyrrole and are a testament to the disorder caused in the pyrrole backbone due to the β-alky groups and head-head and tail-tail linkages that were mentioned earlier.[26]

The poly(3-octyl pyrrole) and poly(3-octadecyl pyrrole) were investigated by Gelling et al. for any corrosion inhibiting properties on aluminum alloy 2024 T3. The two forms of poly(alkyl-pyrrole) were cast as primer films onto AA 2024 T3 panels and then coated with a polyurethane top coat.[27]

After 600 hours of prohesion exposure, the poly(3-octyl pyrrole) was outperforming a hexavalent chromate control sample and the poly(3-octadecyl pyrrole) sample. This is evident by the blistering seen on the chromate and the poly(3-octadecyl pyrrole) panels and the absence of blistering on the poly(3-octyl pyrrole) in Figure 1.9 which indicates corrosion is taking place under the chromate and poly(3-octadecyl pyrrole) coatings.[27]

**Optical Microscopy Images**


Figure 1.9. Optical microscope pictures of the chromate control (left), poly(3-octyl pyrrole) (center), and poly(3-octadecyl pyrrole) (right) panels after 600 hours of immersion exposure.[27]

*Reprinted from Progress in Organic Coatings. 43(1-3), Gelling V., Wiest M., Tallman D., Bierwagen G., and Wallace G., Electroactive-conducting polymers for corrosion control - 4. Studies of poly(3-octyl pyrrole) and poly(3-octadecyl pyrrole) on aluminum 2024-T3 alloy.: p. 149-157. 2001 with permission from Elsevier.*

Another strategy used to increase the processability of polypyrrole is to form copolymers with other monomers which impart some solubility and other properties to the polypyrrole. One such polymer was synthesized by Springer et al.[31] The basic strategy employed in this study was to first synthesize a trimer containing toluidine, polypyrrole, or a mixture of the two and then oxidatively polymerize the trimer using a chemical oxidation method such as incorporation into a solution with ammonium persulfate or some other

strong oxidizing agent. This method would be favorable for industry because not only is it fairly simple, but it is also performed in an aqueous solution. It is also a chemical oxidation method which could be done in bulk as long as the heat given off by the reaction is kept under control.[31]

It was found that this synthesis did form a copolymer between the pyrrole and the toluidine with toluidine rings in the polymer backbone which was verified using FTIR, UV-VIS, and H-NMR measurements. As was expected, the toluidine imparted some of its solubility into the co-polymer. It was found that the copolymer was soluble in NMP, DMSO, $CHCl_3$, THF, benzene, and $CH_2Cl_2$. No comment was made on its conductivity which would surely be affected in some way by the addition of the toluidine ring in the polymer backbone. This same group also synthesized a polypyrrole anisidine copolymer that was soluble in solvents such as NMP and DMSO.[31-32]

Another study by Ikan et al. showed how to synthesize a polypyrrole silicone copolymer in an effort not only to improve its processability but its mechanical properties as well. This study was largely a success in that it produced a single step aqueous synthesis by chemical oxidation and produced a copolymer with a conductivity of 6.1 S/cm, which is quite impressive for a polymer that is not pure polypyrrole. These copolymers were soluble in solvents such as DMF and acetone. Films cast from solutions in these solvents had much improved flexibility. The structure of this copolymer can be seen in Figure 1.10.[33-34]

A sol-gel chemistry has also been developed whereby a methyl methacrylate functional siloxane is attached via the methacrylate moiety to the β position on the polypyrrole ring. The siloxane functional end of the monomer was then bonded to a glass

surface. The bonding with the substrate was verified using diffuse reflectance FTIR. An aqueous ammonium persulfate solution was then used to polymerize the pyrrole moieties. While this method was shown to increase adhesion on glass and metal oxide surfaces, which could be useful for a great many applications, when it comes to corrosion protection, this method is somewhat problematic. The covalently bonded siloxane ends of the monomers would act as a nonconductive barrier between the metal surface and the polypyrrole film preventing, or at least hindering, coupling or other electrochemical reactions. Coupling current or open circuit potential measurements were not carried out in this study so it is unknown if electrochemical interactions with the substrate are possible but it is likely that the siloxane moieties connecting the polypyrrole films to the substrate would reduce those interactions significantly.[35]

**PPY/Silicone Tegomer**

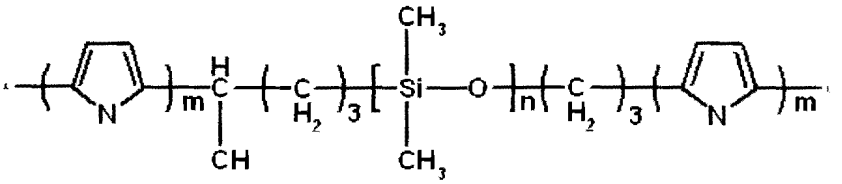


Figure 1.10. A proposed structure for the pyrrole/silicone tegomer copolymer reproduced from [33].

*Reprinted from K z lcan N., Ustamehmeto lu B., Oez N., Sezai Sarac A., and Akar A., Soluble and conductive polypyrrole copolymers containing silicone tegomers. Journal of Applied Polymer Science, **89**(11): p. 2896-2901. 2003 with permission from John Wiley and Sons.*

Other groups have begun to use the strategy of copolymerizing pyrrole with other conductive polymers that are known to have better processability. One example is from Toparre et al. who have copolymerized pyrrole and thiophene with a flourophenyl

group attached to the N position on the pyrrole ring. This synthesis process can be seen in Figure 1.11.[36-37]

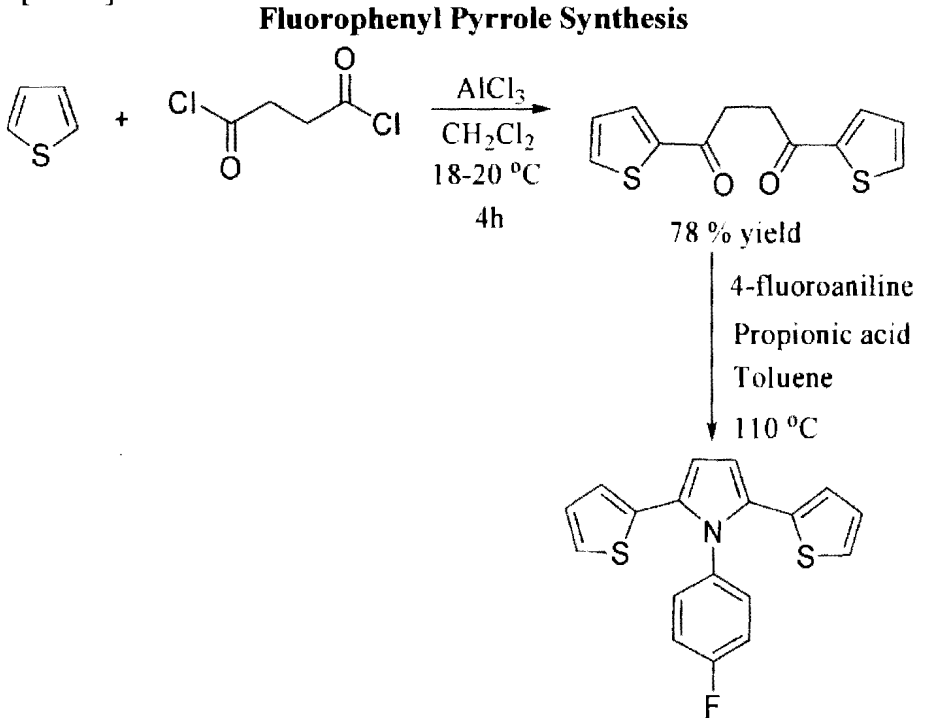


Figure 1.11. The synthetic route to 1-(4-fluorophenyl)-2,5-di(thiophen-2-yl)-1H-pyrrole (FPTP).[36]

*Reprinted from Materials Chemistry and Physics, **104**(2-3), Arslan A., Türkarslan Ö., Tanyeli C., Akhmedov M., and Toppare L., Electrochromic properties of a soluble conducting polymer: Poly (1-(4-fluorophenyl)-2, 5-di (thiophen-2-yl)-1H-pyrrole). Materials Chemistry & Physics: p. 410-416. 2007 with permission from Elsevier.*

This monomer was then polymerized through a chemical oxidation using $FeCl_3$ as the oxidizing agent in a nitromethane solvent. The resulting polymer, linked through the α positions on the thiophene rings, was soluble in chloroform and an electrochromic device was able to be constructed out of it in conjunction with poly(3,4-ethylenedioxythiophene) (PEDOT). The device switched from green to yellow to blue depending on what potential was applied to the conducting polymer. This transition can be seen in Figure 1.12.[36-37]

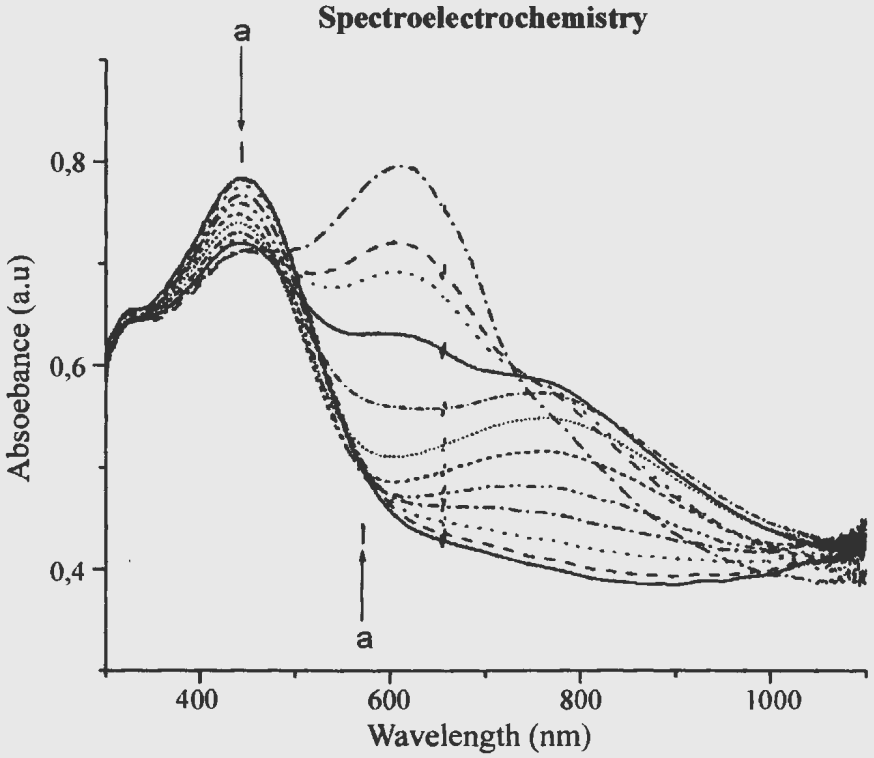


Figure 1.12. The spectroelectrochemistry of the P(FPTP)/PEDOT device with potentials from -0.8V on the bottom to 1.1 V on the top.[36]

*Reprinted from Materials Chemistry and Physics,* ***104****(2-3), Arslan A., Türkarslan Ö., Tanyeli C., Akhmedov M., and Toppare L., Electrochromic properties of a soluble conducting polymer: Poly (1-(4-fluorophenyl)-2, 5-di (thiophen-2-yl)-1H-pyrrole). Materials Chemistry & Physics: p. 410-416. 2007 with permission from Elsevier.*

As can be seen in the spectroelectrograph shown in Figure 1.12, the color of the film is green at -0.8 V but as the potential is raised to 1.1 V, it turns more yellow and eventually turns blue with the disappearance of the absorption peak around 400 nm and the growth of the peak around 600 nm. This is notable because many electrochromic devices are only capable of producing 2 colors as the potential applied is varied. This material is also notable because of its stability. After 1000 oxidation/reduction cycles taking the device through its range of colors, it still retained 88% of its electroactivity. This can be seen in Figure 1.13.[36]

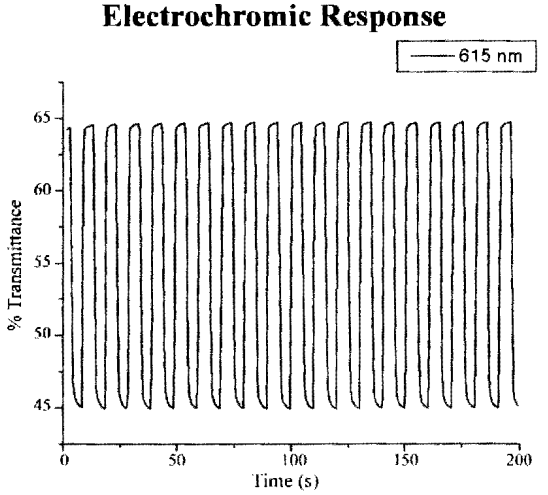


Figure 1.13. The percent transmittance as a function of time showing how the transmittance of the P(FPTP)/PEDOT device changes with each electrochromic switching cycle.[36]

*Reprinted from Materials Chemistry and Physics, **104**(2-3), Arslan A., Türkarslan Ö., Tanyeli C., Akhmedov M., and Toppare L., Electrochromic properties of a soluble conducting polymer: Poly (1-(4-fluorophenyl)-2, 5-di (thiophen-2-yl)-1H-pyrrole). Materials Chemistry & Physics: p. 410-416. 2007 with permission from Elsevier.*

The FPTP synthesized in this paper was a remarkable material, not only because of its processability, but its excellent electrochemical properties which make it useful for electrochromic applications where the color of an object is required to change as a result of a potential change. This could be used for example in a display screen to produce colors with little electronic hardware required.[36]

A similar method was used in which a thiophene trimer that was substituted in the α-position with alkyl sodium solfonate was copolymerized with pyrrole. It was found that this reaction was self doping; meaning the negatively charged sulfonate moieties on the thiophene trimers acted as the dopant for the conducting polymer. Therefore no other salts were required to produce a conductive product. It is also these sulfonate moieties that imparted water solubility to the polymer. While this is an interesting result, it would not lend itself to applications where the polymer is exposed to the elements as it would

dissolve and be eroded overtime when in contact with water. It could, however, be used as a prepolymer to be polymerized with pyrrole monomer to possibly synthesize higher molecular weight polypyrrole in an aqueous solution.[38]

While there are many ways to improve the processability of polypyrrole by changing its chemical structure, many tend to be complex and, therefore, expensive. Many also use organic solvents which are coming under more and more scrutiny making aqueous chemistries more appealing to industry. There are some promising exceptions however which hold great promise for future research.

### 1.4. Dopant Ion Solutions

Another method by which the properties of polypyrrole can be modified is by the dopant counterion that was mentioned earlier. These ions are held to the polymer structure by coulombic forces tightly enough that the ions will start to affect its solubility in various solvents as well as other properties of the polypyrrole.[39-40] The ions can also act to sterically hinder chain interactions such as Van Der Waals forces or $\pi$-$\pi$ stacking. One of the first reports of this behavior was in 1989 by Peres et al. where galvanostatic polymerization was used in the presence of sodium dodecylsulfate as the dopant. While this method did not produce soluble polypyrrole, it did produce an electrodeposited film with greater flexibility in comparison to polypyrrole doped with smaller dopant ions.[39]

Alkyl benzene sulfonates are also used as a dopant to impart some flexibility to polypyrrole films. With these dopants, the factors that have the greatest effect on the end properties of the polypyrrole is the length of the alky chain that is attached to the benzene ring and the monomer to oxidant ratio which directly correlates to the doping level of the

polymer. It has been found that the doping level directly correlates to the density of states in the polymer which affects properties such as conductivity and transport coefficients of charge carriers. It has also been found that with shorter alkyl chains there is more short range order in the polypyrrole chains and, therefore, greater overlap of $\pi$ orbitals and greater interchain interactions. This results in higher conductivities of the product but also lower solubility and mechanical properties. Longer chains act as spacers between the polypyrrole chains thereby by decreasing conductivity but increasing solubility and flexibility.[40-42] These findings agree with Bay et al. who also investigated the effect of alkyl chain length on the mechanical and electrical properties of polypyrrole films. It was found that by increasing the alkyl chain length, the Young's Modulous could be reduced by approximately a factor of 10. It was also found that elongation at break could be increased from 1% to 4% while the measured tensile strength of the films was approximately 35 MPa.[43]

There is also an azobenzene sulfonic acid based surfactant that was investigated as a dopant to produce processable polypyrrole which is synthesized from cardanol. Cardonal can be synthesized from anacardic acid which is a waste product from the cashew industry that. The tri-unsaturated structure of cardonal can be seen in Figure1.14 but it exists as a mixture of tri, bi, and mono-unsaturated cardonal with a small percentage of saturated cardonal.[44] It was found that this compound was able to produce nanospheres of a controlled size due to micelle formation which acted as a soft template for the nanospheres formation. These nanospheres were easily dispersed in water by simply stirring the mixture by hand and were slightly soluble in both water and dimethylformamide.[45]

Another natural and renewable product that has been used in the synthesis of polypyrrole is horseradish peroxidase which is an enzyme found in the horseradish plant that can catalyze the oxidative polymerization of polypyrrole in the presence of hydrogen peroxide. By using sulfonated polystyrene as a dopant, an electroactive and water soluble polypyrrole could be synthesized.[47]

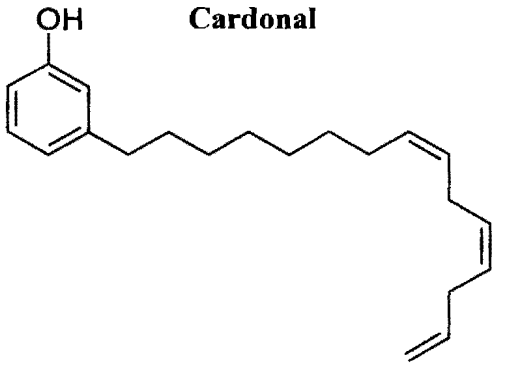


Figure 1.14. The structure of tri-unsaturated cardonal.[46]

*Reproduced with permission from Kumar P. P., Paramashivappa R., Vithayathil P. J., Rao P. V. S., and Rao A. S., Process for isolation of cardanol from technical cashew (Anacardium occidentale L.) nut shell liquid. J. Agric. Food Chem,* ***50****(16): p. 4705-4708. 2002 American Chemical Society.*

Dodecyl benzene sulfonic acid is yet another example of an alky benzene sulfonate which can be used to produce soluble polypyrrole. It was reported by Lee et al. that the use of this dopant could produce polypyrrole powder that was soluble in m-cresol and could be cast into a smooth film that was resistant to acetone. The bulk conductivity of the cast films was found to be 10 S/cm at -2° C which is impressive considering the large amount of nonconducting surfactant in the films.[48] In a later paper it was found that the addition of $[BF_4]^-$ ions as a codopant with dodecyl benzene sulfonic acid increased interchain interactions and improved the conductivity when compared to polypyrrole that

was doped with only dodecyl benzene sulfonic acid.[49] Poly-2-acrylamido-2-methyl-1-propane sulfonic acid has also been used as a codopant along with dodecyl benzene sulfonic acid to impart greater flexibility than dodecyl benzene sulfonic acid alone. With this codopant, films with 25% elongation at break and a toughness of 3.36 MPa were achieved. This is a large improvement over the mechanical properties of polypyrrole that is doped with small anions such as chloride which, typically, is quite brittle.[50] Indeed the use of codopants to alter the properties of polypyrrole has been a successful technique. Others examples have been used to improve, conductivity, mechanical properties, and transport properties of polypyrrole.[51-53] Another study reports the synthesis of dodecyl benzene sulfonic acid doped polypyrrole that is soluble in chloroform, dichloromethane, and 1,1,2,2-tetrachloroethane with comparable conductivity.[54]

Jang et al. also studied the effect of an alkyl benzene sulfonate, as well as several other dopants, on the resulting properties of polypyrrole. The dopants used were: 2-naphthalenesulfonic acid sodium salt (NaNSA), dodecylbenzene sulfonic acid sodium salt (NaDBSA), butylnaphthalene sulfonic acid sodium salt (NaBNS), and di(2-ethylhexyl) sulfosuccinic acid sodium salt (NaDEHS). The dopants were incorporated using a very simple one step aqueous reaction using ammonium persulfate as the oxidant. This process is desirable because of its sheer simplicity which does not require purification of the product, but also because of its relatively environmentally friendly nature. Without the need for organic solvents, there would be no volatile organic compounds (VOC's) produced by the reaction which can be an environmental and health concern. The only byproducts would be, hydrogen gas evolved out of the solution which could be collected

and sold, and waste water contaminated by pyrrole, sulfate and ammonium which could be recoverable as well if it were economical to do so.[55]

The downside to this technique, is that the products are only soluble in organic solvents such as 1,2-dichloroethane, which was used to determine the solubility of the doped polypyrrole. Because the polypyrrole produced in this way would likely use VOC containing chemicals for its application and would be restricted in Europe and the United States. However, by using a two step process in 1,2-dichloroethane outlined in Figure 1.15, the authors were able to add a sulfonic acid functionality to the pyrrole rings which induced water solubility. Although this reaction does take place in 1,2-dichloroethane, the end product is water soluble up to 4% w/v. It was also fairly conductive with a conductivity of $5 \times 10^{-1}$ S/cm which while being admittedly low for polypyrrole, does place it well within the conductivity range of semiconductors.[55]

The key feature of this technique is that bulky dopants with either large non-polar or polar substituents are used. The larger these dopants are, the larger their affect will be on the solubility of the resulting polypyrrole. Another example of this comes from MacDiarmid et al. who use the dopant di(ethylhexyl) sulfosuccinate sodium salt, whose structure can be seen in Figure 1.16, to induce not only solubility but flexibility into highly conductive polypyrrole.[56]

It was reported by the authors that the polypyrrole synthesized via a chemical oxidation reaction had a high number average molecular weight of 62,296 g/mol determined via GPC with polystyrene standards. This is fairly high for polypyrrole. The polymer was readily soluble in slightly polar solvents such as DMF, DMSO, and NMP and had slightly lower solubility in the non-polar solvents like chloroform and m-cresol. It was

also flexible with a cast films being able to be stretched up 2.5 times its original length. Because the conductivity is affected by the alignment of the polypyrrole chains, and therefore increased π orbital interaction allowing for more efficient electron transfer between chains, the stretching of cast films can result in changes in conductivity as the stretched polymer chains become more aligned. This effect was demonstrated when a di(ethylhexyl) sulfosuccinate doped polypyrrole film cast from NMP was stretched to 2.5 times its original length. Due to the stretching and simultaneous chain alignment, an increase in conductivity from 7.2 x $10^{-1}$ S/cm to 60 S/cm was observed.[56]

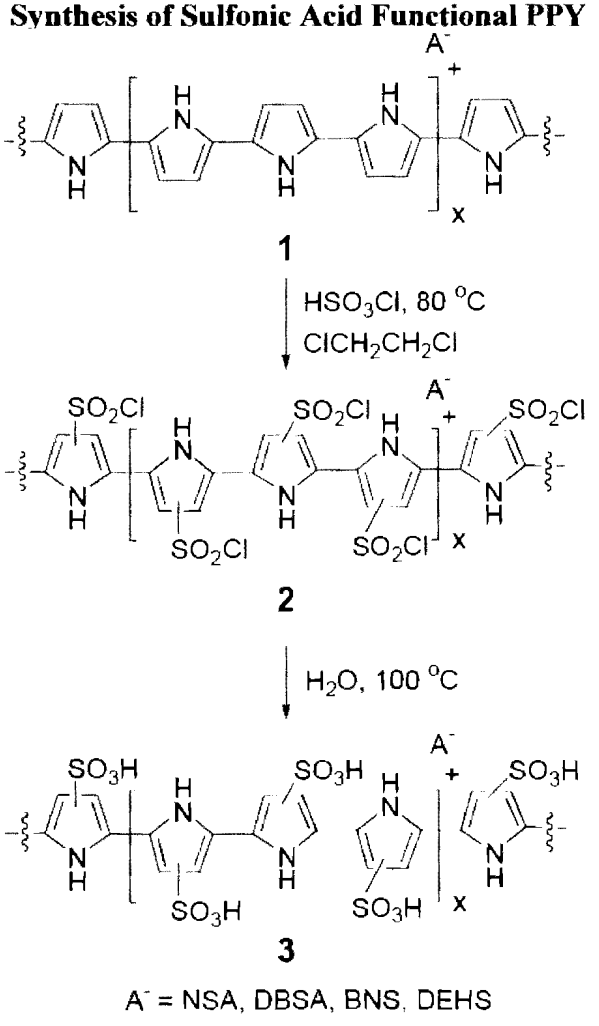


Figure 1.15. The synthesis scheme for sulfonic acid functional polypyrrole.[55]

*Reprinted from Jang K., Lee H., and Moon B. Synthetic Metals, **143**(3), Synthesis and characterization of water soluble polypyrrole doped with functional dopants.: p. 289-294. 2004 with permission from Elsevier.*

**Di(ethylhexyl) Sulfosuccinate Sodium Salt**

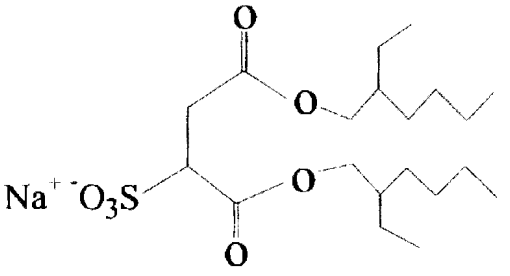


Figure 1.16. The structure of di(ethylhexyl) sulfosuccinate sodium salt.[56]

*Reprinted from Synthetic Metals, **125**(3) Oh E., Jang K., and MacDiarmid A., High molecular weight soluble polypyrrole: p. 267-272. 2002 with permission from Elsevier.*

Napthalene based dopants are another class of compounds that have been studied for the properties that are imparted to polypyrrole. β-naphthalene sulphonic acid is one example of this class of compounds. The doped polypyrrole took on a fibril morphology with a conductivity of 27 S/cm and was soluble in m-cresol. A scanning electron micrograph showing this morphology can be seen in Figure 1.17. The thermal stability, determined by TGA, of the polypyrrole was also increased. The fibril morphology is quite interesting as it is less than a μm across, and with a conductivity of 27 S/cm, some possible applications as wires in nanoscale electronic devices can be imagined.[57-58]

1,5-napthalene disulphonic acid has also been studied and was found to greatly increase the crystallinity of polypyrrole which usually only has short range order. Upon dedoping through exposure to an ammonia solution this crystallinity was lost and the polypyrrole was almost totally amorphous. When the polypyrrole was redoped with 1,5-

napthalene disulphonic acid crystallinity was not regained indicating that this effect is only possible during the initial polymerization reaction.[59]

**Scanning Electron Microscopy**


Figure 1.17. Fibrils of polypyrrole doped with β-naphthalene sulphonic acid.[57]

*Reprinted from Shen Y. and Wan M., Soluble conductive polypyrrole synthesized by in situ doping with beta-naphthalene sulphonic acid. Journal of Polymer Science Part A: Polymer Chemistry, 1997. 35(17): p. 3689-3695. With permission from John Wiley and Sons.*

Other dopants that are used which can impart solubility, modify the ion transport properties, or even produce thermoplastic and elastic films of polypyrrole include functionalized forms of poly(β-hydroxyethers), poly-(butadienes), poly(imides), poly(methacrylates), and polystyrene sulfonates where an anionic group is grafted somewhere onto the polymer.[60-61]

The use of different dopant ionic materials to impart different properties into the resulting polypyrrole is attractive because of its shear simplicity and ease of preparation, reduced cost in comparison to changes in the chemical structure and the large range of

properties that can be imparted to the polypyrrole. For most applications, this method would be more than sufficient but in the case of corrosion inhibition there is one necessary component that is not present in the first two methods for improving the properties of polypyrrole and that is the interruption of percolation networks.[62]

It was found by Rohwerder et al. that in pure polypyrrole films where conduction occurs on a fairly long scale on the order of several hundred μm, the film becomes a very efficient cation conductor along defects that are too large to be fully passivated by the polypyrrole. This happens via a hopping mechanism where the cations hop from fixed dopant ion to fixed dopant ion within the polypyrrole film. When this happens it results in a rapidly moving reduction front within the polypyrrole film, as a result of the metal substrate corroding, which keeps proceeding as long as there is a supply of cations. Once the polypyrrole film is reduced, the oxygen reduction reaction, which is one of the cathodic corrosion reactions that produces hydroxide ions and hydroxide radicals, takes place at the polypyrrole-metal interface instead of on the surface or within the bulk of the polypyrrole. Hydroxide radicals are then produced at the coating/metal interface as a result of oxygen reduction. These radicals then begin to degrade the coating at the interface which results in rapid delamination of the polypyrrole coating and, therefore, coating failure. Creating a percolation network by adding polypyrrole pigment particles to a polymer matrix that is interrupted by nonconducting materials, is one way in which the fast incorporation of cations can be slowed or contained to a small area so the coating will fail gradually instead of catastrophically. This is where composite materials containing polypyrrole may be useful.[62]

### 1.5. Composite Materials Solutions

Another group of researchers has tried to circumvent the shortcomings of polypyrrole by creating composites with polypyrrole and one or more other materials which gives a mix of properties with each material making some contribution to the properties of the material as a whole.[63] One way to do this is by coating particles in polypyrrole and then incorporating those particles into a polymer matrix. When a sufficiently high concentration of polypyrrole coated particles is used, an interconnected conductive network is formed. This point in pigment volume concentration is called the percolation threshold. The polymer matrix gives the mechanical properties, namely adhesion and flexibility, which unmodified polypyrrole typically lacks and the polypyrrole imparts electroactive properties to the composite.

The Handbook of Conducting Polymers details a colloidal approach to the synthesis of the composite materials which forms a raspberry morphology.[64] In this process, a sterically stabilized silica nano-particle colloid is prepared via a surfactant and 20 nm silica particles. An oxidant is then added along with the conducting polymer at 100° C. These composites were made with both polyaniline and polypyrrole and it was found that the polypyrrole colloids had greater colloidal stability.[64]

A paper looking at the effect that different parameters have on the products of this reaction found that the reaction is notably insensitive to oxidant, monomer and silica concentrations, silica diameter, polymerization temperature, stirring rate, and oxidant type. Additionally it was found that the particle size, polypyrrole content and conductivity of the resulting polypyrrole silica colloidal nanocomposites underwent little change as a result of changes in these parameters.[63] This would make this synthesis procedure ideal for

industrial use due to the robustness of the process. The reaction would be aqueous with few hazardous chemicals and the end product would be somewhat insensitive to the conditions under which the reaction was carried out.[65]

Another group used chitosan which is a polysaccharide produced from chitin which is found in the shells of crustaceans to modify the surfaces of silica spheres that were approximately 500 nm across. The chitosan acted as an anchoring point on the silica surface which hydrogen bonded with the polypyrrole and resulted in its adsorption onto the silica surface. The resulting particles had a conductivity of 8 S/cm and a morphology that was composed of a spherical silica particle surrounded by smaller spheres of polypyrrole.[66]

Montmorillonite, clay is another inorganic particle that has been looked at as a possible material with which to form polypyrrole composites. The structure of montmorillonite can be seen in Figure 1.18. The advantage of using these high aspect ratio, flake shaped materials, is that conductive pathways can be formed through a matrix material at lower pigment volume concentrations than spherical particles. They also can provide barrier properties to a coating, if the pigment volume concentration within the coating is high enough, the flakes will tend to overlay one another and provide a longer diffusion pathway for ions. What is typically done to synthesize these composites is the clay is either swelled in an organic solvent such as chloroform to allow pyrrole monomer to diffuse into the gallery space between silicate sheets in the clay structure where it is then polymerized via an oxidizing agent or the clay is exfoliated in an aqueous environment via sonication. The oxidant is then added, followed by pyrrole monomer which polymerizes and is deposited on the flake surface. Often times the flakes need to be modified by

exchanging the sodium or potassium ions that are intercalated in the structures with organic cations such as an alkyl ammonium ion which causes the flakes to have an organophilic character. The alkyl moiety could be caprolactam, vinyl pyrollidone, or any other moiety that has some affinity for polypyrrole. Typically these composites exhibit fairly low conductivity. One such composite had a conductivity of $1.2 \times 10^{-2}$ S/cm. Despite this low conductivity however, these composites materials have been shown to inhibit corrosion inhibit corrosion. On a sample of cold rolled steel in a 5% NaCl solution by weight, the composite was able to reduce the corrosion rate of the steel down to 0.044 mils/year.[67-90]

**Montmorillonite Clay Structure**

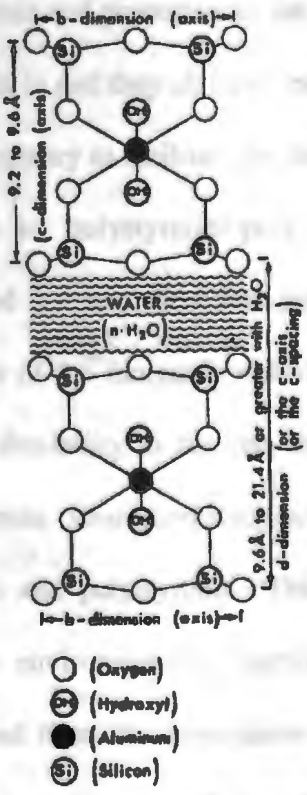


Figure 1.18. The structure of montmorillonite clay.[91]

*Reproduced from Lipids in Health and Disease an open access publication.*

Graphite oxide is another lamellar material that can form polypyrrole composites. The polypyrrole tends to form in the gallery spaces between the graphite oxide sheets and the polymerization process can result in exfoliation of the graphite. This served to increase the conductivity of the graphite oxide and tended to make a stable and completely exfoliated composite dispersion.[92]

Other inorganic materials that have been used in composite materials with polypyrrole include zirconium oxide, tin (IV) oxide, alumina, manganese (IV) oxide, zinc phosphate, and titanium dioxide. PPY composite with zirconium oxide are interesting because they can exhibit higher conductivities at room temperature than pure polypyrrole. All of these materials give different end properties to the composite depending on what the ratio of materials in the composite is and they all have special synthetic considerations such as surface treatments that are necessary to facilitate the deposition of polypyrrole.[93-100]

Organic materials, such as polystyrene, poly methyl methacrylate, and other commodity plastics, are also used in composites with polypyrrole. Organic materials tend to be more expensive than some of the inorganic materials but have the added benefit of imparting some toughness and flexibility to the end composites as opposed to the high modulus, brittle, inorganic materials. One interesting technique uses supercritical $CO_2$ as a solvent to combine polypyrrole and polystyrene. This is a very interesting technique because it is trying to replace environmentally harmful organic solvents with carbon dioxide which can be sequestered from the atmosphere and then released again after the reaction. As a synthesis technique, this approach was quite successful. Images of the pristine polystyrene, the undoped polypyrrole-polystyrene composite, and the doped composite can be seen in Figure 1.19.[101]

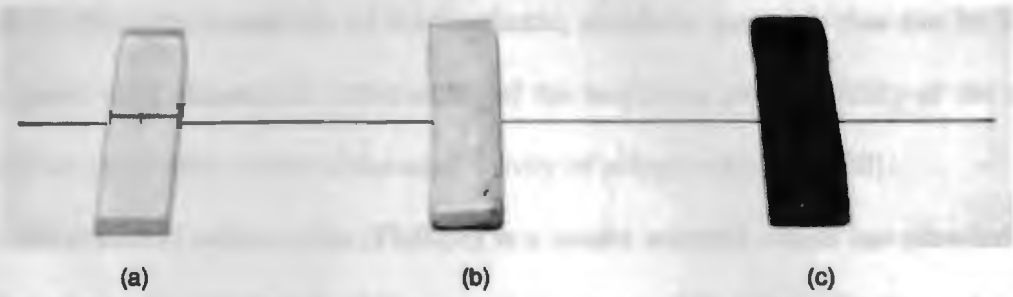


Figure 1.19. An image of a) the polystyrene matrix, b) the undoped PPY composite, c) the doped composite.[101]

*Reprinted from European Polymer Journal, 39(1), Tang M., Wen T., Du T., and Chen Y., Synthesis of electrically conductive polypyrrole-polystyrene composites using supercritical carbon dioxide:: I. Effects of the blending condition: p. 143-149. 2003 with permission from Elsevier.*

As can be seen, the polypyrrole is readily doped when exposed to anions which results in the color change from white to black as the polypyrrole band gap decreases. A bulk conductivity of $1.12 \times 10^{-2}$ was reported for this material. The mechanical properties of these materials were not studied in this paper but they are most certainly an improvement over the properties of pure polypyrrole. It is also likely that this technique would be applicable with other polymers which could give different properties based on their composition.[101-102]

Compression molding and extrusion are two other processing methods that can be used when forming composite materials using polypyrrole and commodity plastics. For compression molding, matrix particles are first coated with polypyrrole via an aqueous reaction, the particles are then compression molded into various shapes including smooth films at an elevated temperature. Conductivities of up 0.1 S/cm were observed for composites made using this method with polyethylene, polypropylene, or poly methyl methacrylate as the matrix. It was also noted that the conductivity of composites formed in

this way exhibited a decreased sensitivity to temperature. This is a useful technique because it offers the possibility of thermoplastic, moldable materials that can be formed into a great many shapes and retain much of the toughness and flexibility of the matrix material but yet displays some of the conductivity of polypyrrole.[103-109]

Poly methyl methacrylate (PMMA) is a matrix material which has attracted some attention due to its exterior durability and resistance to UV light. Coating polypyrrole nanospheres with a PMMA shell only a few nanometers thick to compatibilize the PPY to a PMMA matrix through a microemulsion technique was found to increase the conductivity of cast films of PMMA containing the nanoparticles. Conductivities of 0.5 S/cm were achieved for the films. Furthermore, it was found that because of the much lower glass transition temperature of the PMMA, the particles could be annealed to cause the PMMA shells to attach PPY particles together to form conducting networks prior to incorporation into a PMMA film.[110]

Hydrogel materials can be synthesized by first synthesizing a polypyrrole colloid and then adding it, through sonication, to a hydrogel solution in ethanol. This mixture is then viscous enough to be extruded to further mix the materials and manufacture whatever cross sectional shape is required for a hydrogel part. This material can then be crosslinked in an oven to keep it from deforming. These materials have some possible applications as components for artificial muscles and other areas where a polymer needs to respond to an electrical signal. It is also possible to form gels that are thermally sensitive by using poly(N-vinylcaprolactam-co-acetoacetoxyethyl methacrylate) as the gel polymer. These materials have many applications where a responsive system is required. Other polymers

such as polyvinyl alcohol, and polyvinyl pyrrolidine, that are not gels, have also been used to form composites with polypyrrole colloids.[111-112]

Emulsion chemistry is also used in the synthesis of PPY composite materials. The incorporation of PPY and elastomers is one technique that can produce materials with some surprising properties. Through a reverse emulsion polymerization with a styrene-isoprene copolymer, a material that could be compression molded at 150° C could be made. Depending on the amount of surfactant in the reaction, a material with a conductivity of 2.7 S/cm, tensile strength of 12.2 MPa, and an elongation at break of 204% could be synthesized. Other polymers with which this technique has been used include polyurethanes, poly(ethylene-*co*-vinyl acetate), polydimethylsiloxane, and polyethylene. Polylactide was used to create a biodegradable composite, through an emulsion pathway, in an effort to decrease the environmental impact of a composite.[113-119]

Polymerization of pyrrole vapor that has diffused into a matrix polymer containing an oxidizing agent is a more obscure yet interesting technique. This has been done with polymers such as polyvinyl alcohol and polyimides. This could be a way to eliminate the problem of hazardous solvents in the production of polymer films. The only problem with this method that would possibly be an impedance to industrial application is that an inordinate amount of time is needed for the pyrrole vapors to diffuse into the matrix and be polymerized. This is usually longer than 24 hours. Heating the matrix and the space surrounding it above the glass transition temperature of the matrix could help speed this process by increasing the diffusion rate of pyrrole monomer and the permeability of the matrix polymer. However, this would result in annealing of the matrix polymer and, depending on the amount of time required to complete the reaction, changes in the

mechanical properties of the matrix polymer may become apparent. Depending on the application in which the polymer composite is being used, this may or may not be a problem.[120-121]

## 1.6. Conclusion

Three general strategies for augmenting the properties of polypyrrole to make its use more practical and in some cases environmentally friendly have been discussed. These are the alteration of the chemical structure of pyrrole, the use of dopant ions, and the incorporation of polypyrrole into composite materials. Each method has its strengths and weaknesses and has the potential to impart different properties to the polypyrrole that the other methods cannot. Each must be evaluated on a case by case basis for specific applications.

The objective of this study was to successfully deposit polypyrrole onto an aluminum flake pigment to form a PPY/Al flake composite pigment, and to determine if this pigment was capable of inhibiting corrosion on aluminum alloy 2024 T3. In the first phase of this study, different phenolic compounds and dopants were investigated for their ability to aid in the deposition of polypyrrole onto the Al flake due to interactions with the aluminum oxide layer on the surface of the flake. Once it had been established, through characterization of the flake, that conductive polypyrrole was in fact being deposited onto the surface of the aluminum flake, and that the corrosion inhibiting dopants were incorporated into the polypyrrole, the second phase of the study investigated the corrosion inhibiting properties of the differently doped pigments. The organization of this thesis roughly follows these two phases of the study chronologically. The second chapter is the

methods and materials section outlining what materials were used and what procedures were carried out during the study. The third chapter describes the synthesis of the composite pigments and the characterization of the pigments proving that polypyrrole was deposited. The fourth chapter describes the evaluation of the synthesized pigments as corrosion inhibitors and what effect the different dopants had on their performance as well as a conclusion reviewing the major findings of this study and a section outlining work that could be done in the future.

## 1.7. References


1. Cusack P. and Perrett T., *The EU RoHS Directive and its implications for the plastics industry.* Plastics, Additives and Compounding, 2006. **8**(3): p. 46-49.
2. Frankel G. S. and McCreery R. L., *Inhibition of Al Alloy Corrosion by Chromates.* The Electrochemical Society: Interface, 2001: p. 34-48.
3. McNeill R., Siudak R., Wardlaw J. H., and Weiss D. E., *Electronic Conduction in Polymers. I. The Chemical Structure of Polypyrrole.* Australian Journal of chemistry, 1963. **16**(6): p. 1056-1075.
4. Bolto B. A. and Weiss D. E., *Electronic Conduction in Polymers. II. The Electrochemical Reduction of Polypyrrole at Controlled Potential.* Australian Journal of Chemistry, 1963. **16**: p. 1076-1089.
5. Bolto B. A., McNeill R., and Weiss D. E., *Electronic Conduction in Polymers III. Electronic Properties of Polypyrrole.* Aust. J. Chem, 1963. **16**: p. 1090-1103.
6. Shirakawa H., Louis E., Macdiarmid A., Chiang C., and Heeger A., *Syntheis of Electrically Conducting Polymers-Halogen Derivatives of Polyacetylene.* J.C.S. Chem. Comm., 1977(16): p. 578-580.
7. Epstein A. J., Mele E. J., and Editors., *The Nobel Prize in Chemistry, 2000: Conductive polymers.* Synthetic Metals, 2001. **125**(1): p. 138.
8. Bredas J. L. and Street G. B., *Polarons, bipolarons, and solitons in conducting polymers.* Accounts of Chemical Research, 1985. **18**(10): p. 309-315.
9. Walczak R., Leonard J., and Reynolds J., *Processable, Electroactive, and Aqueous Compatible Poly (3, 4-alkylenedioxypyrrole) s through a Functionally Tolerant Deiodination Condensation Polymerization.* Macromolecules, 2008. **41**(3): p. 691-700.
10. Wang W., Yu D., and Tian F., *Synthesis and characterization of a new polypyrrole based on N-vinyl pyrrole.* Synthetic Metals, 2008. **158**(17-18): p. 717-721.
11. Stanke D., Hallensleben M., and Toppare L., *Graft copolymers and composites of poly (methyl methacrylate) and polypyrrole Part I.* Synthetic Metals, 1995. **72**(1): p. 89-94.

12. Balci N., Akbulut U., Toppare L., Stanke D., and Hallensleben M., *Polypyrrole grafts with poly [(methyl methacrylate)-co-(2-(N-pyrrolyl) ethyl methacrylate)].* Materials Research Bulletin, 1997. **32**(10): p. 1449-1458.
13. Ng S., Chan H., Xia J., and Yu W., *Electrically conductive graft copolymers of poly (methyl methacrylate) with varying polypyrrole and poly (3-alkylpyrroles) contents.* Journal of Materials Chemistry, 1998. **8**(11): p. 2347-2352.
14. Alkan S., Toppare L., Hepuzer Y., and Yagci Y., *Block copolymers of thiophene-capped poly (methyl methacrylate) with pyrrole.* Journal of Polymer Science Part A Polymer Chemistry, 1999. **37**: p. 4218-4225.
15. Cirpan A., Alkan S., Toppare L., Hepuzer Y., and Yagci Y., *Conducting graft copolymers of poly (3-methylthienyl methacrylate) with pyrrole and thiophene.* Journal of Polymer Science Part A Polymer Chemistry, 2002. **40**(23): p. 4131-4140.
16. Guner Y., Toppare L., Hepuzer Y., and Yagci Y., *Conducting graft copolymers of pyrrole and thiophene with random copolymers of methyl methacrylate and 3-methylthienyl methacrylate.* European Polymer Journal, 2004. **40**(8): p. 1799-1806.
17. Park Y. and Park S., *Preparation and electroactivity of poly (methyl methacrylate-co-pyrrolylmethylstyrene)–g-polypyrrole.* Synthetic Metals, 2002. **128**(2): p. 229-234.
18. Mecerreyes D., Pomposo J., Bengoetxea M., and Grande H., *Novel pyrrole end-functional macromonomers prepared by ring-opening and atom-transfer radical polymerizations.* Macromolecules, 2000. **33**(16): p. 5846-5849.
19. Stanke D., Hallensleben M., and Toppare L., *Electrically conductive poly (methyl methacrylate-g-pyrrole) via chemical oxidative polymerization.* Synthetic Metals, 1993. **55**(2-3): p. 1108-1113.
20. Ruckenstein E. and Yang S., *Processable conductive polypyrrole/poly (alkyl methacrylate) composite prepared by an emulsion pathway.* Polymer(Guildford), 1993. **34**(22): p. 4655-4660.
21. Xia Y., Su Q., and Lu Y., *Synthesis and application of conducting graft copolymer with viable processability.* Polymer, 2009. **50**(21): p. 5065-5070.
22. Arsalani N. and Geckeler K., *Novel electrically conducting polymer hybrids with polypyrrole.* Reactive and Functional Polymers, 1997. **33**(2-3): p. 167-172.
23. Mecerreyes D., Stevens R., Nguyen C., Pomposo J., Bengoetxea M., and Grande H., *Synthesis and characterization of polypyrrole-graft-poly ( -caprolactone) copolymers: new electrically conductive nanocomposites.* Synthetic Metals, 2002. **126**(2-3): p. 173-178.
24. Stanke D., Hallensleben M., and Toppare L., *Oxidative polymerization of some N-alkylpyrroles with ferric chloride.* Synthetic Metals, 1995. **73**(3): p. 267-272.
25. Van Dijk H., Aagaard O., and Schellekens R., *Precursor monomer route: a novel concept for producing highly conductive polypyrrole films.* Synthetic Metals, 1993. **55**(2-3): p. 1085-1090.
26. Ashraf S., Chen F., Too C., and Wallace G., *Bulk electropolymerization of alkylpyrroles.* Polymer, 1996. **37**(13): p. 2811-2819.
27. Gelling V., Wiest M., Tallman D., Bierwagen G., and Wallace G., *Electroactive-conducting polymers for corrosion control - 4. Studies of poly(3-octyl pyrrole) and poly(3-octadecyl pyrrole) on aluminum 2024-T3 alloy.* Progress in Organic Coatings, 2001. **43**(1-3): p. 149-157.

28. Masuda H., Tanaka S., and Kaeriyama K., *Preparation of poly (3-octylpyrrole) by oxidative coupling.* Synthetic Metals, 1989. **33**(3): p. 365-372.
29. Guernion N., de Lacy Costello B., and Ratcliffe N., *The synthesis of 3-octadecyl- and 3-docosylpyrrole, their polymerisation and incorporation into novel composite gas sensitive resistors.* Synthetic Metals, 2002. **128**(2): p. 139-147.
30. Audebert P., Aldebert P., Girault N., and Kaneko T., *Soluble and film-forming substituted polypyrroles from pyrrole monomers substituted in the 3-and 4-positions by alkyl and ester groups.* Synthetic Metals, 1993. **53**(3): p. 251-262.
31. Li X., Huang M., Wang L., Zhu M., Menner A., and Springer J., *Synthesis and characterization of pyrrole and m-toluidine copolymers.* Synthetic Metals, 2001. **123**(3): p. 435-441.
32. Li X., Wang L., Huang M., Lu Y., Zhu M., Menner A., and Springer J., *Synthesis and characterization of pyrrole and anisidine copolymers.* Polymer, 2001. **42**(14): p. 6095-6103.
33. K z lcan N., Ustamehmeto lu B., Oez N., Sezai Sarac A., and Akar A., *Soluble and conductive polypyrrole copolymers containing silicone tegomers.* Journal of Applied Polymer Science, 2003. **89**(11): p. 2896-2901.
34. K z lcan N., Öz N., Ustamehmeto lu B., and Akar A., *High conductive copolymers of polypyrrole- , -diamine polydimethylsiloxane.* European Polymer Journal, 2006. **42**(10): p. 2361-2368.
35. Cho G., Jang J., Moon I., Lee J., and Glatzhofer D., *Enhanced adhesion of polypyrrole film through a novel grafting method.* Journal of Materials Chemistry, 1999. **9**(2): p. 345-347.
36. Arslan A., Türkarslan Ö., Tanyeli C., Akhmedov M., and Toppare L., *Electrochromic properties of a soluble conducting polymer: Poly (1-(4-fluorophenyl)-2, 5-di (thiophen-2-yl)-1H-pyrrole).* Materials Chemistry & Physics, 2007. **104**(2-3): p. 410-416.
37. Yigitsoy B., Varis S., Tanyeli C., Akhmedov I., and Toppare L., *A soluble conducting polymer of 2, 5-di (thiophen-2-yl)-1-p-tolyl-1H-pyrrole and its electrochromic device.* Thin Solid Films, 2007. **515**(7-8): p. 3898-3904.
38. Havinga E., Horssen L., Hoeve W., Wynberg H., and Meijer E., *Self-doped water-soluble conducting polymers.* Polymer Bulletin, 1987. **18**(3): p. 277-281.
39. Peres R., Pernaut J., and De Paoli M., *Properties of poly (pyrrole) films electrochemically synthesized in the presence of surfactants.* Synthetic Metals, 1989. **28**(1-2): p. 59-64.
40. Song M., Kim Y., Kim B., Kim J., Char K., and Rhee H., *Synthesis and characterization of soluble polypyrrole doped with alkylbenzenesulfonic acids.* Synthetic Metals, 2004. **141**(3): p. 315-319.
41. Joo J., Lee J., Baeck J., Kim K., Oh E., and Epstein J., *Electrical, magnetic, and structural properties of chemically and electrochemically synthesized polypyrroles.* Synthetic Metals, 2001. **117**(1-3): p. 45-51.
42. G. P. Triberis X. Z., A. N. Yannacopoulos and V. C. Karavolas *The effect of the density of states on the conductivity of the small-polaron hopping regime in disordered systems* Journal of Physics: Condensed Matter 1991. **3**(3): p. 337.

43. Bay L., Mogensen N., Skaarup S., Sommer-Larsen P., Jorgensen M., and West K., *Polypyrrole doped with alkyl benzenesulfonates.* Macromolecules, 2002. **35**(25): p. 9345-9351.
44. Ikeda R., Tanaka H., Uyama H., and Kobayashi S., *A new crosslinkable polyphenol from a renewable resource.* Macromolecular Rapid Communications, 2000. **21**(8): p. 496-499.
45. Antony M. and Jayakannan M., *Amphiphilic azobenzenesulfonic acid anionic surfactant for water-soluble, ordered, and luminescent polypyrrole nanospheres.* J. Phys. Chem. B, 2007. **111**(44): p. 12772-12780.
46. Kumar P. P., Paramashivappa R., Vithayathil P. J., Rao P. V. S., and Rao A. S., *Process for isolation of cardanol from technical cashew (Anacardium occidentale L.) nut shell liquid.* J. Agric. Food Chem, 2002. **50**(16): p. 4705-4708.
47. Nabid M. and Entezami A., *A novel method for synthesis of water-soluble polypyrrole with horseradish peroxidase enzyme.* Journal of Applied Polymer Science, 2004. **94**(1): p. 254-258.
48. Lee J., Song K., Kim S., Kim Y., Kim D., and Kim C., *Synthesis and characterization of soluble polypyrrole.* Synthetic Metals, 1997. **84**(1-3): p. 137-140.
49. Lee G., Lee S., Ahn K., and Kim K., *Synthesis and characterization of soluble polypyrrole with improved electrical conductivity.* Journal of Applied Polymer Science, 2002. **84**(14): p. 2583-2590.
50. Lee Y., Lee J., and Lee D., *A novel conducting soluble polypyrrole composite with a polymeric co-dopant.* Synthetic Metals, 2000. **114**(3): p. 347-353.
51. Oh E., Jang K., Suh J., and Yo C., *Synthesis and characteristics of soluble polypyrroles with mixed dopants.* Molecular Crystals and Liquid Crystals, 1999. **337**(1): p. 101-104.
52. Shen Y. and Wan M., *Soluble conducting polypyrrole doped with DBSA-CSA mixed acid.* Journal of Applied Polymer Science, 1998. **68**(8): p. 1277-1284.
53. Aleshin A., Lee K., Lee J., Kim D., and Kim C., *Comparison of electronic transport properties of soluble polypyrrole and soluble polyaniline doped with dodecylbenzene-sulfonic acid.* Synthetic Metals, 1999. **99**(1): p. 27-33.
54. Lee J., Kim D., and Kim C., *Synthesis of soluble polypyrrole of the doped state in organic solvents.* Synthetic Metals, 1995. **74**(2): p. 103-106.
55. Jang K., Lee H., and Moon B., *Synthesis and characterization of water soluble polypyrrole doped with functional dopants.* Synthetic Metals, 2004. **143**(3): p. 289-294.
56. Oh E., Jang K., and MacDiarmid A., *High molecular weight soluble polypyrrole.* Synthetic Metals, 2002. **125**(3): p. 267-272.
57. Shen Y. and Wan M., *Soluble conductive polypyrrole synthesized by in situ doping with beta-naphthalene sulphonic acid.* Journal of Polymer Science Part A: Polymer Chemistry, 1997. **35**(17): p. 3689-3695.
58. Liu J., Wang X., Hu X., Xiao A., and Wan M., *Studies of influence of naphthalene mono/disulfonic acid dopant on thermal stability of polypyrrole.* Journal of Applied Polymer Science, 2008. **109**(2): p. 997-1001.
59. Liu J. and Wan M., *Polypyrrole doped with 1, 5-naphthalenedisulfonic acid.* Synthetic Metals, 2001. **124**(2-3): p. 317-321.

60. Wernet W., *Thermoplastic and elastic conducting polypyrrole films.* Synthetic Metals, 1991. **41**(3): p. 843-848.
61. Nagaoka T., Nakao H., Suyama T., Ogura K., Oyama M., and Okazaki S., *Electrochemical characterization of soluble conducting polymers as ion exchangers.* Anal. Chem, 1997. **69**(6): p. 1030-1037.
62. Rohwerder M. and Michalik A., *Conducting polymers for corrosion protection: What makes the difference between failure and success?* Electrochemica Acta, 2007. **53**(3): p. 1300-1313.
63. Hollaway L., ed. *Handbook of polymer composites for engineers.* 1994, CRC: Cambridge, England.
64. Skotheim T. and Reynolds J., *Handbook of conducting polymers.* 2007, New York: CRC Press.
65. Lascelles S., McCarthy G., Butterworth M., and Armes S., *Effect of synthesis parameters on the particle size, composition and colloid stability of polypyrrole–silica nanocomposite particles.* Colloid & Polymer Science, 1998. **276**(10): p. 893-902.
66. Yang X., Dai T., and Lu Y., *Synthesis of novel sunflower-like silica/polypyrrole nanocomposites via self-assembly polymerization.* Polymer, 2006. **47**(1): p. 441-447.
67. Yeh J., Chin C., and Chang S., *Enhanced corrosion protection coatings prepared from soluble electronically conductive polypyrrole-clay nanocomposite materials.* journal of Applied Polymer Science, 2003. **88**(14): p. 3264-3272.
68. Boukerma K., Piquemal J., Chehimi M., Mravcáková M., Omastová M., and Beaunier P., *Synthesis and interfacial properties of montmorillonite/polypyrrole nanocomposites.* Polymer, 2006. **47**(2): p. 569-576.
69. Park D., Sung J., Lim S., Choi H., and Jhon M., *Synthesis and characterization of soluble polypyrrole and polypyrrole/organoclay nanocomposites.* Journal of Materials Science Letters, 2003. **22**(18): p. 1299-1302.
70. Mravcáková M., Boukerma K., Omastová M., and Chehimi M., *Montmorillonite/polypyrrole nanocomposites. The effect of organic modification of clay on the chemical and electrical properties.* Materials Science and Engineering: C, 2006. **26**(2-3): p. 306-313.
71. Shakoor A., Anwar H., and Rizvi T., *Preparation, Characterization and Conductivity Study of Polypyrrole-Pillared Clay Nanocomposites.* Journal of Composite Materials, 2008. **42**(20): p. 2101.
72. Liu Y. and Tsai C., *Enhancements in conductivity and thermal and conductive stabilities of electropolymerized polypyrrole with caprolactam-modified clay.* Synth. Met, 1985. **10**: p. 303.
73. Anuar K., Murali S., Fariz A., and Ekramul H., *Conducting Polymer/Clay Composites: Preparation and Characterization.* Materials Science, 2004. **10**: p. 255-258.
74. Liu Y. and Ger M., *Modification of electropolymerized polypyrrole with Na+-montmorillonite.* Chemical Physics Letters, 2002. **362**(5-6): p. 491-496.
75. Faguy P., Ma W., and Lowe J., *Conducting polymer-clay composites for electrochemical applications.* Journal of Materials Chemistry, 1994. **4**(5): p. 771-772.

76. Fang F. and Choi H., *Shear Stress Analysis of a Polypyrrole/Clay Nanocomposite-based Electrorheological Fluid.* Journal of Industrial and Engineering Chemistry, 2006. **12**(6): p. 843-845.
77. Bae W., Kim K., Jo W., and Park Y., *Fully exfoliated nanocomposite from polypyrrole graft copolymer/clay.* Polymer, 2005. **46**(23): p. 10085-10091.
78. Hong S., Kim B., Joo J., Kim J., and Choi H., *Polypyrrole-montmorillonite nanocomposites synthesized by emulsion polymerization* 1.* Current Applied Physics, 2001. **1**(6): p. 447-450.
79. Leta ef S., Aranda P., and Ruiz-Hitzky E., *Influence of iron in the formation of conductive polypyrrole-clay nanocomposites.* Applied Clay Science, 2005. **28**(1-4): p. 183-198.
80. SinhaRay S. and Biswas M., *Preparation and evaluation of composites from montmorillonite and some heterocyclic polymers: 3. a water dispersible nanocomposite from pyrrole-montmorillonite polymerization system.* Materials Research Bulletin, 1999. **34**(8): p. 1187-1194.
81. Kim J., Liu F., Choi H., Hong S., and Joo J., *Intercalated polypyrrole/Na+-montmorillonite nanocomposite via an inverted emulsion pathway method.* Polymer, 2003. **44**(1): p. 289-293.
82. Kim B., Hong S., Joo J., Park I., Epstein A., Kim J., and Choi H., *Electron spin resonance signal of nanocomposite of conducting polypyrrole with inorganic clay.* Journal of Applied Physics, 2004. **95**: p. 2697.
83. Krishantha D., Rajapakse R., Tennakoon D., and Dias H., *Polypyrrole-Montmorillonite Nanocomposite: A Composite Fast Ion Conductor.* Journal of Composite Materials, 2005.
84. Omastová M., Mrav, and cbreve M., *Conductive polypropylene/clay/polypyrrole nanocomposites.* Polymer Engineering & Science, 2006. **46**(8): p. 1069-1078.
85. Mrav and ccaron M., *Poly (propylene)/montmorillonite/polypyrrole composites: structure and conductivity.* Polymers for Advanced Technologies, 2006. **17**(9-10): p. 715-726.
86. Jun X., Xing-rong Z., Peng L., Hui-ping D., and Hai-xia S., *Preparation and Conductivity of Polypyrrole/Silica Composite* Chemistry and Adhesion, 2005. **1**.
87. Mravcáková M., Omastová M., Olejníková K., Pukánszky B., and Chehimi M., *The preparation and properties of sodium and organomodified-montmorillonite/polypyrrole composites: A comparative study.* Synthetic Metals, 2007. **157**(8-9): p. 347-357.
88. Peighambardoust S. and Pourabbas B. *Synthesis and Characterization of Conductive Polypyrrole/Montmorillonite Nanocomposites via One-pot Emulsion Polymerization.* 2007: John Wiley & Sons.
89. Ruiz-Hitzky E. and Van Meerbeek A., *.3 Clay Mineral-and Organoclay-Polymer Nanocomposite.* Developments in Clay Science, 2006: p. 583-621.
90. Ramírez-Valle V., Lerf A., Wagner F., Poyato J., and Pérez-Rodríguez J., *Thermal study of polypyrrole complexes with vermiculites of different layer charge.* Journal of thermal analysis and calorimetry, 2008. **92**(1): p. 43-51.
91. Sivak O., Darlington J., Gershkovich P., Constantinides P., and Wasan K., *Protonated nanostructured aluminosilicate(NSAS) reduces plasma cholesterol concentrations and atherosclerotic lesions in Apolipoprotein E deficient mice fed a*

*high cholesterol and high fat diet.* Lipids in Health and Disease, 2009. **8**(1): p. 30-35.
92. Han Y. and Lu Y., *Characterization and electrical properties of conductive polymer/colloidal graphite oxide nanocomposites.* Composites Science and Technology, 2009. **69**(7-8): p. 1231-1237.
93. Bhattacharya A., Ganguly K., De A., and Sarkar S., *A new conducting nanocomposite--PPy-zirconium (IV) oxide.* Materials Research Bulletin, 1996. **31**(5): p. 527-530.
94. Maeda S. and Ames S., *Preparation and characterization of polypyrrole-Tin (IV) oxide nanocomposite colloids.* Chemistry of Materials, 1995. **7**(1): p. 171-178.
95. Tallman D., Levine K., Siripirom C., Gelling V., Bierwagen G., and Croll S., *Nanocomposite of polypyrrole and alumina nanoparticles as a coating filler for the corrosion protection of aluminium alloy 2024-T3.* Applied Surface Science, 2008. **254**(17): p. 5452-5459.
96. Biswas M. and Ray S., *Water dispersible conducting nanocomposites of poly (N-vinylcarbazole), polypyrrole and polyaniline with nanodimensional manganese (IV) oxide.* Synthetic Metals, 1999. **105**(2): p. 99-105.
97. Sinha Ray S., *Synthesis and evaluation of conducting polypyrrole/Al2O3 nanocomposites in aqueous and non-aqueous medium.* Materials Research Bulletin, 2002. **37**(5): p. 813-824.
98. Su S. and Kuramoto N., *Processable polyaniline-titanium dioxide nanocomposites: effect of titanium dioxide on the conductivity.* Synthetic Metals, 2000. **114**(2): p. 147-153.
99. Lenz D., Delamar M., and Ferreira C., *Application of polypyrrole/TiO2 composite films as corrosion protection of mild steel.* Journal of Electroanalytical Chemistry, 2003. **540**: p. 35-44.
100. Lenz D., Ferreira C., and Delamar M., *Distribution analysis of TiO2 and commercial zinc phosphate in polypyrrole matrix by XPS.* Synthetic Metals, 2002. **126**(2-3): p. 179-182.
101. Tang M., Wen T., Du T., and Chen Y., *Synthesis of electrically conductive polypyrrole-polystyrene composites using supercritical carbon dioxide:: I. Effects of the blending conditions.* European Polymer Journal, 2003. **39**(1): p. 143-149.
102. Teja A. and Webb K., *In Situ Blending of Electrically Conducting Polymers in Supercritical Carbon Dioxide.* Supercritical fluid technology in materials science and engineering: syntheses, properties, and applications, 2002: p. 285.
103. Omastova M., Pavlinec J., Pionteck J., and Simon F., *Synthesis, electrical properties and stability of polypyrrole-containing conducting polymer composites.* Polymer International, 1997. **43**(2): p. 109-116.
104. Omastová M., Kosina S., Pionteck J., Janke A., and Pavlinec J., *Electrical properties and stability of polypyrrole containing conducting polymer composites.* Synthetic Metals, 1996. **81**(1): p. 49-57.
105. Yoshino K., Yin X., Morita S., Nakanishi Y., Nakagawa S., Yamamoto H., Watanuki T., and Isa I., *Preparation and Electrical Property of Polypyrrole-Polyethylene Composite.* Jpn. J. Appi. Phys. Vol, 1993. **32**(2 Pt 1): p. 979-981.

106. Yoshino K., Morita S., Yin X., Onoda M., Yamamoto H., Watanuki T., and Isa I., *Electrical property of polypyrrole-insulating polymer composite.* Synthetic Metals, 1993. **57**(1): p. 3562-3565.
107. Ruckenstein E. and Yang S., *Processable conductive polypyrrole/poly (alkyl methacrylate) composites prepared by an emulsion pathway.* Polymer, 1993. **34**(22): p. 4655-4660.
108. Omastová M., Pavlinec J., Pionteck J., Simon F., and Kosina S., *Chemical preparation and characterization of conductive poly (methyl methacrylate)/polypyrrole composites.* Polymer-London-, 1998. **39**: p. 6559-6566.
109. Cairns D., Khan M., Perruchot C., Riede A., and Armes S., *Synthesis and characterization of polypyrrole-coated poly (alkyl methacrylate) latex particles.* Chem. Mater., 2003. **15**(1): p. 233-239.
110. Jang J. and Oh J., *Fabrication of a highly transparent conductive thin film from polypyrrole/poly (methyl methacrylate) core/shell nanospheres.* Advanced Functional Materials, 2005. **15**(3): p. 494-502.
111. Kim B., Spinks G., Too C., Wallace G., and Bae Y., *Preparation and characterisation of processable conducting polymer-hydrogel composites.* Reactive and Functional Polymers, 2000. **44**(1): p. 31-40.
112. Boyko V., Pich A., Lu Y., Richter S., Arndt K., and Adler H., *Thermo-sensitive poly (N-vinylcaprolactam-co-acetoacetoxyethyl methacrylate) microgels: 1-- synthesis and characterization.* Polymer, 2003. **44**(26): p. 7821-7827.
113. Sun Y. and Ruckenstein E., *Polypyrrole-bearing conductive composite prepared by an inverted emulsion pathway involving nonionic surfactants.* Synthetic Metals, 1995. **72**(3): p. 261-267.
114. Ruckenstein E. and Hong L., *Inverted emulsion pathway to polypyrrole and polypyrrole elastomer composites.* Synthetic Metals, 1994. **66**(3): p. 249-256.
115. Yang S. and Ruckenstein E., *Preparation and mechanical properties of electrically conductive polypyrrole-poly (ethylene-co-vinyl acetate) composites.* Synthetic Metals, 1993. **60**(3): p. 249-254.
116. Zhou D., Subramaniam S., and Mark J., *In situ Synthesis of Polyaniline in Poly (dimethylsiloxane) Networks Using an Inverse Emulsion Route.* Journal of Macromolecular Science, Part A, 2005. **42**(2): p. 113-126.
117. Ruckenstein E. and Chen J., *Polypyrrole conductive composites prepared by coprecipitation.* Polymer, 1991. **32**(7): p. 1230-1235.
118. Shi G., Rouabhia M., Wang Z., Dao L., and Zhang Z., *A novel electrically conductive and biodegradable composite made of polypyrrole nanoparticles and polylactide.* Biomaterials, 2004. **25**(13): p. 2477-2488.
119. Wang Z., Roberge C., Dao L., Wan Y., Shi G., Rouabhia M., Guidoin R., and Zhang Z., *In vivo evaluation of a novel electrically conductive polypyrrole/poly (D, L-lactide) composite and polypyrrole-coated poly (D, L-lactide-co-glycolide) membranes.* Journal of Biomedical Materials Research Part A, 2004. **70**(1): p. 28-38.
120. Ojio T. and Miyata S., *Highly transparent and conducting polypyrrole–poly (vinyl alcohol) composite films prepared by gas state polymerization.* Polymer Journal, 1986. **18**(1): p. 95-98.

121. Iroh J. O., et al., *Electrochemical behaviour of conducting polymer/polyimide composite.* Surface Engineering, 2004. **20**(2): p. 93-98.

# CHAPTER 2.

# MATERIALS AND METHODS

Most chemicals were used as received such as catechol (TCI America); ammonium persulfate, phloroglucide, and phloroglucinol (Sigma-Aldrich); ethanol, sodium molybdate dihydrate, sodium stannate dihydrate, and tetrachloroethylene (J.T. Baker); epon 828 and epikure 3175 (Hexion); methyl isobutyl ketone (Aqua Solutions); resorcinol (MP Biomedicals); monobasic sodium phosphate (BDH); methyl ethyl ketone and sodium metavanadate (Alfa Aesar). The aluminum flake used was an automotive pigment, Stapa Aloxal PM 2010 (Eckhart America). The pyrrole monomer (TCI America) was distilled before use.

The procedure for the synthesis of the polypyrrole/aluminum flake composite pigment proceeded as follows, as is detailed in Table 2.1 and Figure 2.1: 3g of aluminum flake was dispersed into 100 ml of 18.2 MΩ Millipore water. To this, 4.56g of ammonium persulfate (APS) was added, followed by one or more phenolic compounds and then pyrrole was added. This mixture was allowed to stir for 24 hours at which point the product was filtered and washed with at least 150 mL of 18.2 MΩ Millipore water. The PPY/Al flake composite was then placed in an oven and allowed to dry for 24 hours at 60° C. Once the PPY/Al flake composite had dried, it was ground using a mortar and pestle and passed through a 106-μm sieve, which was obtained from VWR.

The composites that were doped with corrosion inhibiting anions were prepared in a similar reaction, with minor differences. The amounts of reactants used for the different reactions can be seen in Table 2.2. In the reactions containing sodium phosphate, sodium

molybdate, or sodium stannate, half of the total amount of corrosion inhibiting salt that was soluble in water at 25° C was used in the reaction. In the case of sodium vanadate, a saturated solution was used due to its lower solubility in water. Such high concentrations were used to increase the probability that the corrosion inhibiting ions would be incorporated into the polypyrrole instead of the competing sulfate ions produced by the reduction of the ammonium persulfate initiator.

Table 2.1. Synthesis reactions for PPY/Al flake composite pigments. Shaded area denotes lack of chemical in the synthesis.

| Reaction # | Catechol (M) | Phloroglucide (M) | Phloroglucinol (M) | Resorcinol (M) | Pyrrole (M) | Phenol + Pyrrole Concentration (M) |
|---|---|---|---|---|---|---|
| 1 | 0.10 | 0.00 | 0.00 | 0.00 | 0.10 | 0.20 |
| 1x | 0.20 | 0.00 | 0.00 | 0.00 | 0.20 | 0.40 |
| 2 | 0.10 | 0.10 | 0.00 | 0.00 | 0.20 | 0.40 |
| 3 | 0.00 | 0.10 | 0.00 | 0.00 | 0.10 | 0.20 |
| 4 | 0.00 | 0.00 | 0.10 | 0.00 | 0.10 | 0.20 |
| 4x | 0.00 | 0.00 | 0.20 | 0.00 | 0.20 | 0.40 |
| 5 | 0.10 | 0.00 | 0.00 | 0.10 | 0.20 | 0.40 |
| 6 | 0.00 | 0.00 | 0.00 | 0.10 | 0.10 | 0.20 |
| 7 | 0.00 | 0.00 | 0.00 | 0.00 | 0.10 | 0.10 |

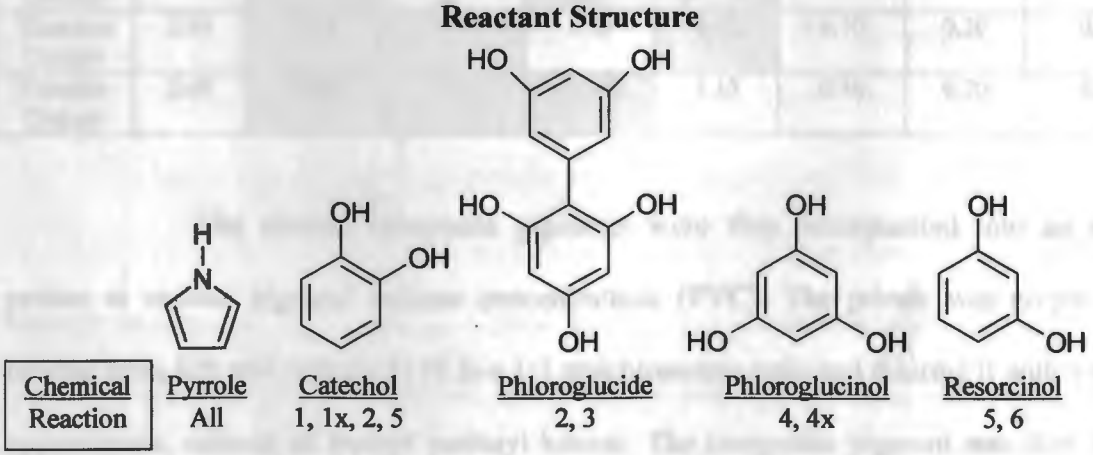


Figure 2.1. The reactants used in the PPY/Al flake synthesis.

The procedure for this reaction was to first dissolve the corrosion inhibiting sodium salt into 90 ml of Millipore 18.2 MΩ water. 3g of Stapa Aloxal PM 2010 aluminum flake

was then dispersed into the solution. The catechol was then added, followed by the pyrrole. 10 ml of a 4 M ammonium persulfate solution was then added via burette over a 45 minute period. As before, the reaction was allowed to stir for 24 hours at which point the insoluble product was filtered out and washed with approximately 1 liter of 18.2 MΩ Millipore water to remove any leftover reactants or ions. A larger amount of water was used to wash the pigments doped with corrosion inhibiting anions to ensure that any ions remaining in the pigment would be bound to the polypyrrole as dopants and not deposited as water soluble salts on the pigment surface. After being dried in an oven at 60° C for 24 hours, the samples were ground using a mortar and pestle and then passed through a 106 μm sieve.

Table 2.2 The synthesis reactions for the PPY/Al flake composite pigments doped with corrosion inhibiting anions.

| | Al Flake g | Sodium Phosphate (M) | Sodium Molybdate (M) | Sodium Vanadate (M) | Sodium Stannate (M) | Catechol (M) | Pyrrole (M) | Ammonium Persulfate (M) |
|---|---|---|---|---|---|---|---|---|
| Phosphate Dopant | 3.00 | 3.62 | 0.00 | 0.00 | 0.00 | 0.10 | 0.20 | 0.40 |
| Molybdate Dopant | 3.00 | 0.00 | 1.35 | 0.00 | 0.00 | 0.10 | 0.20 | 0.40 |
| Vanadate Dopant | 3.00 | 0.00 | 0.00 | 1.73 | 0.00 | 0.10 | 0.20 | 0.40 |
| Stannate Dopant | 3.00 | 0.00 | 0.00 | 0.00 | 1.15 | 0.10 | 0.20 | 0.40 |

The ground composite pigments were then incorporated into an epoxy primer at various pigment volume concentrations (PVC). The primer was prepared by mixing epon 828 and epikure 3175 in a 1:1 stoichiometric ratio and diluting it with a small, approximate, amount of methyl isobutyl ketone. The composite pigment was then added and more methyl isobutyl ketone was added with stirring until a proper application viscosity was reached. The primer was then shaken vigorously by hand for approximately

10 minutes. The panels used as substrates were supplied by Q-Panel and were composed of aluminum alloy 2024 T3. The panels that were to be exposed without a top coat had their surfaces prepared by first being sanded using 160-grit sandpaper and a Master Mechanic® palm sander and then degreased using ethanol. Samples that were to undergo ASTM B117 salt spray exposure (B117) were applied using an ATD Air-6900 high volume low-pressure spray gun with a 1.8 mm orifice. All other coatings were applied using a drawdown bar supplied by Gardco at 8 mils wet thickness. The panels were allowed to flash off for 40 minutes before being placed in an oven at 80° C to cure for 4 Hrs. The final cured thickness of the primers was from 5 to 7 mils. The higher the pigment volume concentration of the coatings, the les they shrank during curing and so the coatings with high pigment volume concentrations had thicknesses closer to 7 mils while lower pigment volume concentration coatings had thicknesses closer to 5 mils. Half of the samples that were to undergo B117 exposure were scribed using a Gravograph IM4 engraver. For the samples that were weathered with a top coat, the panels were sand blasted using 100 μm alumina grit and then washed with ethanol. All other application procedures were kept the same for these panels.

A PHI model 555 XPS instrument was used to perform XPS measurements using Mg K-alpha X-ray excitation with a cylindrical mirror electron energy analyzer. A pass energy of 100 eV was used to collect survey photoelectron spectra. High-resolution photoelectron spectra were collected using a 25 eV pass energy. To neutralize the samples during measurements, a low energy flux (1.0 eV, 0.9 mA) was applied. Charge compensations were done during curve fittings by setting the C 1s peaks for C-C/H at 285.0 eV, and a Gaussian-Lorentzian model with a 90:10 ratio was applied.

To prepare samples for SEM, the ground composite pigment was sprinkled onto carbon tape which was attached to aluminum mounts. Compressed air was blown onto the sample to remove any loose particles and the sample was then sputter coated with gold using a Balzers SCD 030 sputter coater. The instrument used to obtain images was a JEOL JSM-6300 Scanning Electron Microscope. The magnification, accelerating voltage used and scale bars are listed on each figure. EDX measurements were made using the instrument and an accelerating voltage of 15 kV.

Ground product was used for the conductive AFM (C-AFM) measurements. The sample substrates were prepared by first sanding a small aluminum panel and then applying a thin layer of conductive silver epoxy to the surface. The sample was dusted onto the surface of the epoxy. This was allowed to cure overnight before measuring. The samples were measured using a Digital Instruments Dimension 3100 AFM from Veeco. The samples were measured in contact mode using platinum/iridium coated tips from Veeco. All samples were first scanned with no applied voltage to ensure a good image could be obtained. After this was verified, a voltage of 100 mV was applied to the sample and the resulting current image was captured. The conductivity was calculated by using the following equation:

$$\sigma = \left(\frac{I_m}{V_{app}}\right)\left(\frac{X}{A}\right) \qquad [1]$$

$\sigma$ = conductivity (S/cm)
$I_m$ = measured current
$V_{app}$ = applied voltage
X = sample thickness
A = contact area of the AFM tip

The contact area of the tip used was calculated to be 19.5 $nm^2$. The sample thickness was determined from the cross section of the height image, and the average current was determined from the cross section of the current image.

Electrochemical impedance spectroscopy (EIS) was used to monitor the samples undergoing constant immersion and B117 salt spray. EIS measurements were performed at non-scribed areas of the panels. EIS were taken by applying a small, AC voltage perturbation to a sample, usually about its open circuit potential. The current flow due to the voltage perturbation is measured and a form of ohms law is used to calculate the impedance (ohms) as the voltage and current are known:

$$Z(\omega) = \frac{V(\omega)}{I(\omega)} \qquad [2]$$

$Z(\omega)$ is the complex impedance which includes the relationship between amplitudes of the voltage and current signals as well as any phase shift that may occur. $V(\omega)$ and $I(\omega)$ are the voltage perturbation and corresponding current; respectively. EIS was performed using Gamry PC-4 or FAS1 instrument with dilute Harrison's Solution (DHS) (0.35% $(NH_4)_2SO_4$ and 0.05% NaCl in 18.2 MΩ Millipore water) as the electrolyte, platinum coated mesh as the counter electrode, and a saturated calomel reference electrode. A 10 mV perturbation was used with a frequency range from 100,000 to 0.01 Hz. The EIS cell consisted of a glass tube with rubber o-ring to seal the tube onto the coating surface. The area of electrolyte contact, on the coating surface, within this cell was 7 $cm^2$. The same experimental setup was used to collect the open circuit potential (OCP) measurements for the samples.

Particle Size measurements were made on an Accusizer Model 780 from Particle Sizing Systems Inc with a LE400-0.5 EXT sensor. The samples were first dispersed in 300

mL. The dispersion was then allowed to flow through the instrument. Data was collected for 300 seconds. To perform the density tests, 0.1 grams of the ground sample was placed in tetrachloroethylene. The samples were given sufficient time to allow the higher density material to settle out of the liquid at which time a digital photograph was taken and the results recorded.

Samples for the SVET and coupling current measurements were prepared by sandblasting an aluminum 2024 T3 panel using 100 μm alumina grit followed by cleaning/degreasing with ethanol. The panel was cut into 1 cm x 1 cm samples using a shear cutter. A small hole was drilled through one corner of the aluminum 2024 T3 squares and a piece of string was tied through the hole. The samples were then dip coated by hand using the above mentioned primer. After the samples had been cured in an oven at 80°C for no less than 8 hours, the string was removed and the samples were sanded using 600 grit sandpaper to give them a uniform shape and surface profile. The coating thickness of these samples after being sanded was approximately between 3 and 4 mils. This alternate method of coating the samples was used because it was found that if a large panel was first coated and then cut with a shear it would cause damage to the coating in areas where the SVET measurement was to be taken.

The current distribution on PPY-coated substrates was measured using a SVET system from Applicable Electronics employing a Pt–Ir microelectrode (tip diameter 10 μm, from Microprobe, Inc.) onto which was deposited a sphere of Pt black (ca. 20 μm diameter with a capacitance of ca. 40 nF). The microprobe was scanned 200 μm above the sample surface with a vibration amplitude of 20 μm in the *X* and *Y* directions at frequencies in the range of 200-300 Hz. The sample (1 cm square) was masked by polyester tape so as to

form a scan area of 2.5 × 2.5 mm. An artificial defect (ca. 0.1 to 0.3 $mm^2$) was introduced in the center of the scan area. The probe made measurements on a 20 × 20 grid (requiring ca. 10 min), generating a 400-point mesh across the surface. The SVET measurements were performed at ambient temperature (ca. 20 °C) under open circuit (free-corrosion) conditions in a cell containing ca. 5 mL dilute Harrison's solution (DHS, 0.35 wt% $(NH_4)_2SO_4$, 0.05 wt% NaCl). Scans were initiated ca. 5 min after immersion and were repeated every 1 h. All solutions were prepared with analytical grade reagents and 18.2 MΩ Milli-Q water.

Display of the SVET data and statistical analysis of the data were performed with Origin software. The current densities are displayed in three-dimensional (3D) maps, showing the spatial distribution of the vertical component of the current density as a function of the ($X$, $Y$) position in the scan region. In these SVET maps, anodic currents are positive and cathodic currents are negative. A contour map of the current density is projected onto the bottom of the 3D map. In some cases, the data is also presented as current vectors superimposed onto an optical micrograph of the sample, showing both horizontal and vertical components of the current.

Galvanic coupling experiments were carried out in a two-compartment enclosed glass cell as described in Yan et al. (5). The cover of each compartment had four openings, one for inserting the working electrode, a Luggin capillary connected to a saturated calomel electrode (SCE), and tubes for the introduction and removal of gases. The working electrode in one compartment was bare AA 2024-T3 (subsequently referred to as the AA-compartment) and the working electrode in the other compartment was coated 2024-T3 (subsequently referred to as the Coating-compartment). The exposed surface of the AA

2024-T3 was a pinhole of 0.04 $cm^2$ (simulating a coating defect) and the area of the conducting polymer was 1.5 $cm^2$, yielding an area ratio of ca. 37. The mixed potential and the coupling current between the Coating and the AA were measured using the Gamry PC4/300 potentiostat in zero resistance ammeter (ZRA) mode. The solution in the coating-compartment was purged with either air or $N_2$ while the solution in the AA-compartment was purged with air.

Samples were prepared for linear polarization measurements by first sandblasting the aluminum 2024 T3 with 100 μm alumina grit and then cleaning the panel with ethanol. The primer was then prepared as mentioned above and drawn down onto the substrate using a drawdown bar at a wet thickness of 8 mils. The panels were then cured in an oven at 60° C for no less than 8 hours. The dry thickness of the coatings was approximately 3 mils. A scribe that was 1.3 cm long and 1 mm wide was placed onto the panels. The area of these scribes was the area used to calculate current density for the linear polarization plots. The measurements were taken using a glass cell with an area of 7 $cm^2$ that was placed over the scribed area. Dilute Harrison's solution (DHS) (0.35 % ammonium sulfate and 0.05% sodium chloride by weight) was the electrolyte used. A platinum mesh counter electrode was used with a saturated calomel reference electrode. Prior to a measurement being taken, the cell was purged with either nitrogen or air for 25 minutes. The cell was then sealed with parafilm® to slow the diffusion of gas into or out of the cell. Measurements were taken using a Gamry PC4 in a linear potential sweep from -0.010 volts to 0.750 volts vs. the open circuit potential. The scan rate used was 0.5 mV/S.

# CHAPTER 3.

# THE CHARACTERIZATION OF A POLYPYRROLE/Al FLAKE COMPOSITE PIGMENT

## 3.1. Introduction

The first step, after synthesizing the PPY/Al flake composite pigments, was to characterize the flakes to determine which of the variables in the synthesis reaction had an effect on the deposition of the PPY onto the aluminum flake. The first part of this chapter, up to Section 3.7 addresses the characterization of the products from reactions 1-6 from Table 2.1. From Section 3.7 on, this chapter addresses the characterization of the products from the reactions in Table 2.2 as well. The set of reactions in Table 2.1 was designed to determine what influence the addition of different phenolic compounds and different pyrrole concentrations would have on the morphology and composition of the product deposited onto the aluminum flakes. The set of reactions in Table 2.2 was designed to determine what effect different corrosion inhibiting dopants would have on the deposited product of the synthesis reaction.

## 3.2. SEM Characterization of the Products from Reactions 1-6

As can be seen in Figure 3.1, the as-received aluminum flakes are approximately uniform in size ranging from approximately 10-30 μm in diameter. According to the MSDS supplied with the flake by the manufacturer, the flake is composed of aluminum, aluminum oxide, and 1-methoxy-2-propanol; a small amount of impurities were also present.[1]

**SEM Image and Composition of As-Received Flake Pigment**

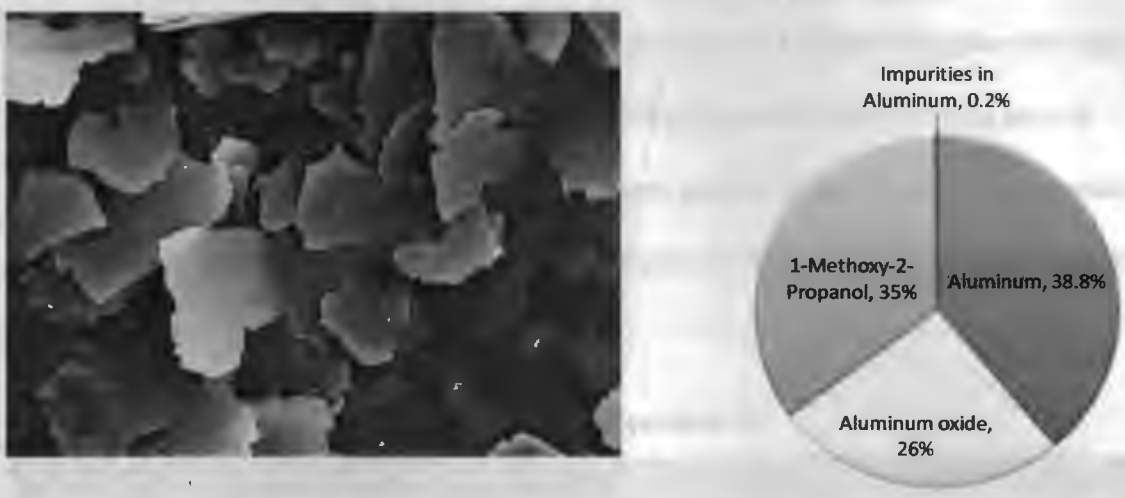


Figure 3.1. SEM micrograph of the as-received aluminum flake (left) and the composition by weight (from MSDS) (right).

It is evident, as shown in Figure 3.2, that the flake-like nature of the pigment was not significantly compromised during the synthesis process. However, in some instances, such as reactions 1 and 1x, large particles are present which are comprised of multiple flakes. It is interesting to note that this only occurs when catechol is the only phenol present during the reaction. The results from reaction 1 are presented in Figure 3.2 where the deposited product on the flakes appears to join flakes together.

**SEM Image of Reaction 1**

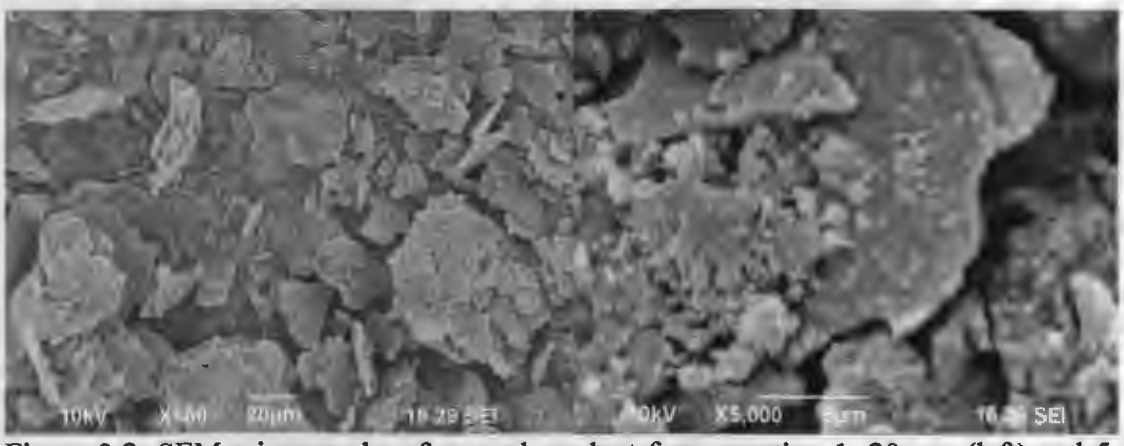

Figure 3.2. SEM micrographs of ground product from reaction 1, 20 μm (left) and 5 μm (right).

In reaction 1x, the result of increasing the reactant concentration in the flake synthesis was studied. The product of this reaction can be seen in Figure 3.3. While it appears that the majority of the aluminum flakes were covered with polypyrrole, the clumping seen in reaction 1 has been amplified resulting in still larger particle sizes. This effect presented a problem in the processing of the pigment, as it was exceptionally hard to grind it to a size that would pass through a 106-μm sieve.

**SEM Image of Reaction 1x**

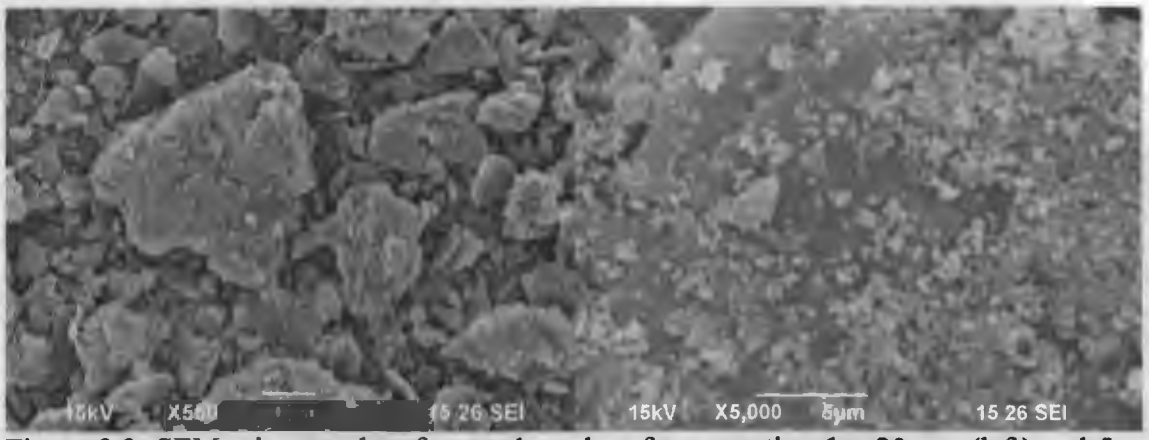


Figure 3.3. SEM micrographs of ground product from reaction 1x, 20 μm (left) and 5 μm (right).

Rather uniform deposition resulted from the combination of catechol and phloroglucide during reaction 2, as can be seen in Figure 3.4. The uniform coating of the flake would most likely facilitate the formation of a conductive epoxy coating. Additionally, the flakes appear to be rather individual in nature when compared with the aforementioned reaction 1. This is particularly interesting as the overall concentration of the reactants is the same between reaction 1x and 2, the only difference being the presence of phloroglucide.

Figures 3.5 and 3.6 (reactions 3 and 4) also show unique polymer growth. In Figure 3.5, when the phloroglucide is the lone phenol, such as in reaction 3, there is the development of lamellar folds of PPY similar in appearance to crumpled tissue paper. In Figure 3.6, when phloroglucinol is the lone phenol, the flakes appear to resemble the as-received flakes with no clumping observed. However, on close examination it appears that the product is rather unevenly distributed on the surface of the flake. It appears that when phloroglucinol is the lone phenol present during the reaction, it tends to direct the polymer growth to the edges of the flake with some wire growth towards the middle.

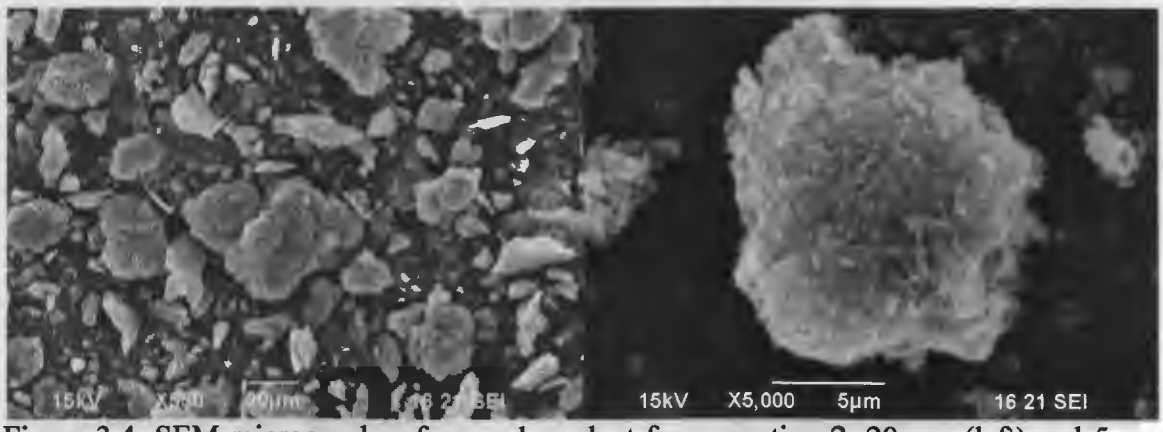

Figure 3.4. SEM micrographs of ground product from reaction 2, 20 µm (left) and 5 µm (right).

Interestingly, when the concentration of reactants used in reaction 4 is increased in reaction 4x, as shown in Figure 3.7, polymer deposition on the center of the flakes is not facilitated. It simply increases the amount deposited on the edges. This is not necessarily desirable for a pigment application. The structures extending from the edges of the flakes would readily break off during the mixing of a paint formulation. It may also be difficult to form a conductive network throughout the coating when the polypyrrole is separated by the resistive flakes.

**SEM Image of Reaction 3**

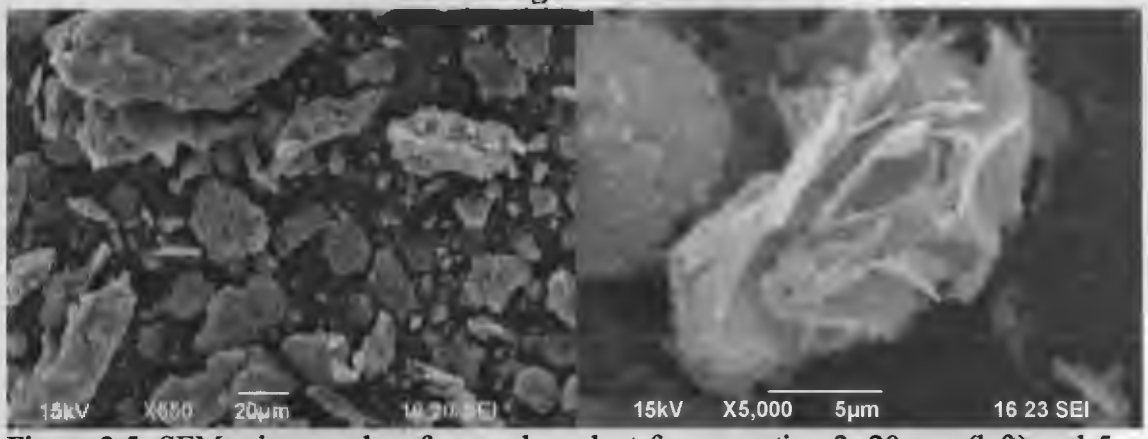


Figure 3.5. SEM micrographs of ground product from reaction 3, 20 µm (left) and 5 µm (right).

**SEM Image of Reaction 4**

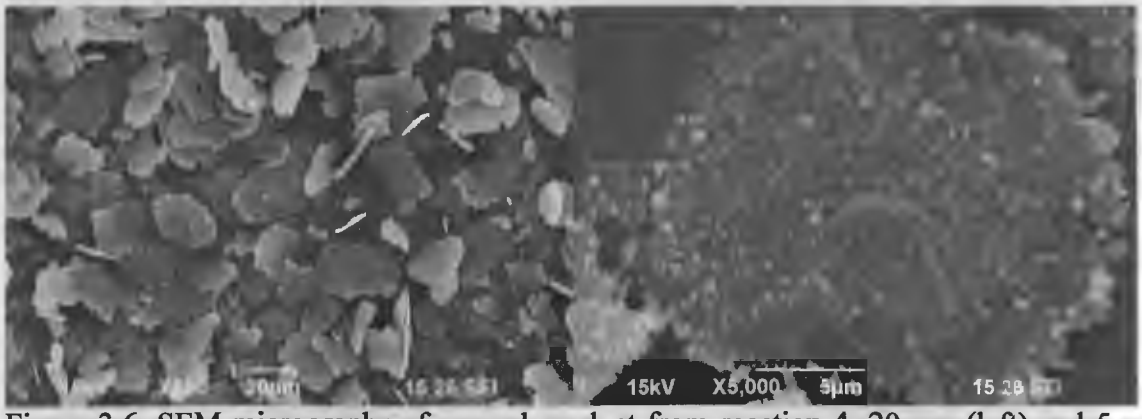


Figure 3.6. SEM micrographs of ground product from reaction 4, 20 µm (left) and 5 µm (right).

The increase in the free product would influence the critical pigment volume concentration (CPVC) for this pigment. This is because the presence of the smaller particles that have been broken off of the larger pigment particles would change the surface area to volume ratio. More binder would be required to wet the larger surface area thereby decreasing the CPVC.[2]

The use of catechol combined with resorcinol, reaction 5, can be seen in Figure 3.8. It was noticed that the joining of multiple flakes together as observed for reactions 1 and 3

was diminished by the addition of resorcinol. This is similar to the result observed for the addition of phloroglucide. While there is some product deposited from this reaction, it is not as uniform and occurs on fewer flakes than is observed in reaction 2.

**SEM Images of Reaction 4x**

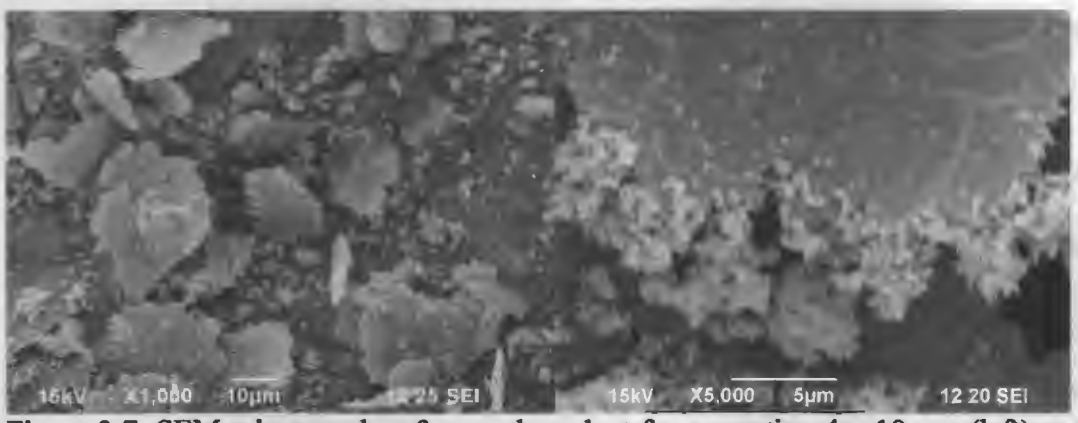


Figure 3.7. SEM micrographs of ground product from reaction 4x, 10 µm (left) and 5 µm (right).

**SEM Images of Reaction 5**


Figure 3.8. SEM micrographs of ground product from reaction 5, 10 µm (left) and 1 µm (right).

In Figure 3.9, there is the presence of wire-like structures on the micro scale. These structures are also observed in Figures 3.6 and 3.7 although they are not as prominent as in Figure 3.9. Because of the sputtered gold coating placed on the samples for SEM

measurements, it is impossible to discern the actual thickness of these wires. The synthesis of these PPY wire structures has been reported by other groups.[3-12] There are presently three ways that these structures have been synthesized. One is by using surfactants to control the polymerization process. Another is by using templates to guide the polymerization as it takes place and a third is by using strictly controlled electrochemical techniques to grow PPY nano-wires.

While there is not a surfactant present during the synthesis, the as-received flakes are prepared with a significant amount of 1-methoxy-2-propanol (35%) present to encourage easy dispersion in aqueous paints. It may be possible that the 1-methoxy-2-propanol is effecting the deposition of the polypyrrole. However, if that were the case, one would assume that the wire-like structures would appear on the products for every reaction, which is not the case.

**SEM Images of Reaction 6**

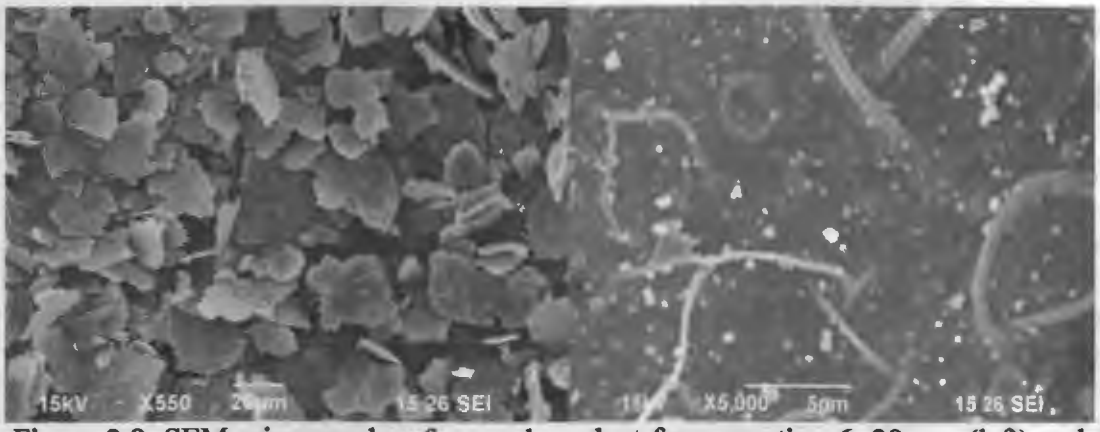


Figure 3.9. SEM micrographs of ground product from reaction 6, 20 µm (left) and 5 µm (right).

Certainly, differences in the resulting morphology of the deposited product appear to be linked to the phenolic compounds used during the synthesis. One explanation,

which was verified via XPS measurements, could be that some degree of copolymerization between the phenolic compounds and the pyrrole monomer unit took place. With the hydroxyl groups present on the catechol ring, the catechol would have some degree of affinity for the aluminum oxide and aluminum hydroxide surfaces of the flakes. An oxidized catechol molecule on the surface of the aluminum flake could act as an initiation point for polypyrrole deposition. Oligomers formed on the surface of the flake would then be preferentially oxidized due to their lower oxidation potentials leading to chain propagation on the surface of the flakes. This hypothesis will be further discussed in section 3.4 of this chapter.

### 3.3. Density Experiments for the Products of Reactions 1-6

The density experiments provided information regarding the adherence of the polypyrrole to the aluminum flake. From Figure 3.10 it is possible to observe the production of any free product for the reactions 1 through 6. For example, any free product, product that is not attached to aluminum flake, will float in the liquid. The aluminum flakes and any adhered product will sink in the liquid due to higher density. It should be noted that the black line on the top of the liquid is the reflection of the product in the meniscus of the liquid. Reaction 1 product was tightly adhered to the flake as the entire product settled to the bottom of the liquid. Reaction 1x product has relatively good adherence, however, there is a higher occurrence of the free particulates in the liquid when compared to the product from reaction 1. Reaction 2 product appears to form larger particulates that became adhered to the glass of the container, therefore, results are inconclusive.

The product from reaction 3 is an anomaly. The product is extremely voluminous when compared with the other product as noticed during the filtering step of the synthesis. Indeed, reaction 3 product does display rather interesting structures that have a tissue-like appearance as observed via SEM. The density experiment would seem to indicate that, indeed, the product is quite different from the other products as shown by the low-density, floating behavior observed during the experiment.

**Density Results for Reactions 1-6**

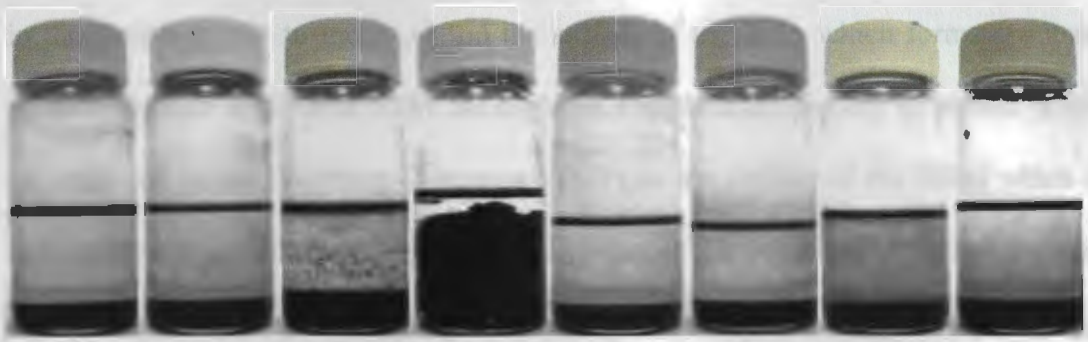


Figure 3.10. Density experiment results for the ground product from reactions 1 through 6.

It is interesting to note that the micrographs indicating uneven deposition and the appearance of rather poorly adherent product did not directly correspond with the findings of free product during the density experiment. Reactions 1, 1x, 4, 4x, 5, and 6 display similar density results with reaction 5 possessing the highest amount of free product as determined visually. When comparing the micrographs there would appear to be a large difference in free product in the reactions. Perhaps some of the small particulates observed in the SEM micrographs are not free product as originally thought, but instead small aluminum particles that resulted from the breakup of some of the larger flakes. This would effectively create small particles that could subsequently undergo deposition.

Additionally, the small particles could be quite well attached to the surface and are not easily removed. These conditions could produce the observed results.

### 3.4. X-Ray Photoelectron Spectroscopy Analysis

The XPS survey scan of the as-received Stapa Aloxal PM 2010 can be seen in Figure 3.11. The majority of the material present in the as-received flake is revealed to be comprised of aluminum, oxygen and carbon. It is likely that the large amount of the oxygen in the sample is due to the $Al_2O_3$ on the surface of the flake which forms spontaneously when aluminum is exposed to the atmosphere. The sizeable quantity of carbon present can be attributed to the 1-methoxy-2-propanol (MP) on the surface of the flakes which is used as a surface treatment by the manufacturer to enable the flakes to become easily dispersed in water-borne coatings. The composition of the aluminum flake pigment according to the MSDS supplied by the manufacturer of the aluminum flake is approximately 26% aluminum oxide, 39% aluminum, and 35% 1-methoxy-2-propanol by weight respectively. The larger amount of oxygen and smaller amount of aluminum in the sample versus what is stated in the MSDS could be due to the oxidation of the aluminum flake after manufacturing. In addition, the difference between the amounts of carbon observed using XPS and the values given in the MSDS could be due to the volatility of the 1-methoxy-2-propanol.

The XPS spectra collected from the sample synthesized without any phenolic reactants (reaction 7) can be seen in Figure 13.12 along with the elemental composition for the sample. From the elemental composition obtained from the XPS spectra in Figure 3.12, it is evident that for the sample synthesized without phenolic reactants, the carbon to

nitrogen ratio is approximately 5:1 and the sulfur to nitrogen ratio is approximately 1:9. For a pure polypyyrole sample, the carbon to nitrogen ratio that would be expected would be 4:1. The elevated carbon content that is observed for this sample is likely to be indicative of the presence of adventitious carbon that has adhered itself to the flake. This data, therefore, serves as a way to determine how much the adventitious carbon will affect the XPS measurements for subsequent samples under these synthesis conditions. The sulfur to nitrogen ratio also gives an idea of the doping level for this pigment which is explained later.

**XPS Results for the As-Received Flake**

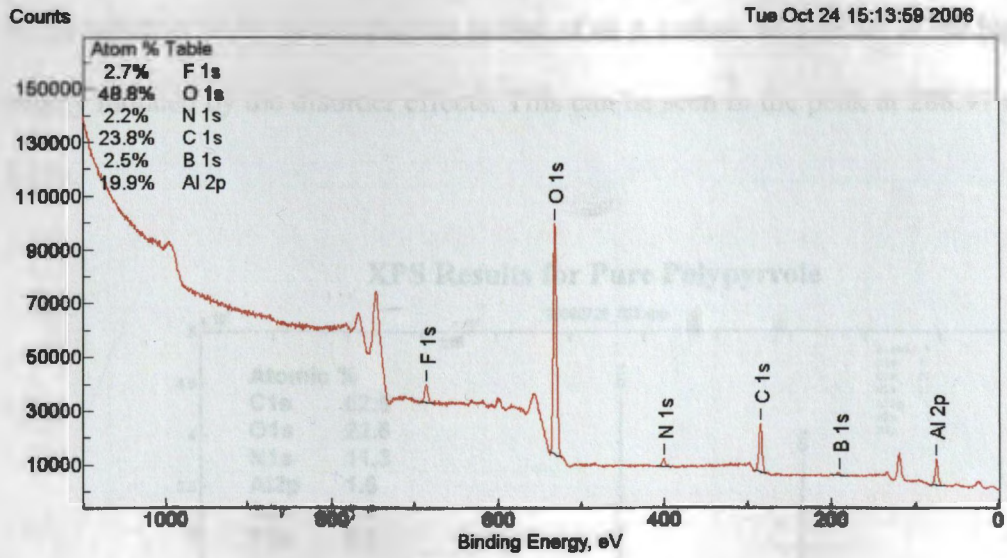


Figure 3.11. An XPS plot of the as received flake.

The core level carbon 1s (C1s) nitrogen 1s (N1s), and aluminum 2p (Al2p) XPS spectra of the polypyrrole/Al flake composite prepared in the presence of catechol, reaction 1, are shown in Figure 3.13. A standard peak shape analysis with Gaussian fittings was used to analyze the core level spectra. Analysis revealed that the C1s main peak is split into three peaks as is shown in Figure 3.13a. The peak at 284.98 eV is associated with the

pyrrole β carbons, while the peak at 286.85 eV is associated with the pyrrole α carbons. The energy gap of 1.87 eV between the two peaks is consistent with, but slightly larger than what has been previously reported for similar samples.[13-15] "Disorder effects" such as inter-chain links, side chains or chain terminations can be allocated to the asymmetry of the C1s spectrum.[13-14] This is not unexpected when a strong oxidant such as ammonium persulfate is used as free radicals formed on β carbons in the pyrrole rings would lead to crosslinking between chains via the β carbons. As a result of these disorder effects, the electron density normally attributed to the hydrogen atom binding with β carbon of the pyrrole ring is mainly attributed to the β carbon itself. The result is a peak width which is wider in comparison to that of an α carbon, as a result of the higher binding energy induced by the disorder effects. This can be seen in the peak at 288.97 eV in Figure 3.13a.

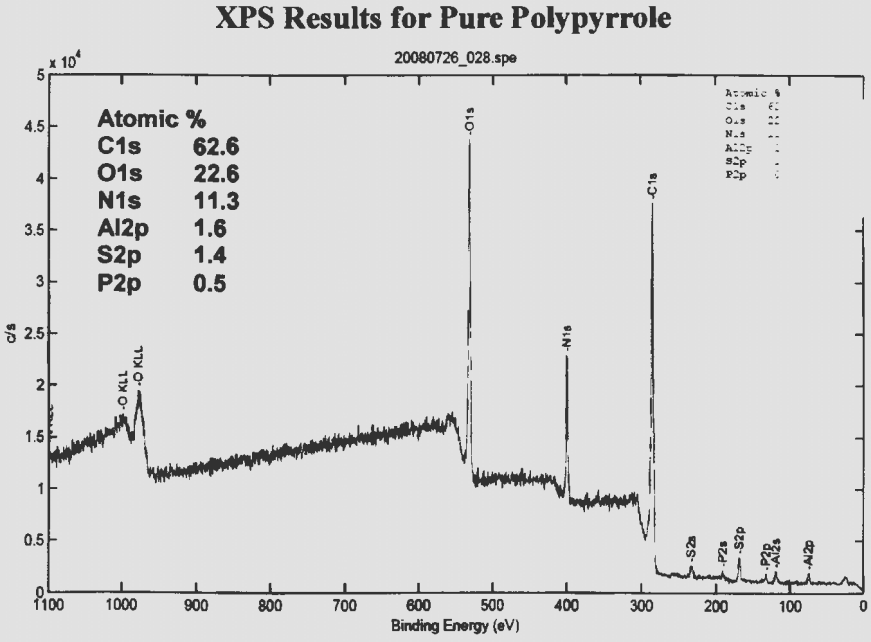


Figure 3.12. An XPS plot for the sample synthesized without phenolic reactants.

The N(1s) spectra spectrum shown in Figure 3.13b is characteristic of oxidized polypyrrole complexes that contain only amine-like and $N^+$ nitrogen atoms with peaks at 399.41 eV and 401.31 eV respectively. The electrostatic effect of the nearest counter ion to the nitrogen can be assigned to the shoulder on the side of the peak that is higher in energy.[13, 16] The nitrogen in the polypyrrole/aluminum composite flakes is composed of approximately 31% N+ which is similar to levels reported by other research groups.[13, 16] There is not a peak present that can be assigned to an imine nitrogen. This indicates that the polypyrrole did not undergo a deprotonation step and an anion is still acting as a counter ion to the polymer.[16]

**Core Level Spectra for Reaction 1**

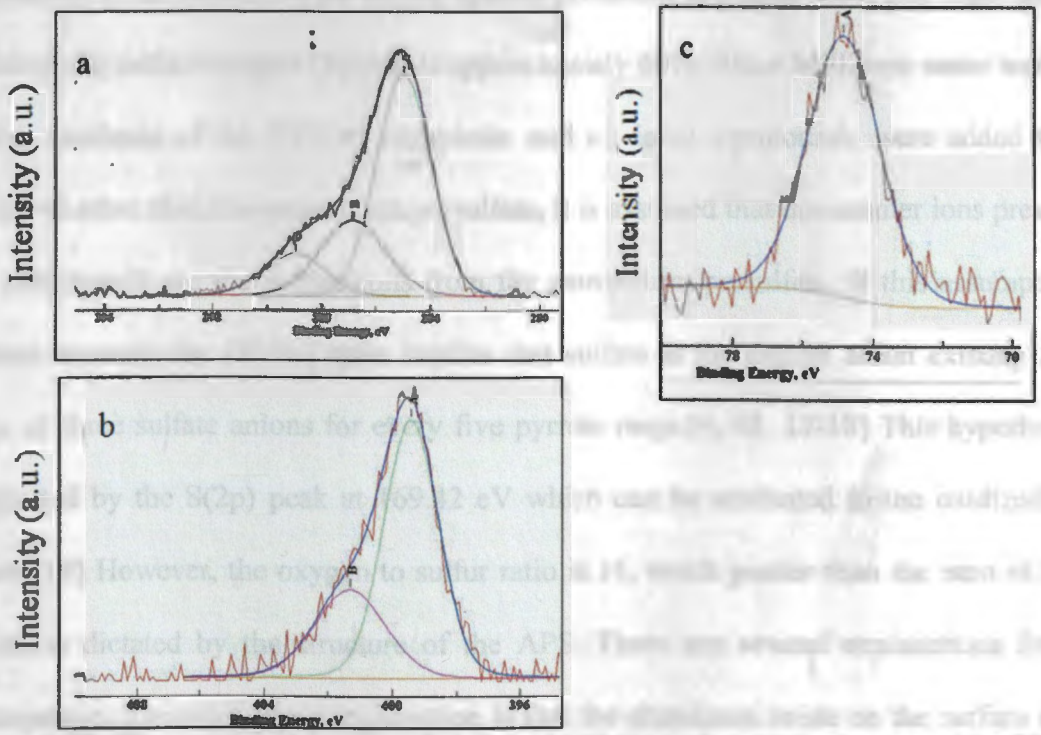


Figure 3.13. The core level spectra of a) C 1s, b) N 1s, and c) Al 2p spectra of the PPY/Al flake composite synthesized in the presence of catechol, reaction 1.

Another possible explanation for the lack of an imine peak would be the formation of complexes between the nitrogen on the pyrrole rings and the aluminum along with other atoms such as oxygen converting the nitrogen to an amine like state. This would cause the disruption of the π-electron conjugation resulting in a N-π-$AlO_z$ peak. The peak associated with N-π-$AlO_z$ is observed at 74.81 eV in Figure 3.13c and could also be a contributing factor responsible for the large amount of oxygen observed.[16] The formation of these complexes with the aluminum on the surface of the flake would greatly increase the adhesion of the deposited product to the flake surface. It may be that the phenolic groups are somehow affecting the formation of these complexes to change the morphology of the deposited product.

The elemental composition of the polypyrrole/Al flake composite pigment prepared in reaction 1 can be seen in the survey spectra presented in Figure 3.14. The reported ratio between the sulfur/nitrogen [S]/[N], is approximately 60%. Since Millipore water was used in the synthesis of the PPY/Al composite and no ionic compounds were added to the synthesis other than the ammonium persulfate, it is assumed that the counter ions present in the polypyrrole are the sulfate ions from the ammonium persulfate. If this assumption is indeed accurate, the [S]/[N] ratio implies that sulfate is the dopant anion existing in the ratio of three sulfate anions for every five pyrrole rings.[4, 13, 17-18] This hypothesis is supported by the S(2p) peak at 169.42 eV which can be attributed to the oxidized $SO_3^-$ anion.[19] However, the oxygen to sulfur ratio is 11, much greater than the ratio of three, which is dictated by the structure of the APS. There are several explanations for this discrepancy. The most likely explanation is that the aluminum oxide on the surface of the flakes that is not covered with the deposited product is making a large contribution to the

oxygen peak. Another possible contribution to the oxygen peak originates from the carbon/nitrogen [C]/[N] ratio which is approximately 7:1. This indicates that catechol may have been incorporated into the deposited product whose hydroxyl groups would also contribute to the oxygen peak. The increased carbon to nitrogen ratio also may be an indication of copolymerization between the phenols and the polypyrrole. This same effect was observed in Figure 3.15 below.

To further investigate the effect that the phenolic compounds may be having on the composition of the PPY/Al flake composite pigment, a survey scan was acquired from the sample synthesized with both catechol and phloroglucide (reaction 2). The results of this scan can be seen in Figure 3.15. With the addition of phloroglucide into the synthesis reaction, the carbon to nitrogen ratio has increased to approximately 10:1 and the sulfur to nitrogen ratio has increased to 1:3. Also, there is a very low amount of aluminum present at the surface of the particles which would be consistent with the SEM images in Figure 3.4 which shows that the majority of the flake surfaces are covered in the deposited product. There is also a lower oxygen content in Figure 3.15 in comparison to Figure 3.14 which may be due to more of the aluminum oxide surface of the flake being covered with the deposited product.

The data in Figures 3.11-3.15 suggest that a copolymer could possibly be forming that contains the polypyrrole and phenolic reactants. There is certainly some adventitious carbon present but Figure 3.12 suggests that it likely would not lead to carbon levels that are more twice what would be expected. Therefore, it may be that the increased carbon to nitrogen ratio observed for the pigments synthesized with phenols are due to a

copolymerization which could be an explanation for the different morphologies observed when different phenols are present in the synthesis reaction.

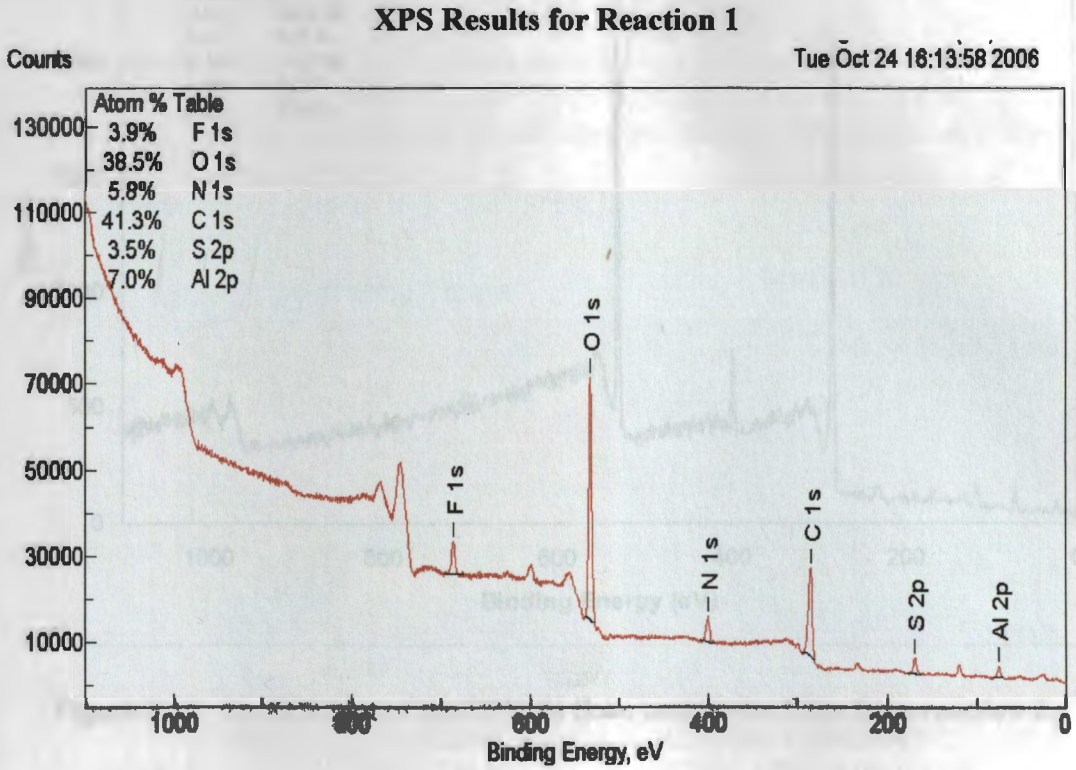


Figure 3.14. An XPS plot of the PPY/Al flake composite flake from reaction 1.

It is possible that the phenols have different affinities for the aluminum oxide surface of the flake based on the number and position of their hydroxyl groups. If an oxidized phenolic molecule becomes attached to the aluminum oxide, on the surface of the flakes, through hydrogen bonding, it could act as an initiation point for the deposition of polypyrrole onto the surface of the flake. Furthermore, the phenolic monomers in the polymer chain would require dopants similar to the pyrrole units in the chain which could also be an explanation for the increased sulfur to nitrogen ratio observed when phenolic reactants were present in the synthesis reaction.

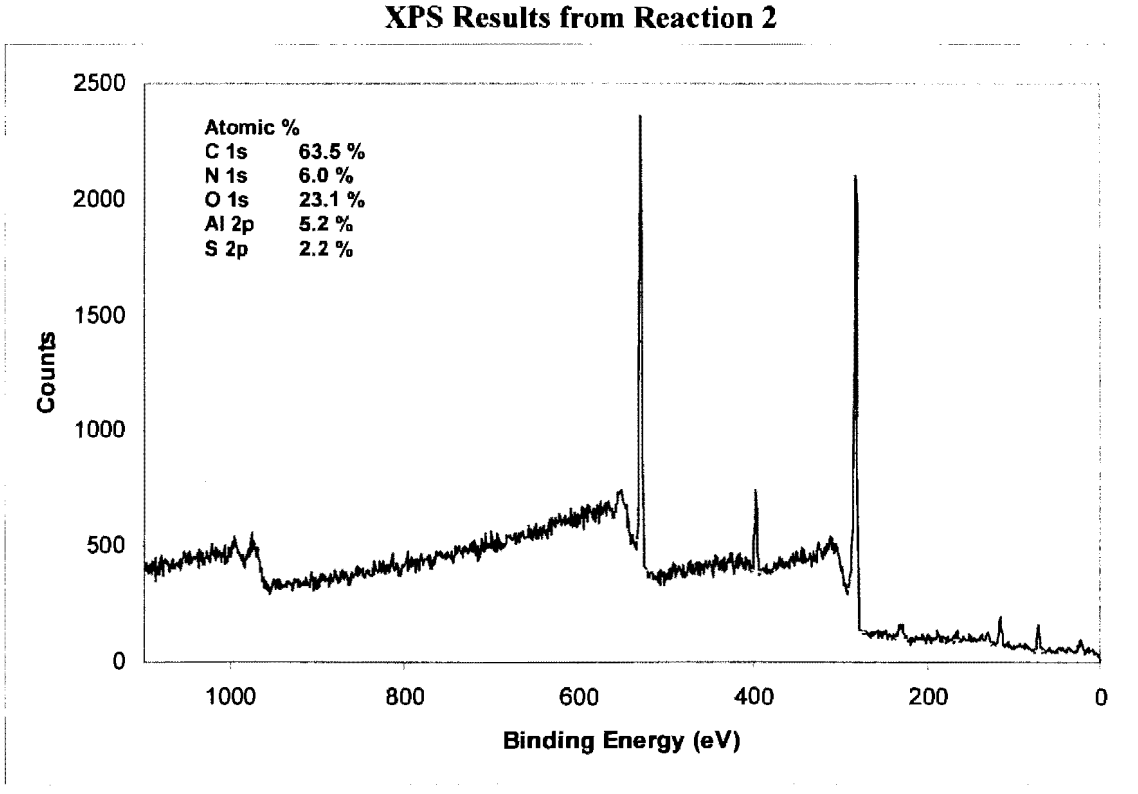


Figure 3.15. An XPS plot of the PPY/Al flake composite flake from reaction 2.

### 3.5. Conductive Atomic Force Microscopy

To help verify that the product deposited onto the flake was indeed conductive, conductive AFM measurements were acquired for the flakes from reactions 1 and 2. As can be seen in Figures 3.16 and 3.17, the aluminum flakes have the majority of their surfaces covered in a conductive layer. The average conductance of the deposited product in Figure 3.16 was found to be 1.6 S/cm. The average conductance of the deposited product in Figure 3.17 was approximately 5.2 S/cm. This conductivity is likely due to the polymeric film deposited on the surface of the flake as the conductivity of the as-received flake was too low to be detected when examined via C-AFM due to the resistive nature of the oxide

layer. These results can be seen in Figure 3.18. Here the blue areas in the image coincide with areas of the sample that have conductivities that are below the detection threshold of the instrument indicating a surface with very low conductivity. In the case of this instrument, the detection threshold for a 5 micron thick sample is 2.56 x $10^{-13}$ S/cm. It is not surprising then that conductivity is not observed for an aluminum oxide surface as aluminum oxide has a conductivity < $10^{-14}$ S/cm.

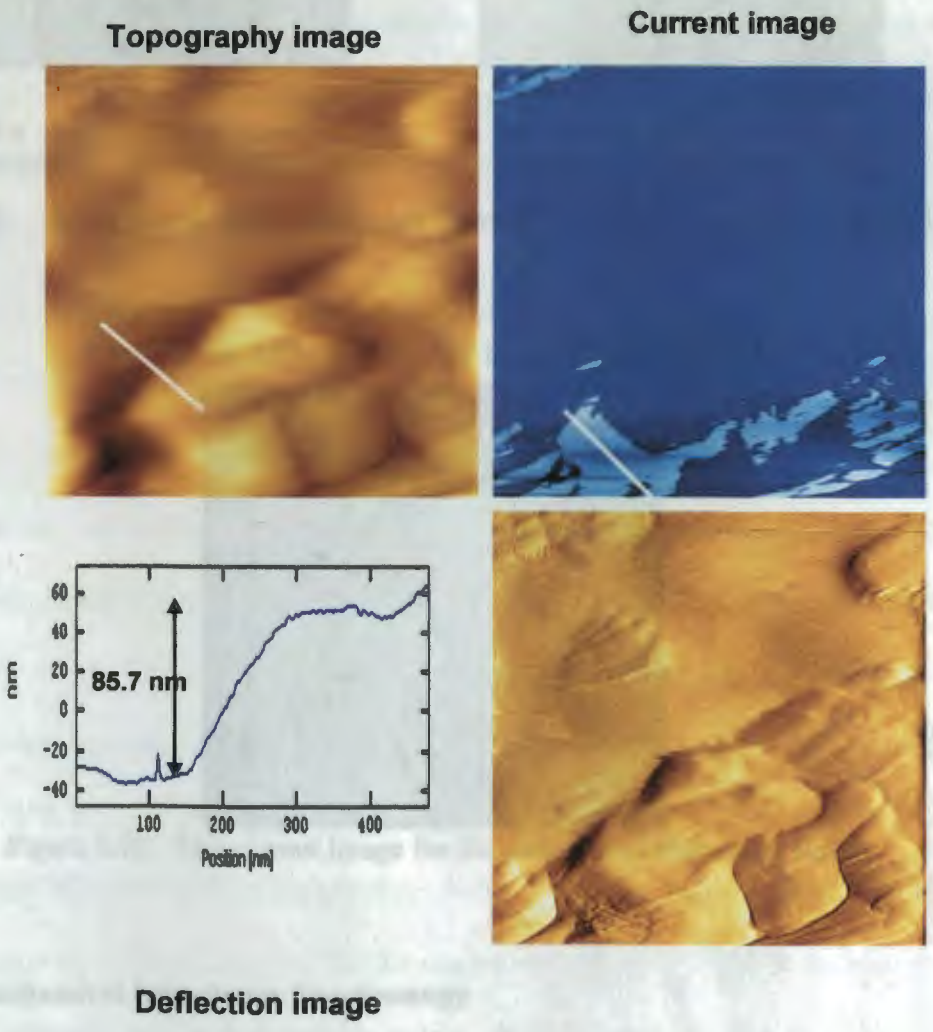


Figure 3.16. A 2.5 μm conductive AFM image showing the conductivity of the product from reaction 1.

**Conductive AFM Results from Reaction 2**

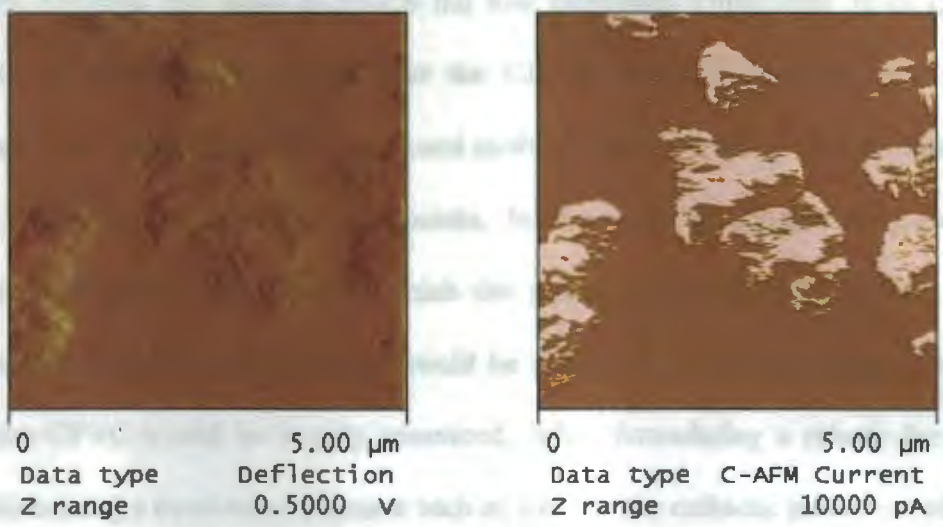


Figure 3.17. 5 µm topographic (left) and current (right) images of the product from reaction 2.

**Conductive AFM Results for the As-Received Flake**

Figure 3.18. The current image for the as-received aluminum flake.

### 3.6. Electrochemical Impedance Spectroscopy

EIS measurement of a coated substrate is typically used to determine the barrier properties of the coating as well as monitor the degradation process of the system. The use of EIS as a formulating tool in determining the critical pigment volume concentration

(CPVC) of a coating was first suggested by Lobnig et al. in 2006 [20]. This technique involves detecting the point at which the low frequency impedance drops due to the presence of voids in the coating near the CPVC. While this would have a definite advantage over many other commonly used methods for determining CPVC, it would seem to be limited to nonconductive pigments. In the case of conducting pigments, the percolation threshold, the point at which the pigment particles start to form electrical connections throughout the coating, would be detected by a drastic drop in impedance while the CPVC would be largely unnoticed. When formulating a primer for corrosion prevention using a conductive pigment such as zinc for the cathodic protection of steel, the percolation threshold is a critical point that must be exceeded if an electrical connection is to be made with the substrate. Because a top coat would be applied over the primer for barrier properties, one would be more concerned with far exceeding the percolation threshold and less concerned with porosity introduced by exceeding the CPVC.

This concept is illustrated in Figure 3.19. The measurements were acquired from epoxy primers containing either nonconductive as-received aluminum flake or a conductive PPY/Al flake composite pigment from reaction 1. Prior to EIS measurements being taken, the samples were immersed in dilute Harrison's solution for 3 hours. Notice that for the conductive PPY/Al flake primer, there is a large drop in impedance between a PVC of 30% and 35% while this same drop is not observed for the as-received flake until a PVC of 45%. The drop observed at the lower PVC for the conductive pigment would be indicative of the percolation threshold while the impedance drop observed at the higher PVC for the non-conductive pigment would be more closely associated with the CPVC. Also it is important to note that at a PVC of 35% the impedance of the PPY/Al flake composite primer drops

below the impedance observed for bare aluminum 2024. There are several ways in which this behavior could be caused. One possibility is that the polypyrrole is interacting with the oxide layer present on the aluminum 2024. If the coating were thinning the resistive oxide layer on the substrate, possibly via the attack of sulfate ions released from the polypyrrole, a lower impedance would be observed. Another possibility is that at a PVC of 35%, the coating is sufficiently above its CPVC to become porous enough to allow the rapid ingress of electrolyte. If the electrolyte was able to move through the coating to areas outside of the electrochemical cell, it would effectively increase the area over which the measurement was made thereby decreasing the observed impedance.

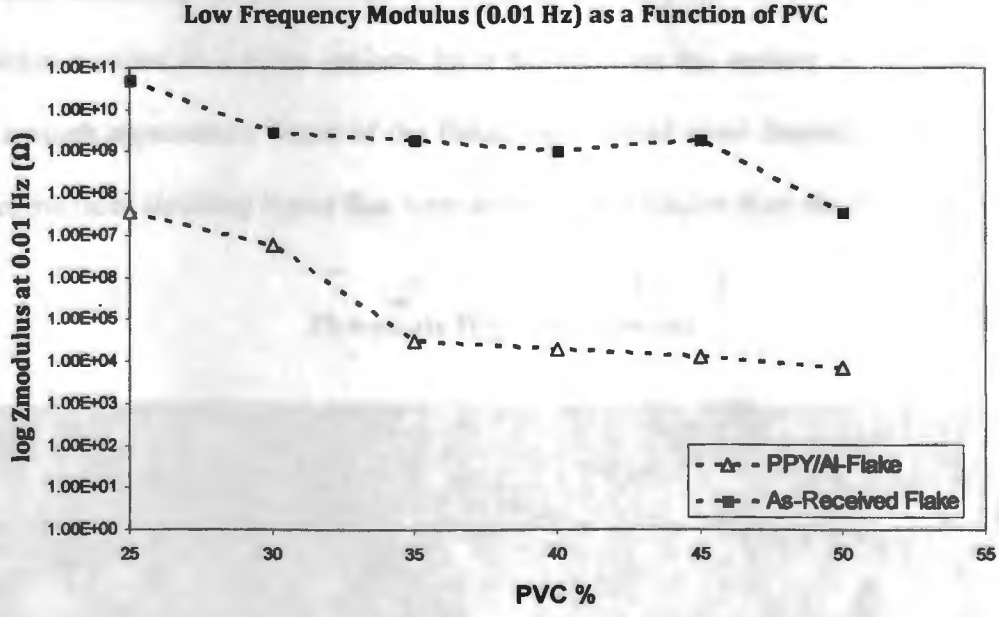


Figure 3.19. A graph of low frequency impedance at 0.01 Hz vs. PVC.

### 3.7. The Effect of Corrosion Inhibiting Dopants

The other synthetic variable that was investigated in this study was the dopant ion. Various dopant ions that have been shown to inhibit corrosion were incorporated into the

polypyrrole composite pigment to determine their effect on the deposition of the polypyrrole and its performance as a corrosion inhibitor.[21-23] The details of these synthesis reactions can be seen in Table 2.2. As can be seen in Figures 3.20-3.23, the different dopant ions had a large effect on the morphology of the product deposited onto the aluminum flake.

It is evident that the sample doped with phosphate displays similar morphology to the sample doped with sulfate with several flakes agglomerated together in lamellar particles that are held together with polypyrrole. The presence of molybdate however resulted in poor deposition of polypyrrole onto the flake with small clumps spread out somewhat uniformly on the surface of the flake. The presence of vanadate during the deposition resulted in a more uniform layer formed over the surface of the flakes giving them a rough appearance. Some of the flakes experienced more deposition of polypyrrole on their surfaces resulting layers that were several times thicker than the flakes themselves.

**Phosphate Doped Composite**

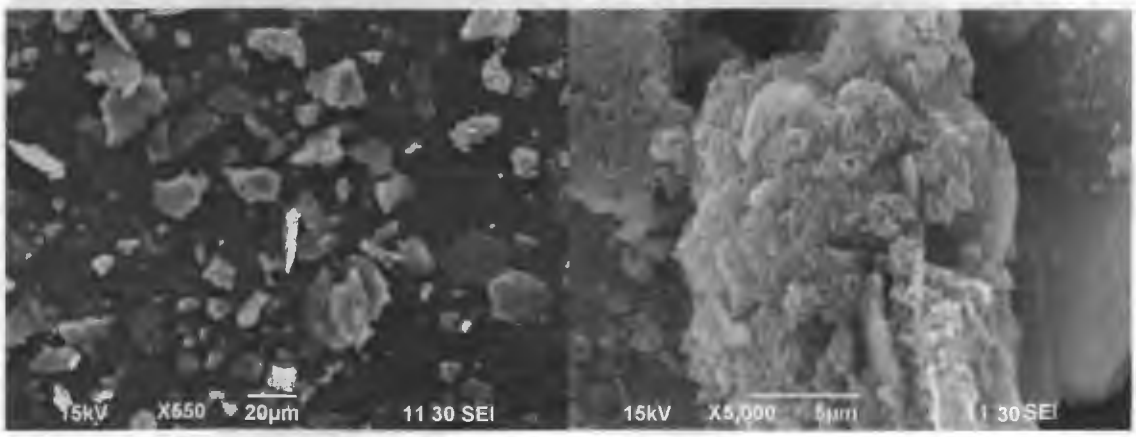


Figure 3.20. SEM micrographs of the flake synthesized in the presence of sodium phosphate.

It has been observed in previous work that the counterion incorporated into polypyrrole can have large effects on the micro-morphology of the deposited pyrrole.[24-26] Indeed, the effect of counterions on the morphology of polypyrrole has been found to be substantial. These effects are related to the size and therefore steric effects of the counterion as well as the charge, solubility, and concentration in the polypyrrole, with higher concentrations resulting in more pronounced effects. Because molybdenum and phosphorous have very similar cationic radii, it is likely that the morphology differences are due to difference in charge as well as solubility. Another factor may be that the molybdate is forming complexes with the catechol in solution which prevents the catechol from reaching the surface of the flake to aid polypyrrole deposition.

**Molybdate Doped Composite**

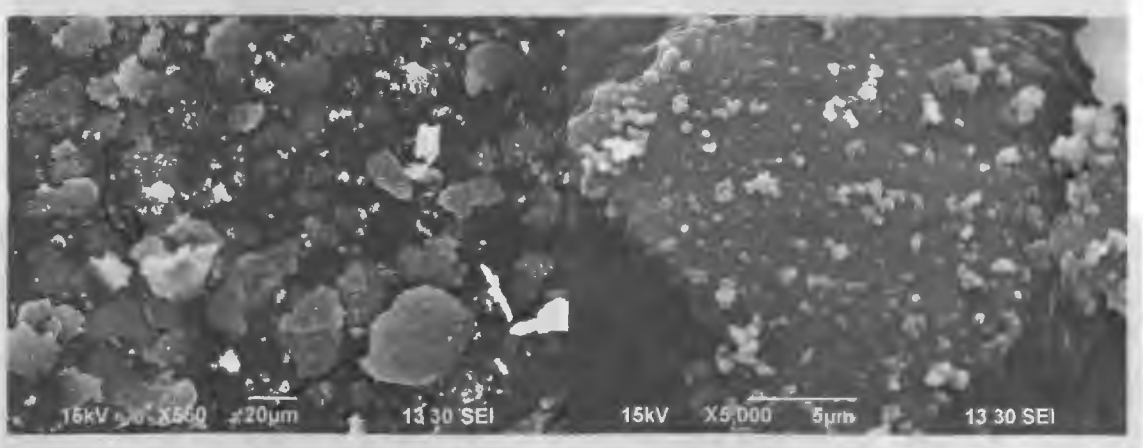


Figure 3.21. SEM micrographs of the flake synthesized in the presence of molybdate.

The reaction carried out with stannate behaved very differently from the other reactions in this study. After 10-15 minutes of stirring in the presence of the aluminum flake, the stannate began to react with the flake evolving a colorless gas and heat. This is

assumed to be hydrogen evolved from the corrosion of the flake. After this reaction had ended, the pH of the mixture was measured with a piece of pH paper which revealed the pH to be between 12 and 13. Once all reactants had been added to the Erlenmeyer flask, the strong odor of ammonia was evident above the flask. This is likely the result of adding ammonium persulfate to a basic solution which would deprotonate the ammonium ions forming ammonia.

**Vanadate Doped Composite**


Figure 3.22. SEM micrographs of the flake synthesized in the presence of vanadate.

**Stannate Doped Composite**

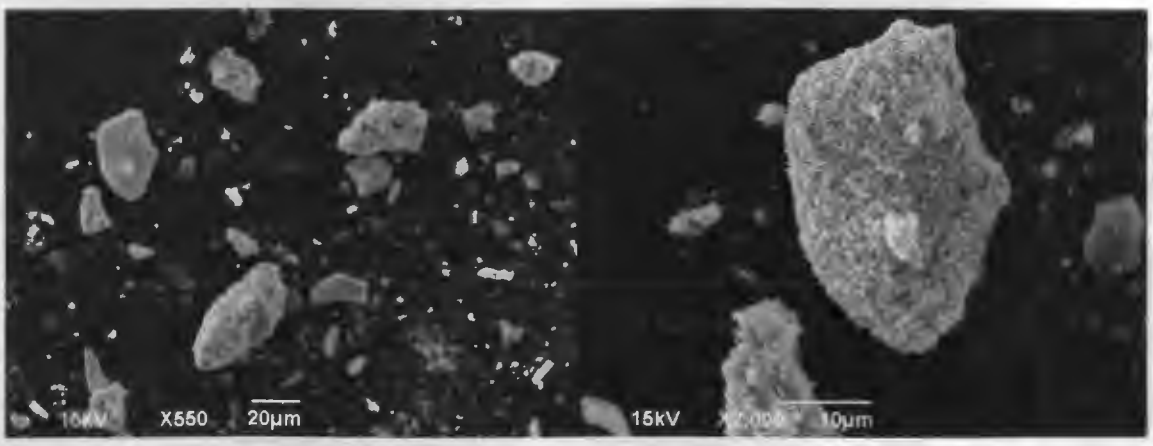


Figure 3.23. SEM micrographs of the flake synthesized in the presence of stannate.

This reaction did not appear to deposit polypyrrole onto the surface of the particles as they were white in color with a slight yellow tint when they were filtered from the reaction mixture. After drying, the particles turned a light brown color. The liquid portion of the reaction mixture retained its dark color after filtration indicating that pyrrole oligomers were likely present. These oligomers were also likely to be overoxidized due to the high pH of the solution which would increase their solubility. It has been shown by Beck et al. that above a pH of 10, the overoxidation potential actually shifts to a negative value.[27] This indicates that there is a negative Gibb's free energy change associated with the overoxidation and therefore, it will happen spontaneously with no driving potential required. Keeping in mind that there are persulfate ions present which are fairly strong oxidizing agents, it is very likely that the polypyrrole is overoxidized and therefore unusable as a corrosion inhibitor.

A density experiment was conducted on the samples to determine if the dopant ion had an effect on the amount of polypyrrole that was unattached to the flake. These results are shown in Figure 3.24. This experiment was not performed for the sample synthesized in the presence of stannate because the product was a light brown powder which quite obviously did not contain polypyrrole. It is apparent from the images that the vanadate doped sample does not have any visible floating particulates indicating that the great majority of the vanadate doped polypyrrole is attached to the aluminum flake. The phosphate doped pigment has a small amount of suspended particles but none that are floating on the surface. The molybdate doped pigment, however, has a large number of suspended particles which is consistent with the SEM images in Figure 3.21. This

indicates that the molybdate, in some way, impedes the deposition of polypyrrole onto the surface of the aluminum flake.

Particle size measurements of the different pigments were taken to determine what effect the dopant ion may have on particle size. These results are shown in Figures 3.25-3.30. The number weighted statistics of these results are summarized in Table 3.1. It is evident that neither the mean size of the pigment nor the standard deviation of that mean was greatly affected by the dopant ion used. The synthesis process did decrease the mean diameter of the flakes which is likely due to the grinding process which could easily fracture the flakes thereby decreasing their diameter and increase the ratio of small particles to larger particles which could be responsible for the change in the particle size distribution with the mode changing from approximately 10 μm in the flake before the synthesis process to 1.6 μm after the synthesis process. The pigment synthesized in the presence of stannate is an exception.

**Effect of Dopant on Density Experiments**

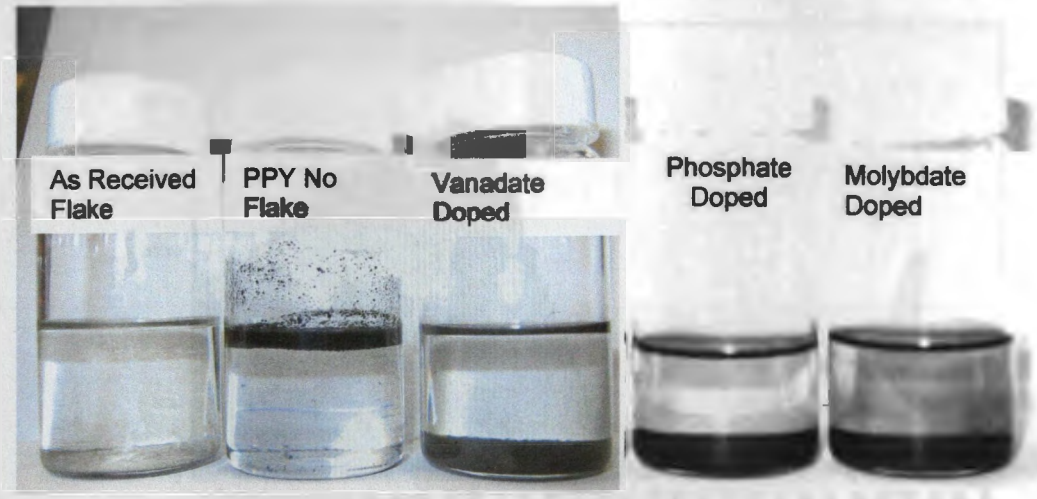


Figure 3.24. The density experiments for the composite pigments doped with corrosion inhibiting pigments.

Table 3.1. The number weighted means and standard deviations for the measured particles size distributions showing the effect of different dopants.

| Sample | Sample Mean Diameter (μm) | Standard Deviation (μm) |
|---|---|---|
| Sulfate Doped | 4.8 | 4.9 |
| Phosphate Doped | 5.6 | 5.6 |
| Molybdate Doped | 4.8 | 5.3 |
| Vanadate Doped | 3.7 | 3.9 |
| Stannate Sample | 5.5 | 4.4 |
| As Received Flake | 8.7 | 6.6 |

*Standard Deviations that are smaller than the means are not necessarily expected because the particle size distributions are not normal distributions.

The synthesis reaction caused the flakes to grow an oxide layer which contained large amounts of tin, oxygen, and nitrogen. The growth of the oxide layer caused the pigment particles to have a more spherical shape that would be harder to break the edges off of. This resulted in a particle size distribution with a more Gaussian shape with the mode around 3.5 μm. The elemental compositions of the samples doped with corrosion inhibiting dopants as measured by EDX are shown in Table 3.2.

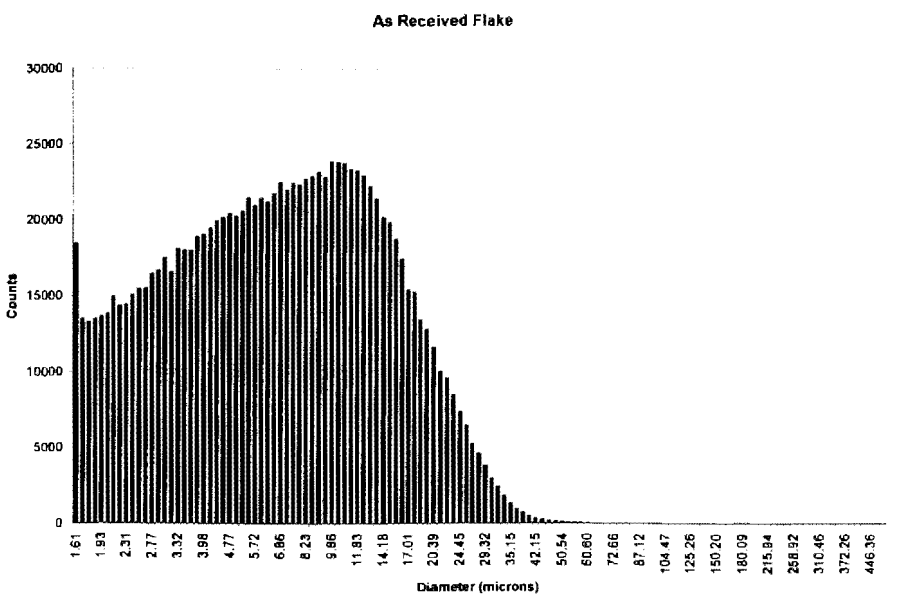


Figure 3.25. The particle size distribution for the as received flake.

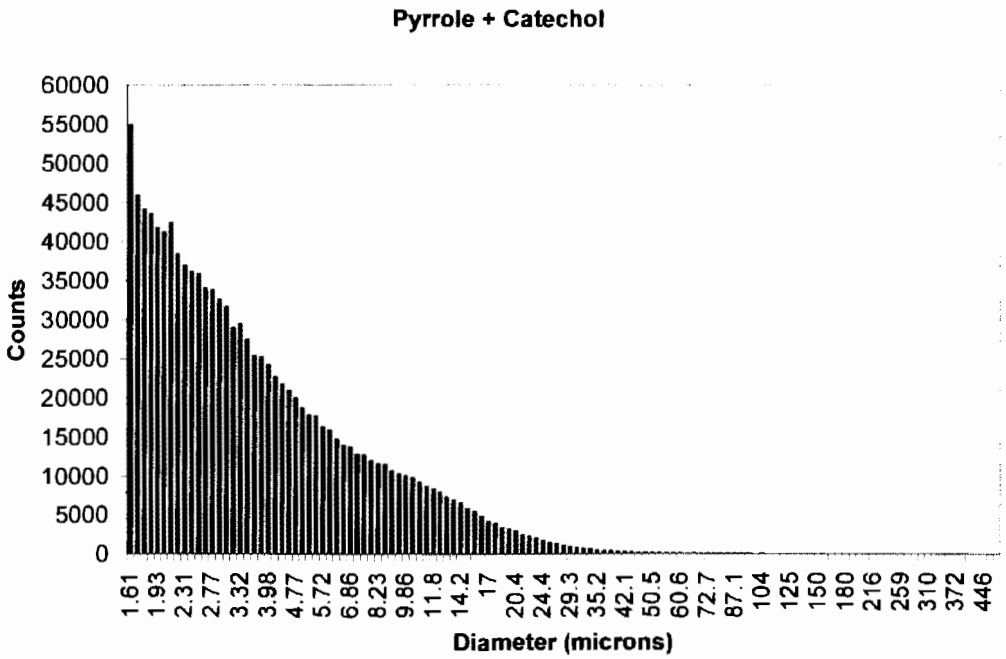


Figure 3.26. The particle size distribution for the pigment doped with sulfate.

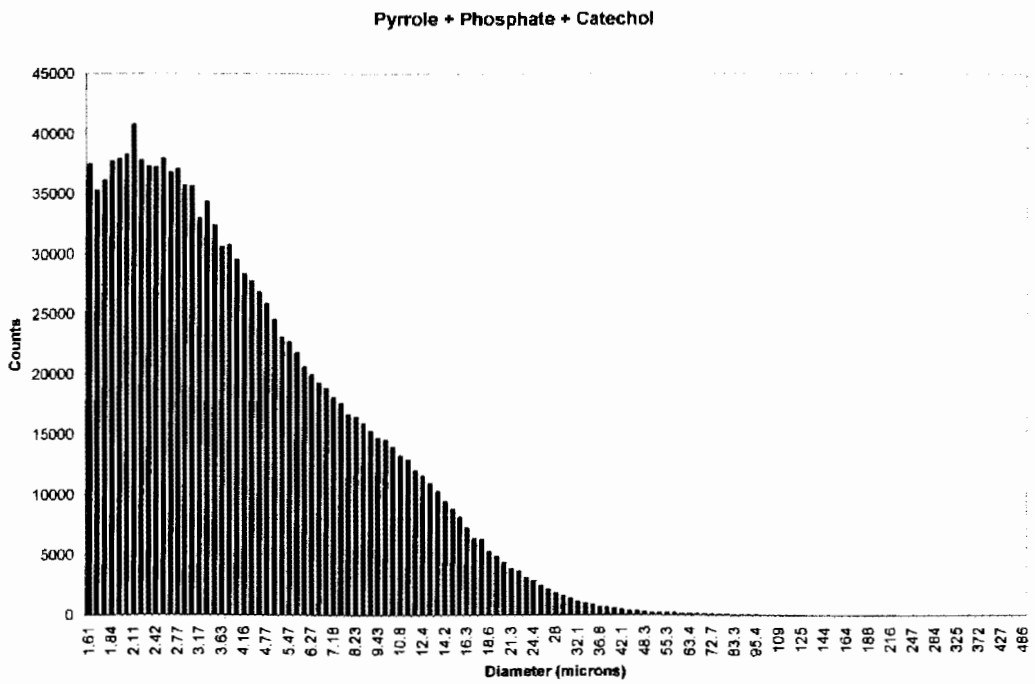


Figure 3.27. Particle size distribution for the pigment doped with phosphate.

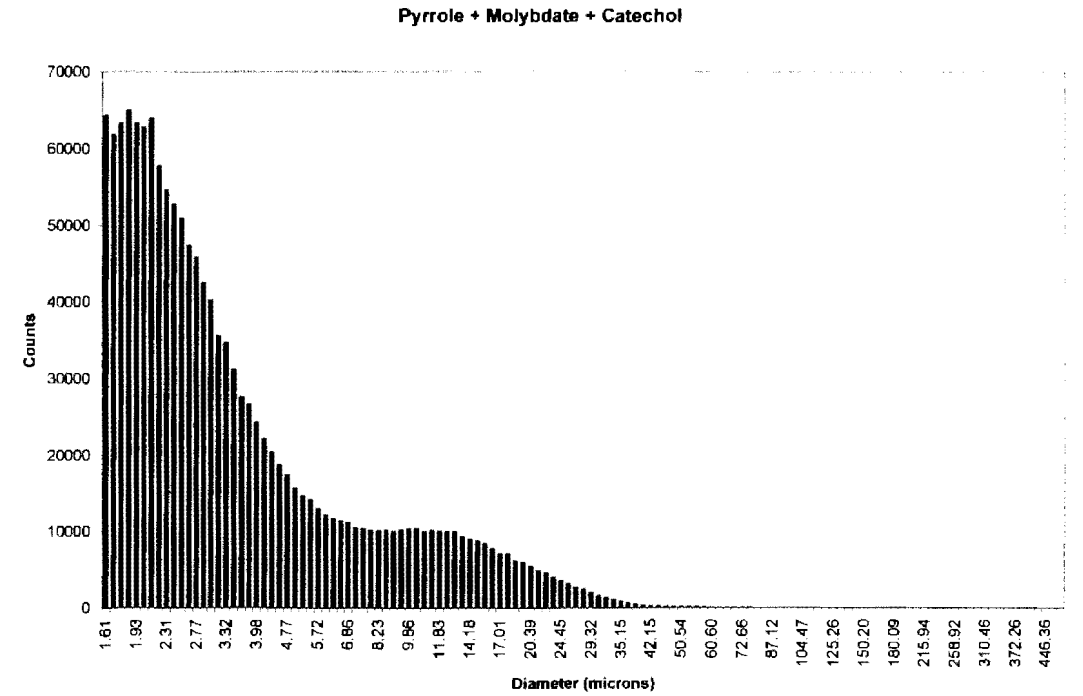


Figure 3.28. The particle size distribution for the pigment doped with molybdate.

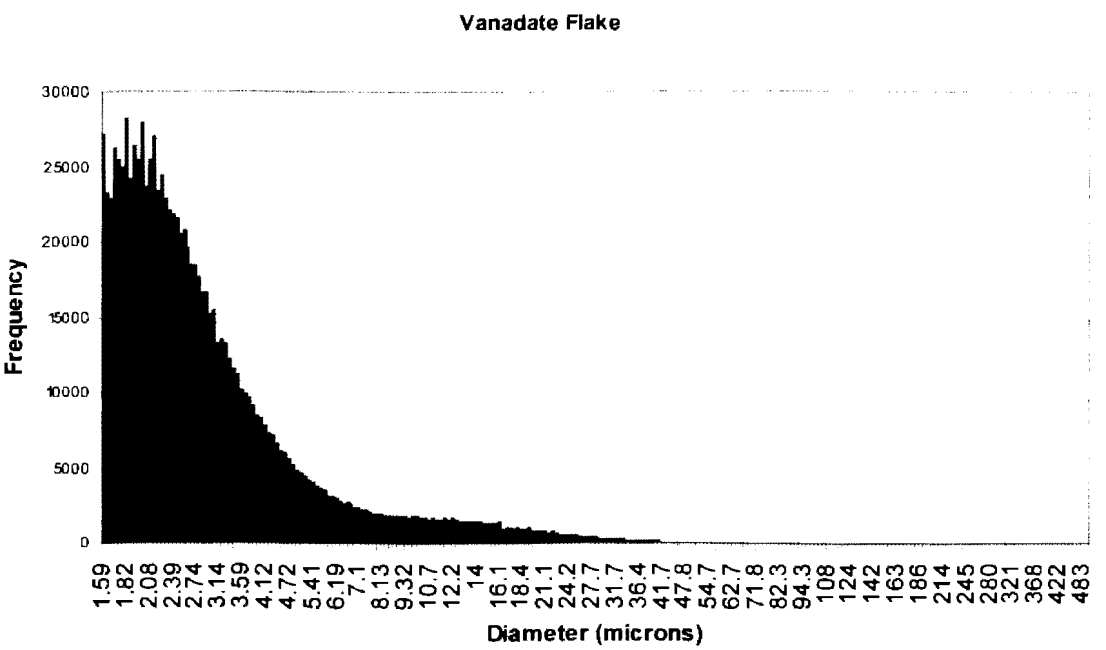


Figure 3.29. The particle size distribution for the pigment doped with vanadate.

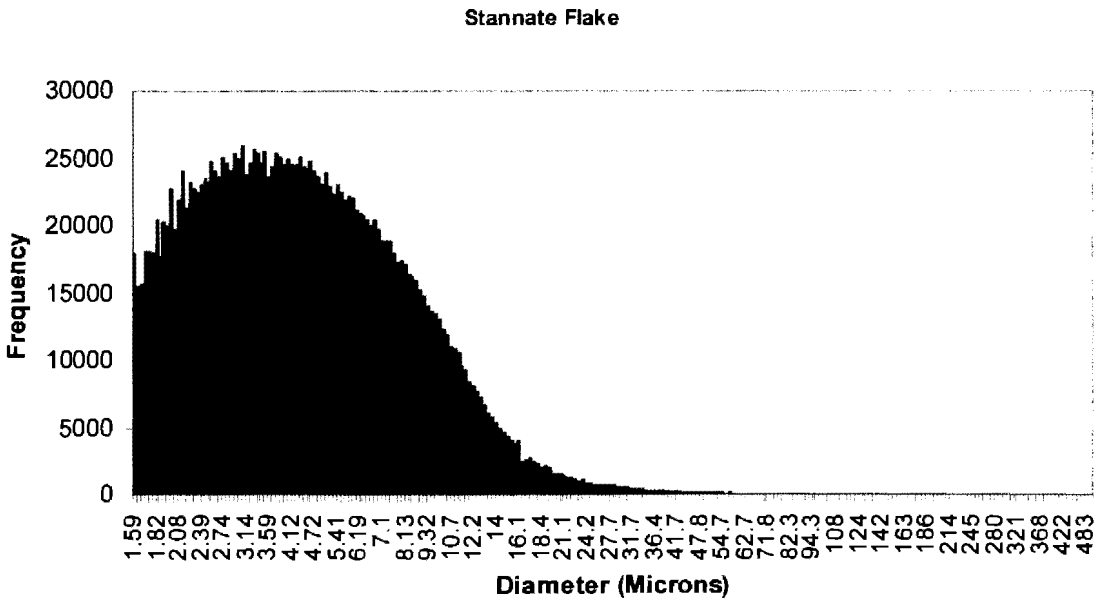


Figure 3.30. The particle size distribution for the pigment synthesized in the presence of stannate.

The pigment that was doped with molybdate had a lower carbon content and a higher aluminum content than the samples that were doped with vanadate or phosphate. This is likely due to the fact that less material appeared to be deposited onto the surface of the flake when molybdate was present. Looking at the sample synthesized in the presence of stannate, there is much less carbon on the surface of the particles and a large amount of oxygen. There is also twice as much tin as aluminum. This indicates that very little carbon was deposited onto the surface and instead, an oxide layer was formed on the surface of the flakes. This is not all that surprising as stannate is used for conversion coatings and therefore forms a stable oxide layer on the metal surface.[28] The high pH produced by this reaction however increases the likelihood that overoxidation of the polypyrrole will take place rendering it useless.

Table 3.2. The elemental composition of the pigments doped with corrosion inhibiting dopants expressed as percentages of the total atoms detected.

| Sample | C ± 3σ | Al ± 3σ | N ± 3σ | O ± 3σ | Mo ± 3σ | V ± 3σ | Sn ± 3σ | P ± 3σ | S ± 3σ |
|---|---|---|---|---|---|---|---|---|---|
| Molybdate Doped | 56.8 ± 2.6 | 24.7 ± 0.2 | 5.3 ± 5.6 | 12.6 ± 1.4 | 0.5 ± 0.2 | 0.0 ± 0.0 | 0.0 ± 0.0 | 0.0 ± 0.0 | 0.0 ± 0.23 |
| Vanadate Doped | 74.1 ± 1.7 | 8.9 ± 0.1 | 6.3 ± 4.0 | 9.3 ± 0.8 | 0.0 ± 0.0 | 1.3 ± 0.1 | 0.0 ± 0.0 | 0.0 ± 0.0 | 0.1 ± 0.0 |
| Phosphate Doped | 71.8 ± 1.7 | 6.3 ± 0.1 | 6.9 ± 4.5 | 13.3 ± 0.9 | 0.0 ± 0.0 | 0.0 ± 0.0 | 0.0 ± 0.1 | 1.4 ± 0.3 | 0.3 ± 0.1 |
| Stannate Doped | 19.6 ± 3.1 | 5.3 ± 0.3 | 15.3 ± 4.1 | 49.4 ± 2.5 | 0.0 ± 0.0 | 0.0 ± 0.0 | 10.4 ± 0.5 | 0.0 ± 0.0 | 0.0 ± 0.0 |

## 3.8. Conclusion

Polypyrrole composites were prepared under various experimental conditions. It was determined through SEM that the morphology of the deposited material depended greatly on the reactants used during the synthesis. Reactions 1, 1x, and 3 resulted in flakes that were joined together. Reactions 4 and 4x resulted in small particulates which preferentially deposited on the edges of the aluminum flake. Reaction 5 produced sporadic coverage of the flakes, with a majority of the flake being uncoated by the deposited product.

The density experiment determined that a majority of the product was attached to the flake for reactions 1, 1x, 2, 4, 4x, 5, and 6. Reaction 3 displayed unique results where all of the product was suspended in the liquid, which is most likely related to the tissue-like appearance of the product that was found during the SEM study.

For the XPS, C-AFM, and electrochemical impedance spectroscopy (EIS) experiments, the study focused on the product from reactions 1 and 2. It was found that the product may be a co-polymer or composite formed between the pyrrole and catechol. The results from reaction 1 also seemed to show that the dopant was sulfate ions from the

ammonium persulfate. The C-AFM detected a conductive surface with a conductivity of 1.6 S/cm for reaction 1 and 5.2 S/cm for reaction 2. EIS was used to assist in the formulating of a conductive coating where it was determined that a 45% PVC would be sufficient for a low impedance coating of the polypyrrole composite flake. These results combined with the Conductive AFM results indicate that conductive polypyrrole was deposited onto the surface of the aluminum flake and that the composite pigment is capable of forming percolation networks through an epoxy binder.

It was also found that the dopant ion had a large effect on the morphology of the deposited polypyrrole and the degree to which the polypyrrole was attached to the aluminum flake. Vanadate and phosphate provided the best deposition of polypyrrole on to the aluminum flake along with sulfate when catechol and phloroglucide were present.

### 3.9. References


1. 2010 S. A. P., *MSDS No. EA-0561G.* 2005, Louisville, KY: Eckhart America.
2. Wicks Z. W., Jones F. N., and Pappas S. P., *Organic Coatings Science and Technology.* 2nd Edition ed. 1999, New York: Wiley-Interscience.
3. Dai T., Yang X., and Lu Y., *Controlled growth of polypyrrole nanotubule/wire in the presence of a cationic surfactant.* Nanotechnology, 2006. **17**: p. 3028-3034.
4. Zhang X., Zhang J., Liu Z., and Robinson C., *Inorganic/organic mesostructure directed synthesis of wire/ribbon-like polypyrrole nanostructures.* Chemical Communications, 2004(16): p. 1852-1853.
5. Lu G., Li C., and Shi G., *Polypyrrole micro- and nanowires synthesized by electrochemical polymerization of pyrrole in the aqueous solutions of pyrenesulfonic acid.* Polymer, 2006. **47**(6): p. 1778-1784.
6. Xu Q., Meng G., Han F., Zhao X., Kong M., and Zhu X., *Controlled fabrication of gold and polypyrrole nanowires with straight and branched morphologies via porous alumina template-assisted approach.* Materials Letters, 2009. **63**(16): p. 1431-1434.
7. Yun M., Myung N., Vasquez R., Lee C., Menke E., and Penners R., *Electrochemically grown wires for individually addressable sensor arrays.* Nano letters, 2004. **4**(3): p. 419-422.
8. Dong B., Krutschke M., Zhang X., Chi L., and Fuchs H., *Fabrication of polypyrrole wires between microelectrodes.* Small, 2005. **1**(5): p. 520-524.

9. Carswell A., Edgar A., and Grady B., *Adsorbed surfactants as templates for the synthesis of morphologically controlled polyaniline and polypyrrole nanostructures on flat surfaces: From spheres to wires to flat films.* J. Am. Chem. Soc, 2003. **125**(48): p. 14793-14800.
10. Jerome C., Labaye D., Bodart I., and Jerome R., *Electrosynthesis of polyacrylic/polypyrrole composites: Formation of polypyrrole wires.* Synthetic Metals, 1999. **101**(1-3): p. 3-4.
11. Kros A., Linhardt J., Bowman H., and Tirrell D., *From giant vesicles to filaments and wires: Templates for conducting polymers.* Advanced Materials, 2004. **16**(8): p. 723-726.
12. Wang J., Mo X., Ge D., Tian Y., Wang Z., and Wang S., *Polypyrrole nanostructures formed by electrochemical method on graphite impregnated with paraffin.* Synthetic Metals, 2006. **156**(7-8): p. 514-518.
13. Joo J., Lee J., Lee S., Jsng K., Oh E., and Epstein A., *Physical characterization of electrochemically and chemically synthesized polypyrroles.* Macromolecules, 2000. **33**(14): p. 5131-5136.
14. Pfluger P. and Street G. B., *Chemical, Electronic, and Structural Properties of Conducting Heterocyclic Polymers: A View by XPS.* Journal of Chemical Physics, 1984. **80**(1): p. 544-553.
15. Atanasoska L., Naoi K., and Smyrl W., *XPS studies on conducting polymers: polypyrrole films doped with perchlorate and polymeric anions.* Chemistry of Materials, 1992. **4**(5): p. 988-994.
16. Lim V., Li S., Kang E., Neoh K., and Tan K., *In situ XPS study of thermally deposited aluminium on chemically synthesized polypyrrole films.* Synthetic Metals, 1999. **106**(1): p. 1-11.
17. Prissanaroon W., Brack N., Pigram P., and Liesegang J., *Electropolymerisation of pyrrole on copper in aqueous media.* Synthetic Metals, 2004. **142**(1-3): p. 25-34.
18. Hepel M., *Composite polypyrrole films switchable between the anion- and cation-exchanger states.* Electrochimica Acta, 1996. **41**(1): p. 63-76.
19. Malitesta C., Losito I., Sabbatini L., and Zambonin P., *Applicability of chemical derivatization - X-ray photoelectron spectroscopy (CD-XPS) to the characterization of complex matrices: case of electrosynthesized polypyrroles.* Journal of Electron Spectroscopy and Related Phenomena, 1998. **97**(3): p. 199-208.
20. Lobnig R., Villalba W., Goll K., Vogelsang J., Winkels I., Schmidt R., Zanger R., and Soetemann J., *Development of a new experimental method to determine critical pigment-volume-concentrations using impedance spectroscopy.* Progress in Organic Coatings, 2006. **55**(4): p. 363-374.
21. Bethencourt M., Botana F. J., Calvino J. J., Marcos M., and Rodriguez-Chacon M. A., *Lanthanide compounds as environmentally-friendly corrosion inhibitors of aluminium alloys: a review.* Corrosion Science, 1998. **40**(11): p. 1803-1819.
22. Jones D., *Corrosion.* 2nd ed. Corrosion in Selected Corrosive Environments. 1996, Upper Saddle River, NJ: Prentice Hall.
23. Inhibitors-Current C., *Inorganic/organic hybrid coatings for aircraft aluminum alloy substrates.* Progress in Organic Coatings, 2001. **41**: p. 226-323.

24. Sengupta P., Kar P., and Adhikari B., *Influence of dopant in the synthesis, characteristics and ammonia sensing behavior of processable polyaniline.* Thin Solid Films, 2009. **517**(13): p. 3770-3775.
25. Osada Y. and De Rossi D., *Polymer sensors and actuators*. 2000: Springer Verlag.
26. Wallace G., Spinks G., Kane-Maguire L., and Teasdale P., *Conductive electroactive polymers: intelligent materials systems*. 2003: CRC.
27. F. Beck P. B., M. Oberst, Ber. Bunsenges, Journal of Physical Chemistry 1987. **91**: p. 967.
28. Lin C., Lin H., Lin K., and Lai W., *Formation and properties of stannate conversion coatings on AZ61 magnesium alloys.* Corrosion Science, 2006. **48**(1): p. 93-109.

# CHAPTER 4.

# THE EVALUATION OF POLYPYRROLE/ALUMINUM FLAKE COMPOSITE PIGMENTS AS CORROSION INHIBITORS

## 4.1. Introduction

After the pigment had been characterized, it was necessary to determine if it would inhibit corrosion on aluminum 2024 and what mechanisms may be responsible for any observed inhibition. The techniques that were used in this evaluation include potentiodynamic polarization, open circuit potential measurements, electrochemical impedance spectroscopy, coupling current measurements, the scanning vibrating electrode technique (SVET), and ASTM B117 accelerated weathering. The variables that were investigated in these experiments were: the oxygen concentration, the presence or absence of aluminum flake, and the dopant ion.

## 4.2. Potentiodynamic Polarization

To determine the effect that the PPY/Al flake composite primer would have on the corrosion of an exposed substrate in a defect area, anodic potentiodynamic polarization was performed on top of a scribe that was 1.5 cm long. This experiment was performed in both an air purged electrolyte and a nitrogen purged electrolyte to determine what role oxygen is playing in the interaction. Pigment synthesized with and without Al flake was also used to determine if the flake was playing a role in the reaction at the defect. The results for the pigment doped with sulfate can be seen in Figures 4.1 and 4.2. These results are useful because they yield information about the thermodynamics and kinetics of a reaction.

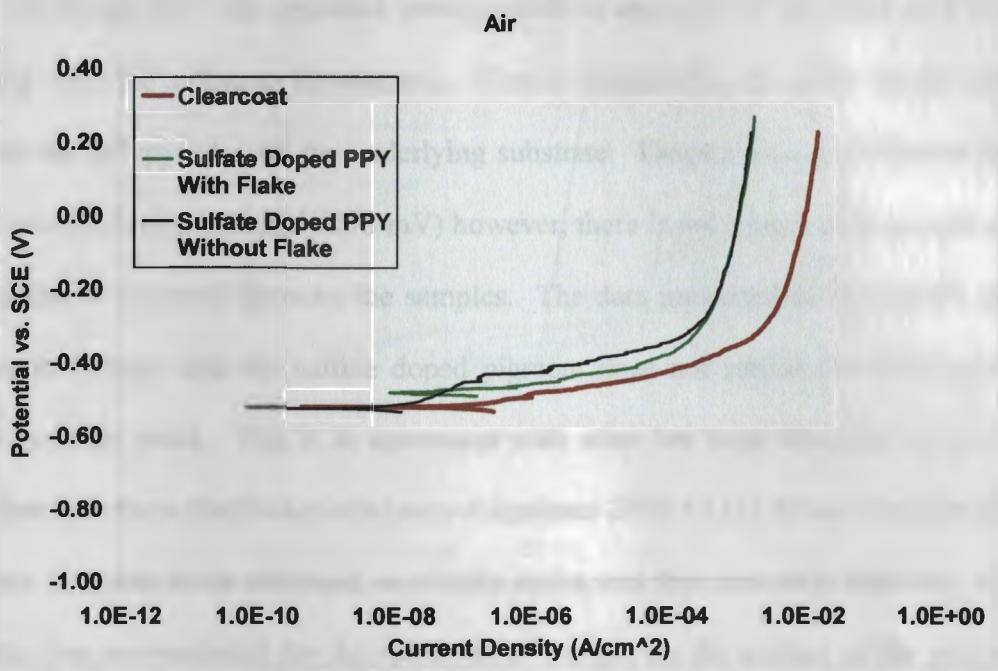


Figure 4.1. The anodic potentiodynamic polarization scan for the sulfate doped pigment in air purged electrolyte.

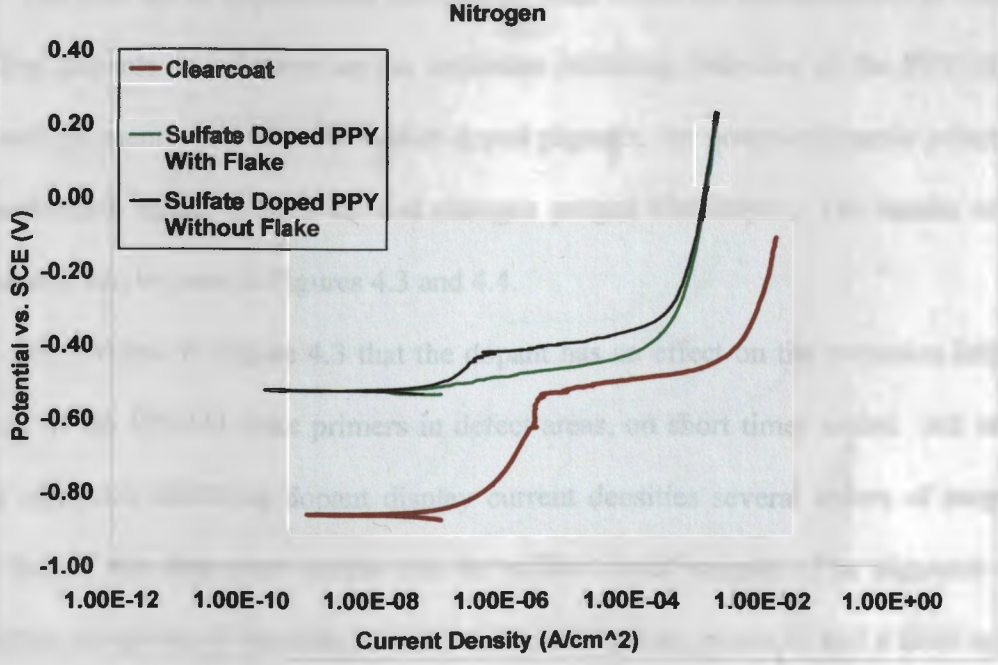


Figure 4.2. The anodic potentiodynamic polarization scan for the sulfate doped pigment in nitrogen purged electrolyte.

In Figure 4.2 , the expected positive shift in open circuit potential as a result of coupling with the substrate is observed. Clearly oxygen has an effect on the coupling between the polypyrrole and the underlying substrate. Despite a large difference in open circuit potential (approximately 275 mV) however, there is not a large difference in current density that is observed between the samples. The data presented in Figures 4.1 and 4.2 appears to indicate that the sulfate doped pigment does not inhibit corrosion to a large extent in defect areas. This is in agreement with what has been observed for pure PPY films that have been electrodeposited onto Aluminum 2024 T3.[1] It was observed that the substrate in defect areas remained anodically active and that corrosion inhibition resulted from the low overpotential for the reduction of oxygen on the surface of the polypyrrole which shifted the location of that reaction to the polypyrrole surface.[1]

The next set of experiments determined what effect the incorporation of corrosion inhibiting dopants would have on the corrosion inhibiting behavior of the PPY/Al flake composite pigments. As with the sulfate doped pigment, the potentiodynamic polarization was performed, again, in both air and nitrogen purged electrolyte. The results of these experiments can be seen in Figures 4.3 and 4.4.

It is evident in Figure 4.3 that the dopant has an effect on the corrosion inhibiting behavior of the PPY/Al flake primers in defect areas, on short times scales. All samples with a corrosion inhibiting dopant display current densities several orders of magnitude below that of the clear coat sample and the sulfate doped sample. The pigments doped with either phosphate or vanadate, display an elevated pitting potential and a more negative open circuit potential (OCP) than the other samples. These open circuit potentials however are still in the range that might be expected for aluminum 2024.

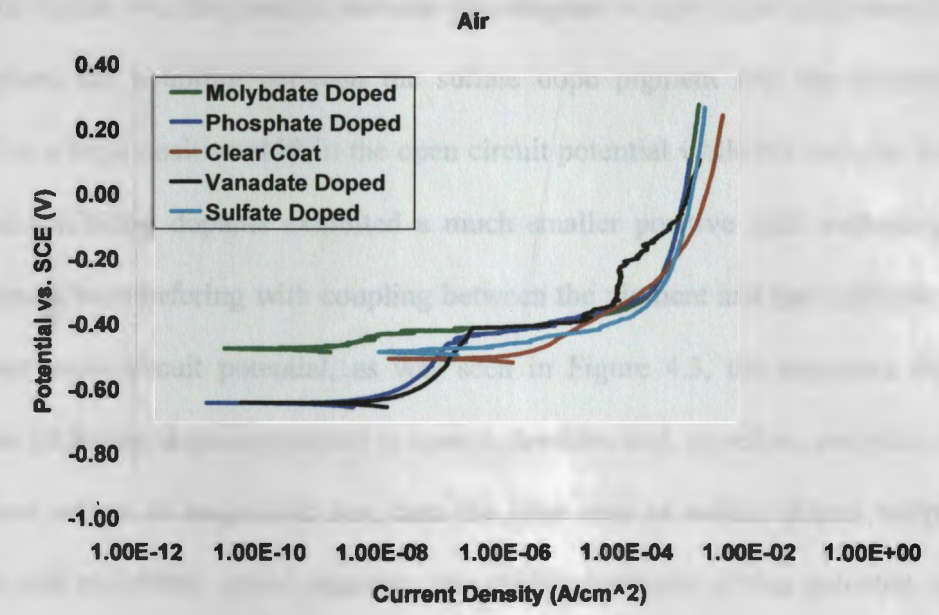


Figure 4.3. The anodic potentiodynamic polarization scan for the differently doped pigments in air purged electrolyte.

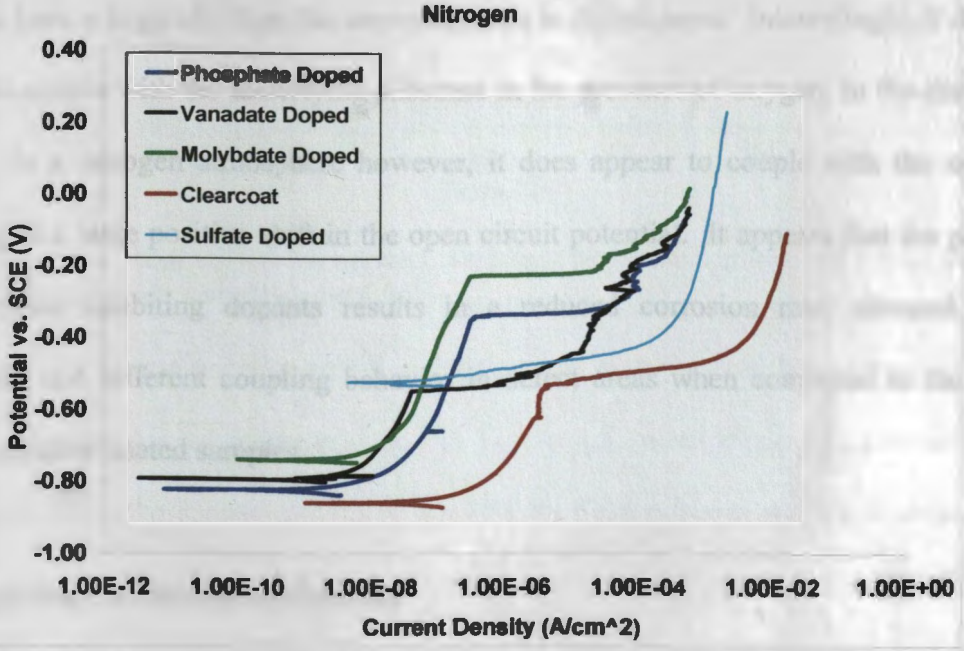


Figure 4.4. The anodic potentiodynamic polarization scan for the differently doped pigments in nitrogen purged electrolyte.

In Figure 4.4, the contrast between the samples is even more pronounced. As was seen before, the coupling between the sulfate dope pigment and the aluminum 2024 resulted in a large positive shift in the open circuit potential while the samples doped with corrosion inhibiting dopants exhibited a much smaller positive shift indicating that the dopants may be interfering with coupling between the pigment and the substrate. Despite this lower open circuit potential, as was seen in Figure 4.3, the pigments doped with corrosion inhibiting dopants resulted in current densities and, therefore, corrosion rates that are several orders of magnitude less than the clear coat or sulfate doped samples. The vanadate and molybdate doped pigments also exhibit increased pitting potential, especially in the case of the molybdate doped sample, which would help prevent rapid pitting corrosion.

From these experiments, it appears that the sulfate doped PPY/Al flake pigment does not have a large effect on the corrosion rates in defect areas. Interestingly, it does not appear to couple with the underlying substrate in the presence of oxygen. In the absence of oxygen, in a nitrogen atmosphere however, it does appear to couple with the substrate resulting in a large positive shift in the open circuit potential. It appears that the presence of corrosion inhibiting dopants results in a reduced corrosion rate, elevated pitting potentials, and different coupling behavior in defect areas when compared to the sulfate doped and clear coated samples.

### 4.3. Coupling Current Measurements

To further investigate the coupling behavior that was observed in the potentiodynamic polarization experiments, coupling current measurements between the

coating and the substrate were performed. As with the potentiodynamic polarization, coupling current measurements were taken in both an air purged electrolyte and a nitrogen purged electrolyte to determine what affect the presence of oxygen has on the coupling behavior of the pigment. In the case of the sulfate doped pigment, samples were made with and without flake to determine what role the flake is playing in the coupling. The results of the measurements for the sulfate doped pigment can be seen in Figures 4.5 and 4.6.

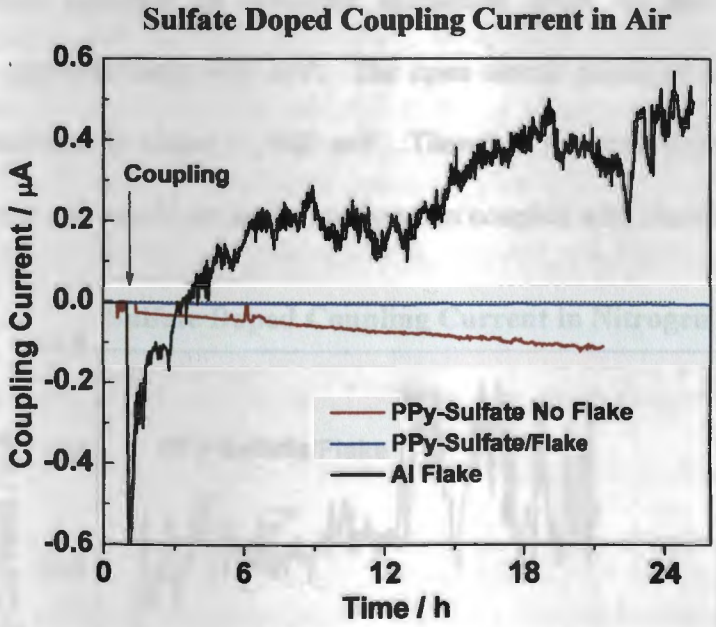


Figure 4.5. The coupling current between variously pigmented primers and their aluminum 2024 substrates in air purged electrolyte.

The data shown in Figure 4.5 and 4.6 agrees with the coupling observations from the potentiodynamic polarization data. In Figure 4.5, when oxygen is present, current flowing between the primer containing the PPY/Al flake pigment and the aluminum 2024 is not observed. Therefore as one would expect, there was not an observed OCP difference between the clear coated sample and the PPY/Al Flake sample in Figure 4.1. When the primer is pigmented with sulfate doped polypyrrole without flake being present, negative

coupling current is observed indicating that the polypyrrole is acting as the cathode in the electrochemical couple. This is to be expected as the polypyrrole has a much more noble OCP than the aluminum 2024 substrate. Interestingly, the primer containing pure aluminum flake displays positive coupling current when coupled with a uncoated sample of aluminum 2024. This indicates that the coating is acting as the anode in the cell, and thus, is sacrificially protecting the uncoated aluminum 2024. This is not entirely unexpected. The open circuit potential of uncoated aluminum 2024, in the conditions of this experiment, is approximately -650 mV. The open circuit potential of pure aluminum in these same conditions is closer to -900 mV. Therefore the pure aluminum would be the more active metal and would act as the anode when coupled with aluminum 2024.

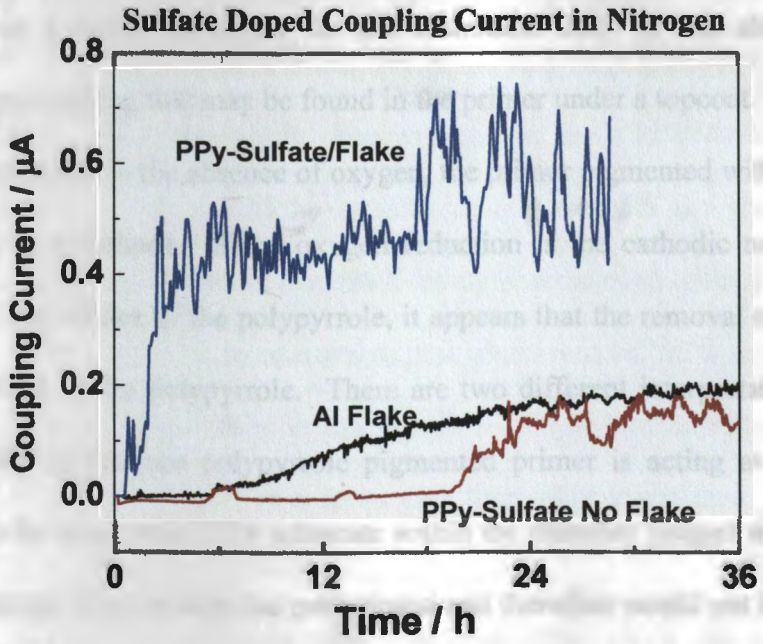


Figure 4.6. The coupling current between variously pigmented primers and their aluminum 2024 substrates in nitrogen purged electrolytes.

*Reprinted from Electrochemica Acta, 54(2), Yan M., Tallman D. E., and Bierwagen G. P., Role of oxygen in the galvanic interaction between polypyrrole and aluminum alloy: p. 220-227. 2008 with permission from Elsevier.*

Figure 4.6 is a plot of the data when the polypyrrole coated sample is in a nitrogen atmosphere during the coupling current measurement. In the absence of oxygen, very different coupling behavior is observed. After a short induction period of 36 minutes, the PPY/Al flake pigmented primer exhibited a sharp increase in positive current indicating that the pigment is acting as the anode in the electrochemical couple with aluminum 2024. In the case of the primer containing only aluminum flake, positive current was also observed but only after a much longer induction period of approximately 6 hours. Also, the current observed for this sample was only half or at some points in time a third as much as was observed for the PPY/Al flake primer. This indicates that the polypyrrole is activating the aluminum flake towards anodic dissolution which increases the flakes ability to function as a sacrificial anode for the aluminum 2024 in the absence of oxygen. Conditions approaching this may be found in the primer under a topcoat.

Interestingly, in the absence of oxygen, the primer pigmented with pure polypyrrole does not act as a cathode. Since oxygen reduction is the cathodic reaction that would dominate on the surface of the polypyrrole, it appears that the removal of oxygen prevents cathodic activity in the polypyrrole. There are two different interpretations for this data. One possibility is that the polypyrrole pigmented primer is acting as the cathode in a reaction with the aluminum 2024 substrate within the chamber purged with nitrogen. This current would not flow through the potentiostat and therefore would not be measured. This reaction would likely be a slow process as it would be happening at the coating/substrate interface and so would be diffusion limited. This reaction would be reducing the polypyrrole which, when reduced, could act as an anode when coupled with the uncoated aluminum 2024. The slow rate of reaction would be the reason for the long induction

period of approximately 21 hours before uninterrupted positive current is observed for the sample.

The other interpretation would be that the polypyrrole is activating the aluminum 2024 sample in the nitrogen purged compartment, which it is in contact with, to anodic activity similar to the effect that it had on the pure aluminum flake. The reason for the much longer induction time and the lower observed current flow would be the large ohmic drop associated with the resistive epoxy binder surrounding the polypyrrole particles as well as the fact that the aluminum 2024 has a more noble OCP than the pure aluminum in these conditions meaning that it would be less anodically active. The polypyrrole would have less contact with the underlying substrate in comparison to the PPY/Al flake coating so diffusion of the electrolyte through the coating would be needed to decrease the ohmic drop to a point where the reaction could take place on a large enough scale to produce the observed current. This same ohmic drop would exist in the PPY/Al flake sample, but in this case, the polypyrrole would be in intimate contact with the aluminum flake. In addition, the pigment particles are dispersed throughout the coating meaning the electrolyte would be in contact with the more reactive pure aluminum before it reaches the substrate. This suggests that the ohmic drop in this sample would be decreased to a point where the anodic reaction can take place at a faster rate than what is observed for the pure PPY pigmented coating resulting in a reduced induction time.

The next set of experiments investigated what effect the different corrosion inhibiting dopants would have on the coupling behavior between the PPY/Al flake composites and the aluminum 2024. From the results obtained for the sulfate doped pigments, it appears that the PPY is activating the aluminum flake to act as a sacrificial

anode. If corrosion inhibitors were released from the PPY however it could conceivably slow or stop this reaction. The results from these experiments can be seen in Figures 4.7 and 4.8.

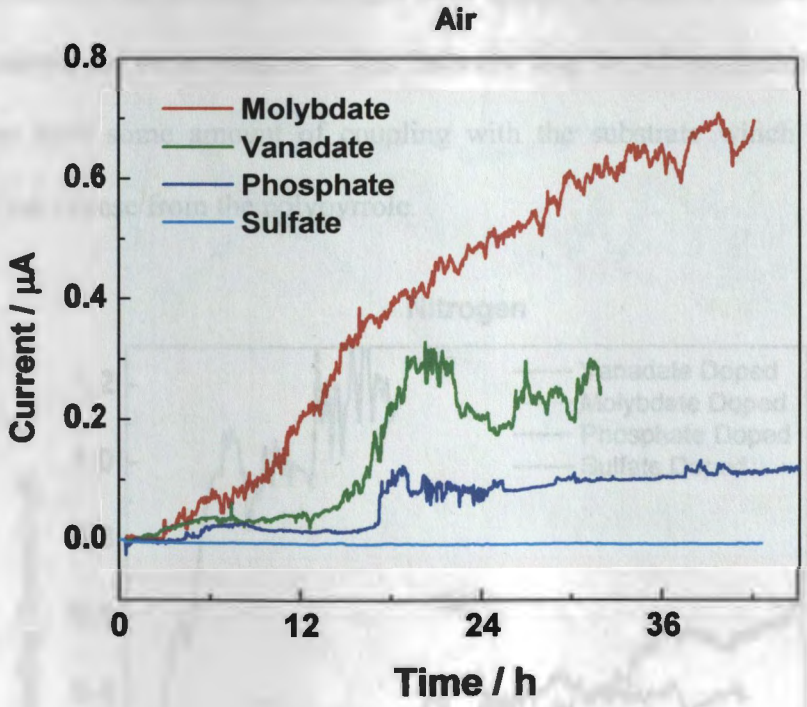


Figure 4.7. The galvanic coupling current between the PPY/Al flake composite pigments with different dopants and aluminum 2024 in air purged electrolyte.

It is evident from Figures 4.7 and 4.8 that the dopants incorporated into the polypyrrole have a large effect on the coupling behavior of the pigment. The sample doped with molybdate in comparison to the sulfate doped sample is one of the most extreme examples. It is observed that the coupling behavior of the molybdate doped pigment reacts in exactly the opposite way to the presence or absence of oxygen in comparison to the sulfate doped sample. While the sulfate doped sample does not exhibit any appreciable coupling in the air purged electrolyte, the molybdate doped sample has the highest amount of coupling current out of all the samples. In the nitrogen purged electrolyte however, it is

the sulfate doped sample that exhibits the highest amount of coupling current while the molybdate has a very small amount of coupling current. The samples that are doped with either phosphate or vanadate appear to couple with the substrate whether oxygen is present or not. However, the absence of oxygen does appear to slightly increase the amount of coupling current for these samples. This behavior may be advantageous as the pigments will always have some amount of coupling with the substrate which could aid in the process of ion release from the polypyrrole.

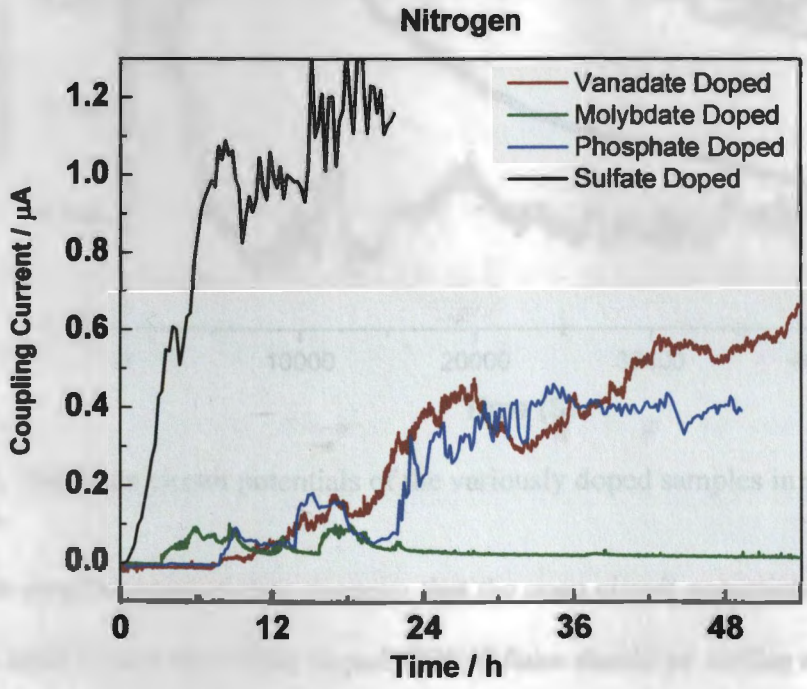


Figure 4.8. The galvanic coupling current between the PPY/Al flake composite pigments with different dopants and aluminum 2024 in nitrogen purged electrolyte.

### 4.4. Open Circuit Potential Measurements

Open circuit potential measurements were performed in air purged electrolyte for 12 hours to investigate what effect the coupling behavior of the coatings had on the open

circuit potentials of the coating/substrate systems. The results from this experiment can be seen in Figure 4.9.

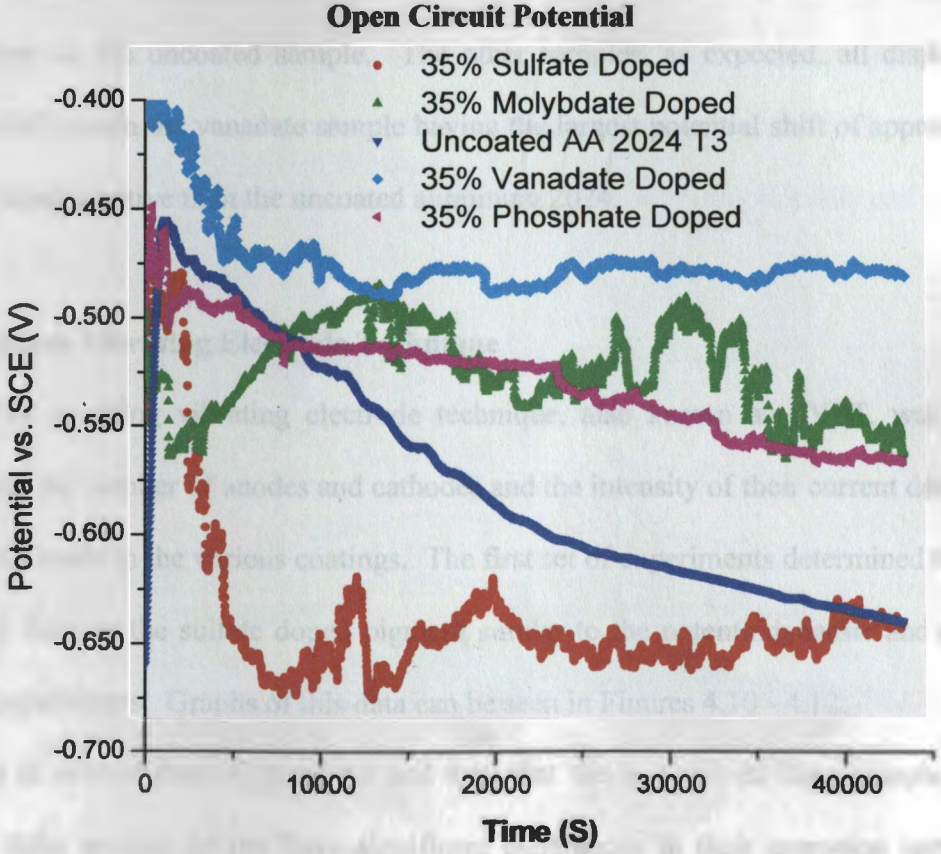


Figure 4.9. The open circuit potentials of the variously doped samples in an oxygen purged electrolyte.

The coupling current data suggests that the open circuit potentials for the uncoated aluminum 2024 T3 and the sulfate doped PPY/Al flake should be similar as the polypyrrole is not coupled to the substrate. In the case of the other pigments, an open circuit potential shifted in the positive direction would be expected. As can be seen in Figure 4.9, the OCPs for the sulfate doped sample and the uncoated aluminum 2024 start at similar potentials and then begin shifting to more negative potentials. The sulfate doped sample reaches an OCP of -0.650 mV vs. SCE, what would be expected for uncoated Al 2024, fairly quickly after immersion while the uncoated sample reaches that potential more slowly. By the end of

the experiment both samples had reached similar potentials. This may be due to interactions between the polypyrrole and the oxide layer on the aluminum 2024 or a thicker oxide layer on the uncoated sample. The other samples, as expected, all display more positive OCPs with the vanadate sample having the largest potential shift of approximately 175 mV more positive than the uncoated aluminum 2024.

### 4.5. Scanning Vibrating Electrode Technique

The scanning vibrating electrode technique, also known as SVET, was used to investigate the number of anodes and cathodes and the intensity of their current density in a defect area made in the various coatings. The first set of experiments determined the effect of the Al flake in the sulfate doped pigment similar to the potentiodynamic and coupling current experiments. Graphs of this data can be seen in Figures 4.10 - 4.12.

It is evident from Figures 4.9 and 4.10 that the as-received flake sample and the PPY/Al flake sample do not have significant differences in their corrosion behavior in defect areas. Both samples have one distinct anode and one distinct cathode within their defect areas with similar current densities. This is in agreement with the potentiodynamic polarization results and show that the sulfate doped PPY/Al flake pigment is not capable of inhibiting corrosion in defect areas. This may be due to the coupling behavior of this pigment. Because this experiment was performed in an electrolyte containing dissolved oxygen, the pigment nearest the defect would be in direct contact with the oxygen containing electrolyte which would prevent coupling between the pigment and the defect area. It also indicates that although the aluminum flake without polypyrrole acts as an anode when coupled with the aluminum 2024, it either does not have enough throwing

power to inhibit corrosion in the defects or does not result in a large enough negative potential shift to result in cathodic inhibition in the defect areas. The sample pigmented with pure PPY also gave results that agree with the potentiodynamic polarization results. Lower current density is observed indicating that the corrosion rate is lower for this sample. The results showing the effect of the corrosion inhibiting dopants can be seen in Figures 4.13, 4.14, and 4.15.

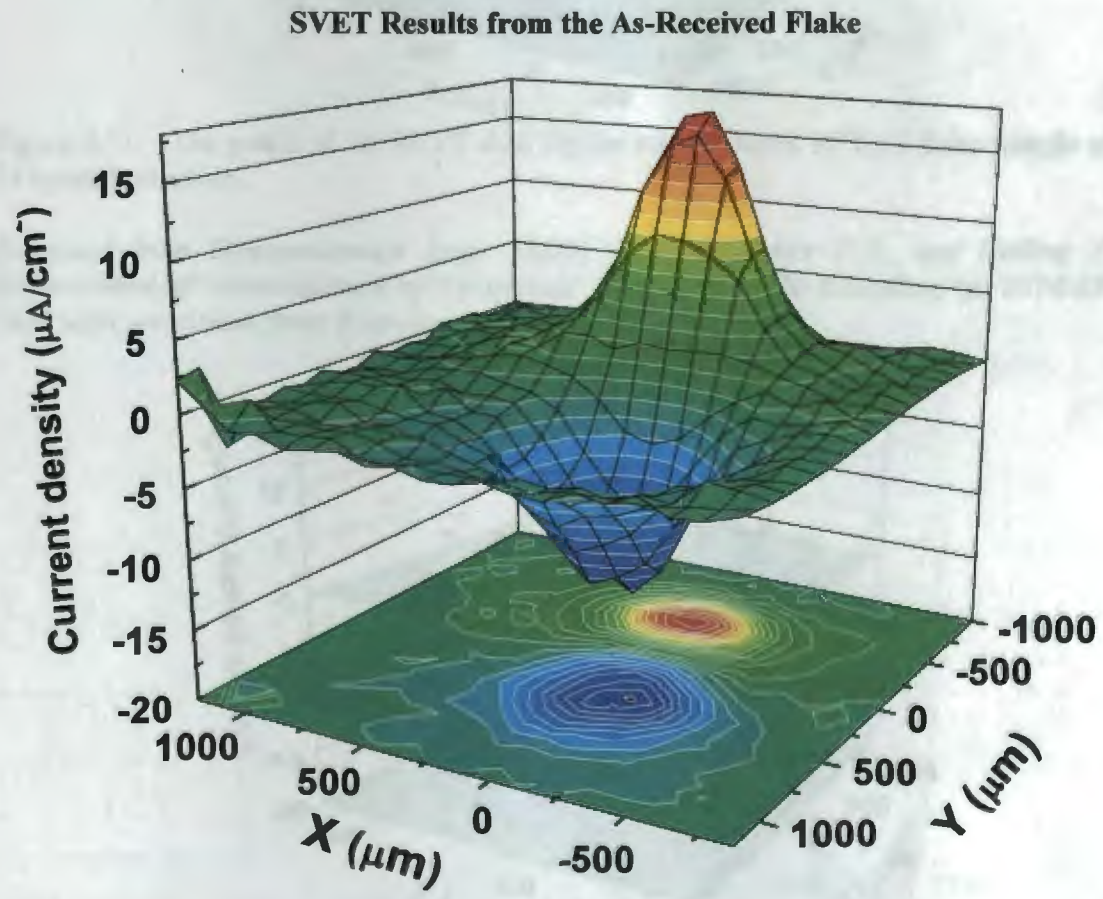


Figure 4.10. The Graph of the SVET data for the as received aluminum flake sample after 24 hours immersion.

*Reprinted from Electrochemica Acta, 55(20), Yan M., Vetter C.A., and Gelling V.J., Electrochemical Investigations of Polypyrole Aluminum Flake Coupling: p. 5576-5583. 2010 with permission from Elsevier.*

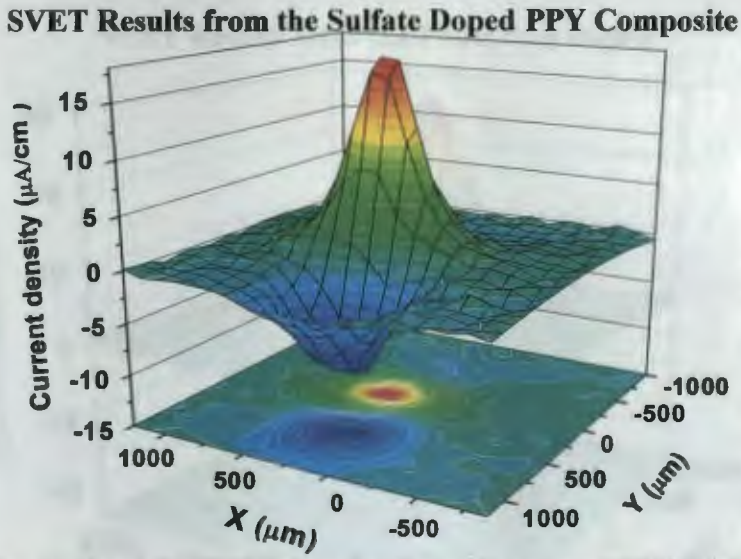


Figure 4.11. The graph of the SVET data for the sulfate doped PPY/Al flake sample after 24 hours Immersion.

*Reprinted from Electrochemica Acta, 55(20), Yan M., Vetter C.A., and Gelling V.J., Electrochemical Investigations of Polypyrole Aluminum Flake Coupling: p. 5576-5583. 2010 with permission from Elsevier.*

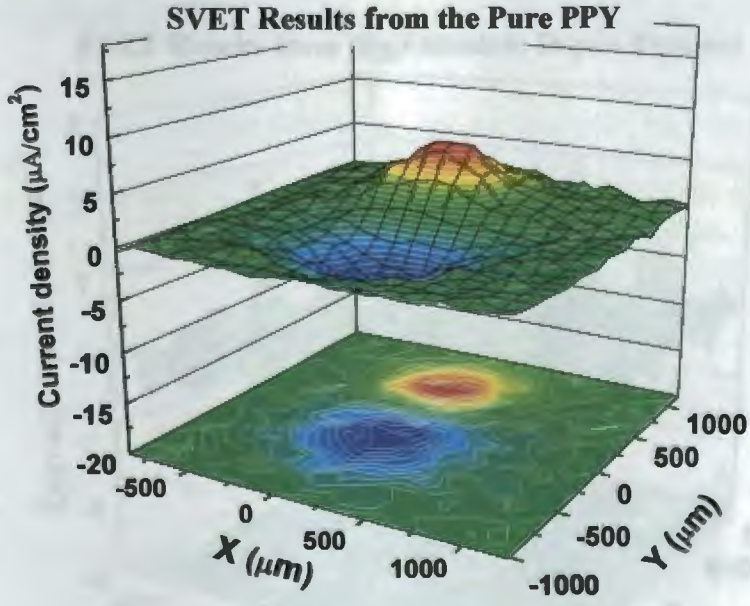


Figure 4.12. The graph of the SVET data for the sulfate doped pure PPY sample after 24 hours immersion.

*Reprinted from Electrochemica Acta, 55(20), Yan M., Vetter C.A., and Gelling V.J., Electrochemical Investigations of Polypyrole Aluminum Flake Coupling: p. 5576-5583. 2010 with permission from Elsevier.*

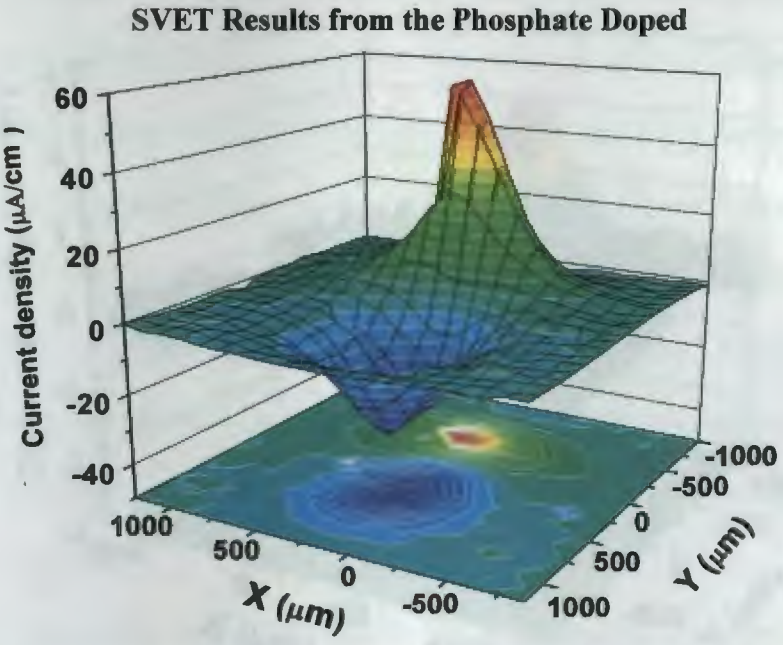


Figure 4.13. The graph of the SVET data for the phosphate doped PPY/Al flake sample after 24 hours immersion.

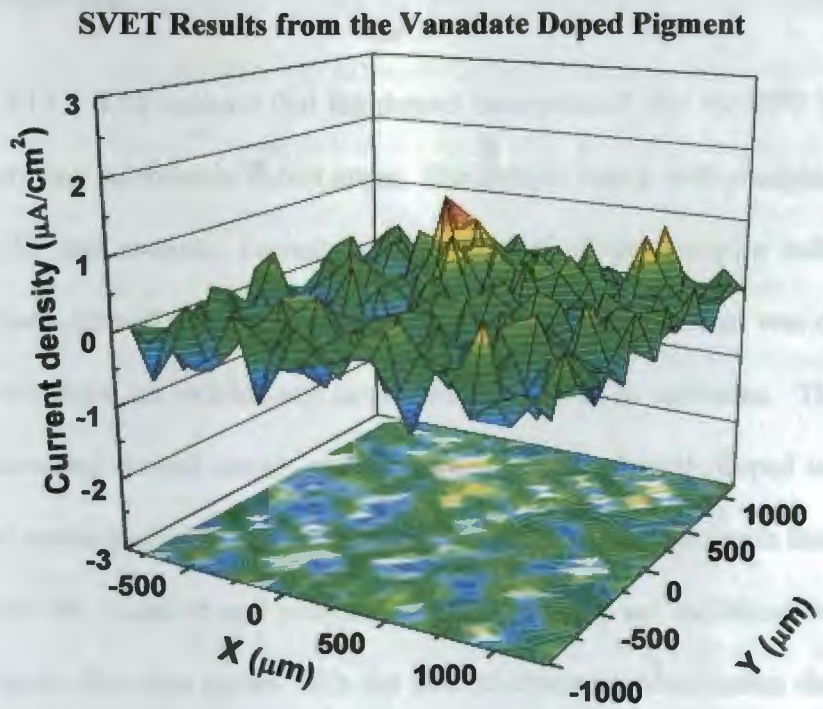


Figure 4.14. The graph of the SVET data for the vanadate doped PPY/Al flake sample after 24 hours immersion.

**SVET Results from the Molybdate Doped Pigment**

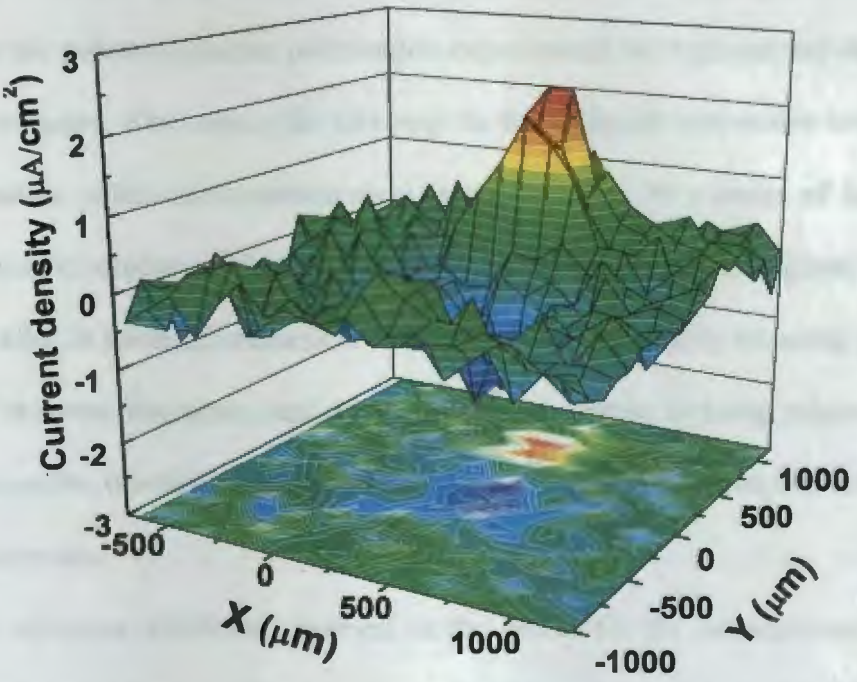


Figure 4.15. The graph of the SVET data for the molybdate doped PPY/Al flake sample after 24 hours immersion.

Figures 4.13 – 4.15 indicate that the dopant incorporated into the PPY has a large effect on the corrosion behavior in defect areas. The sample doped with phosphate exhibits the highest anodic and cathodic current densities out of all the samples indicating the strongest corrosion cell and the highest corrosion rates. The sample that was doped with vanadate however, does not exhibit any large, distinct, anode or cathodes. There is one weakly anodic area and several weakly cathodic areas. The molybdate doped sample does exhibit a distinct anode and cathode but the current densities associated with them are low. This indicates that the vanadate and molybdate doped samples are inhibiting corrosion in defect areas. Again, this data agrees with the potentiodynamic polarization data. Lower current densities in the potentiodynamic polarization data coincide with lower current densities in the SVET data and therefore lower corrosion rates in defect areas.

The exception to this is the phosphate doped sample which had low current densities in the potentiodynamic polarization experiments but high current density in the SVET experiments. One reason for this may be the different time scales involved. The potentiodynamic polarization measurement is taken within 30 minutes of immersion in dilute Harrison's solution while the SVET measurements shown in Figures 4.10 – 4.15 were taken after 24 hours of immersion. If the primer is not actively releasing phosphate as a result of substrate corrosion, and some residual phosphate is being released from the edges of the scribe, it would be possible to observe short term corrosion inhibition followed by active corrosion.

The corrosion inhibition observed in the defect for the vanadate and molybdate doped samples may indicate that ion release is taking place on large length scales (100 μm). It is evident from the coupling current results that the vanadate and molybdate doped samples are adequately coupled with the substrate to allow the reduction of polypyrrole as a result of substrate oxidation. It is also evident that the PPY/Al flake pigment that is not doped with corrosion inhibiting dopants does not inhibit corrosion in defect areas. It is unlikely that the dopants could have an effect on such large length scales while trapped in the polypyrrole matrix. It is suggested that the vanadate and molybdate dopants are being released to have this effect.

### 4.6. Accelerated Weathering

To investigate how these coatings would perform longer term in a corrosive environment, samples were spray coated onto panels at a pigment volume concentration (PVC) of 45%, scribed, and exposed to ASTM B117 salt spray. During the exposure, the

panels were monitored with EIS measurements and visual inspection. The visual assessment of the first set of panels containing as-received flake primers and sulfate doped PPY/Al flake primers can be seen in Figure 4.16. These images indicate that after only 139 hours of ASTM B117 salt spray exposure, the samples coated with the as-received flake pigmented primer begun to fail as determined by the blisters forming along the scribes. The blisters forming along the scribe are indicative of cathodic delamination caused either by the entrapment of hydrogen produced by the cathodic hydrogen evolution reaction or by the degradative attack by hydroxyl radicals produced by oxygen reduction.[2] This indicates that corrosion has spread from the scribes and is taking place underneath the coating. At 1378 hours and 1650 hours, blistering across a large area on the panels indicate that there is rampant corrosion taking place under the coating. This behavior for the as-received flake samples agrees with the prior electrochemical experiments which indicated that this primer is not capable of inhibiting corrosion in defect areas. This same observation was made for the sulfate doped PPY/Al flake sample but curiously the same level of corrosive attack is not observed for these samples.

The sulfate doped PPY/Al flake samples do not exhibit the blistering that is observed for the as-received flake samples. To ensure that corrosion was not taking place despite the absence of blistering in the coating, the coatings of one of the sulfate doped PPY/Al flake samples and one of the as-received flake samples were removed after 627 hours of exposure by swelling the coatings in methyl ethyl ketone. The results of the coating removal can be seen in Figure 4.17. It is evident that the as-received flake panel was corroding over much of its surface while the sulfate doped PPY/Al flake panel was only corroding in the defect area. This indicates that although the sulfate doped PPY/Al

flake pigment does not inhibit corrosion in defect areas; it does prevent the corrosion from spreading to areas outside of the defect. Essentially the coating does not undergo cathodic or anodic delamination. This is likely due to the increased coupling current observed in the presence of the PPY/Al flake under a nitrogen atmosphere. It may be that away from the scribe area the coating is able to sacrificially protect the aluminum 2024 T3 substrate. This is further supported by the results seen at 1650 hours.

**ASTM B117 Salt Spray**

Figure 4.16. The visual evaluation of the as-received flake coated panels (top) and the sulfate doped PPY/Al Flake panels (bottom) at (from left to right) 0, 139, 1378, and 1650 hours of B117 exposure.

After removal of the coating as this point in weathering, it was evident that there was corrosion over the entire surface of the panel coated with the sulfate doped PPY/Al flake pigment. The failure did not initiate at the scribe. This coincided with a large amount of white material in the coating. The white material is likely the corrosion products produced by the anodic reaction of the aluminum flake at or near the coating surface. As the flake corrodes to form white aluminum oxide it becomes visible. Therefore, it may be that the aluminum flake was acting as a sacrificial anode for the aluminum 2024 until it had corroded away. Once the aluminum flake had corroded to the point where an electrical connection was lost with the substrate, the panel began corroding across its entire surface. It is also possible that this pigment is acting as an oxygen scavenger even when it is not coupled with the substrate. Keeping in mind the low overpotential for the reduction of oxygen on the surface of the polypyrrole, it may be that and oxygen diffusing through the coating is reduced on the surface of the polypyrrole with the aluminum flake acting as the electron source for this reaction instead of the aluminum 2024 substrate.

**Coating Removal**

Figure 4.17. The as-received flake and sulfate doped PPY/Al flake panel before coating removal (left) and after coating removal (right).

These panels were also monitored via EIS measurements to get more detailed data on the performance of the coatings during B117 exposure. Bode plots of these results can be seen in Figures 4.18 and 4.19.

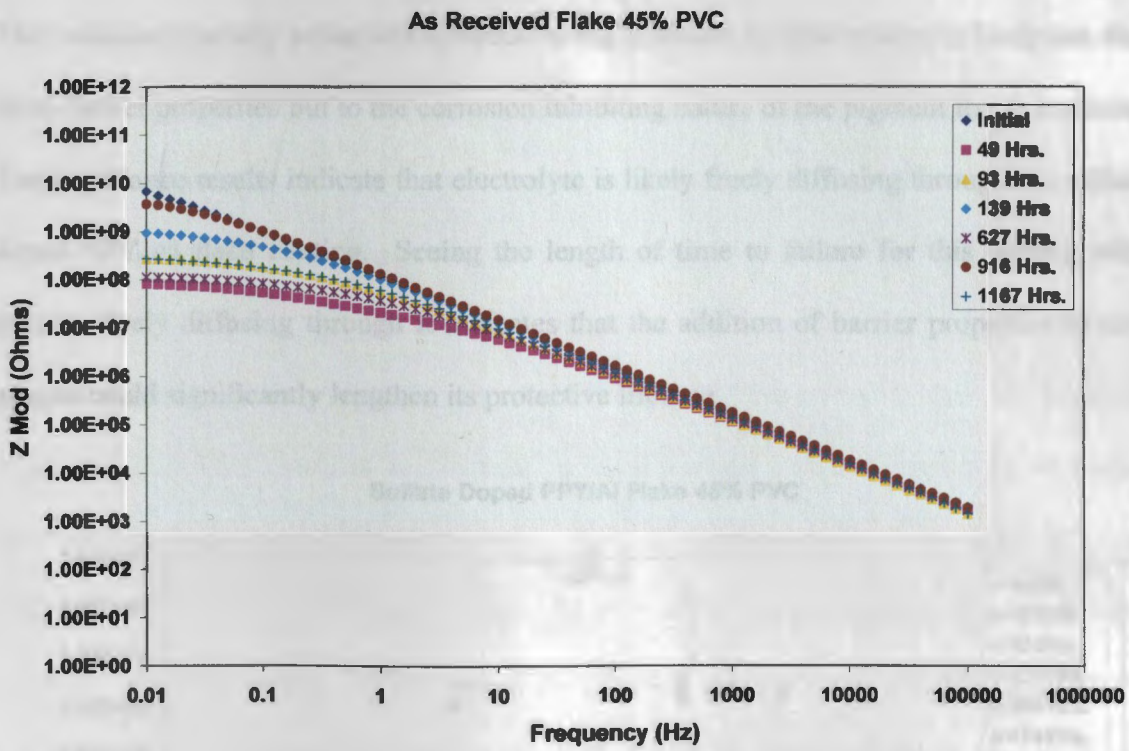


Figure 4.18. A bode plot of the EIS data obtained from an as-received flake sample during B117 exposure.

It can be observed from Figures 4.18 and 4.19 that the two different coatings systems exhibit very different impedance behavior during B117 exposure. The coating pigmented with the as-received flake behaves in a way that would be expected for a non-active barrier coating. This sample has an initial impedance of $10^{10}$ ohms at 0.01 Hz which is indicative of the barrier properties of the coatings. It also displays capacitive behavior at all measured frequencies. As exposure continues, the low frequency impedance drops two orders of magnitude and begins to display resistive behavior in the low frequencies

indicating that electrolyte diffusion is forming conductive pathways through the coating. The sulfate doped PPY/Al flake panel exhibits an initial impedance at 0.01 Hz that is a full five orders of magnitude lower than that of the as-received flake sample. It also displays much more resistive behavior indicating that conduction is occurring through the coating. This indicates that any protection afforded to the substrate by this coating is likely not due to its barrier properties but to the corrosion inhibiting nature of the pigment that it contains. The impedance results indicate that electrolyte is likely freely diffusing through the sulfate doped PPY/Al flake coating. Seeing the length of time to failure for this coating with species freely diffusing through it indicates that the addition of barrier properties to this system could significantly lengthen its protective lifetime.

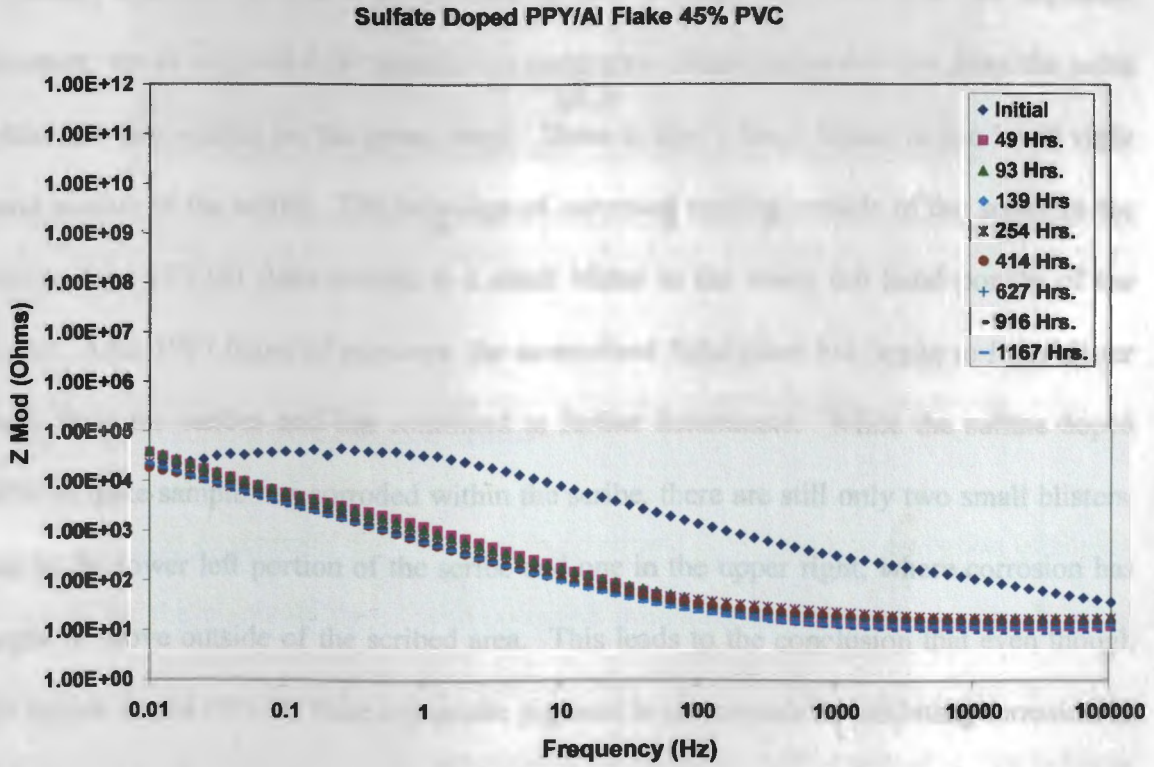


Figure 4.19. A bode plot of the EIS data obtained from a PPY/Al flake sample during B117 exposure.

These results indicate that a top coat could significantly improve the performance of these coatings as it would limit the amount oxygen and electrolyte that areas away from the scribe are exposed to thereby increasing coupling and possibly lengthening the amount of time that the PPY/Al flake would be actively protecting the substrate. To determine what effect a top coat would have on the performance of this system, a new set of samples was made up at the same pigment volume concentration and a clearcoat of the same epoxy resin used in the primer was sprayed over the top of the primers and exposed to B117 salt spray. The visual assessment of these coatings can be seen in Figure 4.20.The added barrier properties from a top coat, as would be expected, improved the performance of both primers regardless which pigment was used in them. In both samples, after 143 hours of exposure, corrosion products are evident in their scribes. At 1453 hours of exposure however, the as received flake sample has undergone delamination 6-7 mm from the point where the two scribes on the panel meet. There is also a large blister in the lower right hand portion of the scribe. The only sign of corrosion moving outside of the scribe in the sulfate dope PPY/Al flake sample is a small blister in the lower left hand portion of the scribe. After 1907 hours of exposure, the as-received flake panel has begun to form blister away from the scribes and has continued to further delaminate. While the sulfate doped PPY/Al flake sample has corroded within the scribe, there are still only two small blisters, one in the lower left portion of the scribe and one in the upper right, where corrosion has begun to move outside of the scribed area. This leads to the conclusion that even though the sulfate doped PPY/Al flake composite pigment is not capable of inhibiting corrosion in defect areas in these conditions, it is capable of keeping corrosion from progressing outside of those areas for long periods of time in accelerated weathering conditions.

**ASTM B117 Results with Top Coat**

Figure 4.20. The visual evaluation of the top coated as-received flake panels (top) and the sulfate doped PPY/Al Flake panels (bottom) at (from left to right) 0, 143, 1453, and 1907 hours of B117 exposure.

*Reprinted from Electrochemica Acta, 54(2), Yan M., Tallman D. E., and Bierwagen G. P., Role of oxygen in the galvanic interaction between polypyrrole and aluminum alloy: p. 220-227. 2008 with permission from Elsevier.*

The next experiment was designed to determine if the superior corrosion inhibition observed for the pigments doped with corrosion inhibiting anions, in the electrochemical evaluation of the pigments would translate into superior performance during B117 accelerated weathering. For this experiment the samples were made at a much lower pigment volume concentration of 10%. This was done with the thought that it may be

more conducive to the release of the corrosion inhibiting ions from the composite coatings. Studies performed by Rohwerder et al. determined that in pure polypyrrole films or polypyrrole composite systems with long range percolation, cation incorporation tends to dominate over anion release when the polypyrrole is reduced as a result of the metal substrate corroding. By selecting a pigment volume concentration that is below the percolation threshold for a particular pigment it is though that cation incorporation can be limited allowing anion release to take place.[3] The visual evaluation of the panels during exposure can be seen in Figure 4.21.

From the results in Figure 4.21, it appears that the corrosion inhibition in defect areas observed for the vanadate doped sample during electrochemical evaluation does take place under the conditions of ASTM B117 weathering. After 72 hours of exposure, corrosion products are evident in the scribed area on the sample coated with the sulfate doped pigment. For the sample coated with the vanadate doped pigment however, the scribes still contain shiny, uncorroded aluminum 2024. There is no visual evidence of corrosion within the scribes whatsoever. At 216 hours, the scribed area on the panel coated with the vanadate doped pigment has completely turned green in color. This indicates the presence of vanadium(III) instead of the vanadium(V) that is present in vanadate.[4] This indicates that at some point during the synthesis process or accelerated weathering the vanadium was reduced from vanadium(V) to vanadium(III). This suggests that the ion release mechanism is taking place and may be responsible for the observed corrosion inhibition in defect areas. The fact that the vanadate is being reduced does not necessarily mean that it isn't inhibiting corrosion. An XPS study was performed by Iannuzzi and Frankel to attempt to determine what oxidation states the vanadium goes through as

vanadate inhibits corrosion. Due to small differences in the binding energy of the different vanadium oxidation states and the possible formation of complexes with the underlying substrate, the results of this study were inconclusive.[5] At 552 hours of exposure, the sulfate doped sample had developed several blisters along its scribes indicating that the pigment is no longer able to stop the corrosion from spreading beyond the scribes. Slightly better performance was observed for the vanadate doped sample. Only one blister with a diameter of approximately 1mm can be observed along the scribe with one larger blister developing along the edge of the taped region. This large blister could be the result of electrolyte being trapped under the tape thereby causing that area to undergo conditions which are closer to constant immersion which is a more aggressive environment.

**Vanadate Doped Salt Spray Results**

Figure 4.21. The visual evaluation of the sulfate doped PPY/Al Flake coated panels (top) and the vanadate doped PPY /Al Flake coated panels (bottom) at 72, 216, and 552 hours of B117 exposure.

## 4.7. Conclusions

In this chapter, various experiments were performed to investigate the ability of a PPY/Al flake composite pigment to inhibit corrosion on aluminum 2024 T3. From the potentiodynamic polarization experiments, it was apparent that the dopant ions have a definite impact on the corrosion inhibiting behavior of the different pigment samples with lower corrosion rates observed for the vanadate, phosphate, and molybdate doped samples in comparison to the sulfate doped sample. The vanadate and molybdate samples also exhibited an elevated pitting potential in nitrogen purged electrolyte. Shifts in the OCPs of the samples were also observed as a result of changing oxygen concentration which indicated that there may have been unique coupling behavior between the coatings and the substrate.

Coupling current measurements indicated that the oxygen concentration did have an effect on the coupling between the pigments and the substrate. While the Al flake itself was capable of coupling with the substrate in both an air and a nitrogen atmosphere, the PPY composite pigment exhibiting more coupling current than the aluminum flake by itself in a nitrogen atmosphere and very little coupling in an air atmosphere. In both cases, the coating acted as the anode in the couple indicating that the polypyrrole was activating the Al flake to anodic activity in a nitrogen atmosphere causing it to act as a sacrificial anode for the aluminum 2024 T3. In air, where coupling was not observed, the pigment is likely acting as an oxygen scavenger which would also result in corrosion inhibition. While polypyrrole can be doped by oxygen which results in oxygen absorption by the polypyrrole, eventually the polymer would reach a perpetually doped state at which point it would serve as a low overpotential surface for the reduction of oxygen which would

increase the corrosion rate.[1] However, in the case of the PPY composite pigment, it is suggested, from the coupling current results, that the aluminum flake would act as the electron source for oxygen reduction in lieu of the aluminum 2024 thereby sustaining the oxygen scavenging behavior of the pigment until the Al flake is consumed. It was also observed that the dopant ions present in the composite pigment had a large effect on the coupling behavior between the coating and the aluminum 2024 substrate. In the case of the molybdate doped sample, the opposite behavior of the sulfate doped sample was observed. The molybdate doped sample exhibited a large amount of coupling with the substrate in air and very little coupling in a nitrogen atmosphere.

SVET measurements indicated that the sulfate and phosphate doped samples were not inhibiting corrosion in defect areas while the molybdate doped and vanadate doped samples did exhibit corrosion inhibition in defect areas. Since similar behavior was observed in defect areas for both the as received flake sample and the sulfate doped sample, it is suggested that the dopant ion is what is responsible for inhibition in defects and no the presence of polypyrrole. This may be due to ion release from the PPY composite pigment.

ASTM B117 exposure of the sulfate doped samples indicated that while corrosion was taking place in the scribe area, it was not taking place underneath the coating. This behavior continued until the panel turned white in color at which point corrosion was present over the entire surface of the coating. Also, EIS measurements during exposure indicated that the corrosion protection that was afforded by the PPY composite coating was not due to the barrier properties of the coating. This supports the hypothesis from the coupling current measurements that the pigment is acting both as a sacrificial anode and possibly an oxygen scavenger with the aluminum flake being the electron source for both

processes. Once the aluminum flake is consumed, which may be evident from the white color of the coating due to the corrosion products of the flake, the coating is no longer able to protect the underlying substrate and corrosion proceeds over the entire surface of the coating. A top coat drastically improved the performance of the coating system as it imparted some barrier properties to the system. When samples that were pigment with the vanadate doped pigment were exposed to B117 salt spray, the scribed areas on the panels turned green in color indicating the presence of vanadium (III) and therefore the release of the dopant from the composite coating.

### 4.8. References


1. Yan M., Tallman D. E., and Bierwagen G. P., *Role of oxygen in the galvanic interaction between polypyrrole and aluminum alloy.* Electrochemica Acta, 2008. **54**(2): p. 220-227.
2. Rohwerder M., Hornung E., and Stratmann M., *Microscopic aspects of electrochemical delamination: an SKPFM study.* Electrochimica Acta, 2003. **48**(9): p. 1235-1243.
3. Rohwerder M. and Michalik A., *Conducting polymers for corrosion protection: What makes the difference between failure and success?* Electrochemica Acta, 2007. **53**(3): p. 1300-1313.
4. Furman S. C. and Garner C. S., *Absorption Spectra of Vanadium (III) and Vanadium (IV) Ions in Complexing and Non-complexing Media.* Journal of The American Chemical Society, 1950. **72**(4): p. 1785-1789.
5. Iannuzzi M. and Frankel G. S., *Mechanisms of corrosion inhibition of AA2024-T3 by vanadates.* Corrosion Science 2007. **49**(5): p. 2371-2391.

# CHAPTER 5.

# CONCLUSION AND FUTURE WORK

## 5.1. Conclusion

This study has outlined an environmentally friendly method by which polypyrrole composites can be prepared under various experimental conditions. It was determined through SEM that the morphology of the deposited material could be altered greatly via the use of phenolic compounds during the synthesis. Reactions 1, 1x, and 3 resulted in agglomerated flakes that were joined together. Reactions 4 and 4x resulted in small particulates which preferentially deposited on the edges of the aluminum flake. Reaction 5 produced sporadic coverage of the flakes, with a majority of the flake being uncoated by the deposited product.

The density experiments determined that a majority of the deposited PPY was attached to the flake for reactions 1, 1x, 2, 4, 4x, 5, and 6. Reaction 3 displayed unique results where a majority of the product was suspended in the liquid, which is most likely related to the tissue-like appearance of the product that was found during the SEM study.

The XPS, C-AFM, and electrochemical impedance spectroscopy (EIS) experiments focused on the product from reactions 1 and 2. It was found that the product may be a co-polymer or composite formed between the pyrrole and catechol. The hydroxyl groups present on the catechol could then allow the deposited product to interact with the aluminum oxide surface of the aluminum flake thereby increasing coverage. The results from reaction 1 also seemed to show that the dopant was sulfate ions from the ammonium persulfate used as the initiator for the polymerization of the PPY. The C-AFM detected a

conductive surface with a conductivity of 1.6 S/cm for reaction 1 and 5.2 S/cm for reaction 2. EIS was used to assist in the formulating of a conductive coating where it was determined that a 45% PVC would be sufficient for a low impedance coating of the polypyrrole composite flake. These results combined with the Conductive AFM results indicate that conductive polypyrrole was deposited onto the surface of the aluminum flake and that the composite pigment is capable of forming percolation networks through an epoxy binder.

It was also found that the dopant ion had a large effect on the morphology of the deposited polypyrrole and the degree to which the polypyrrole was attached to the aluminum flake. Vanadate and phosphate provided the best deposition of polypyrrole on to the aluminum flake along with sulfate when catechol and phloroglucide were present.

After the PPY/Al flake composite pigment had been synthesized and characterized, various experiments were performed to investigate the ability of the composite pigment to inhibit corrosion on aluminum 2024 T3. The potentiodynamic polarization experiments revealed that the ions used as dopant, to render the polypyrrole conductive, have a definite impact on the corrosion inhibiting behavior of the different pigment samples with lower corrosion rates observed for the vanadate, phosphate, and molybdate doped samples in comparison to the sulfate doped sample. The vanadate and molybdate doped samples also exhibited an elevated pitting potential in nitrogen purged electrolyte. Shifts in the OCPs of the samples were also observed as a result of changing oxygen concentration which indicated that there may have been unique coupling behavior between the coatings and the substrate.

Coupling current measurements indicated that the oxygen concentration did have an effect on the coupling between the pigments and the substrate. While the Al flake itself was capable of coupling with the substrate in both an air and a nitrogen atmosphere, the PPY composite pigment exhibiting more coupling current than the aluminum flake by itself in a nitrogen atmosphere and very little coupling in an air atmosphere. In both cases, the coating acted as the anode in the couple indicating that the polypyrrole was activating the Al flake to anodic activity in a nitrogen atmosphere causing it to act as a sacrificial anode for the aluminum 2024 T3. In air, where coupling was not observed, the pigment is likely acting as an oxygen scavenger which would also result in corrosion inhibition. While polypyrrole can be doped by oxygen which results in oxygen absorption by the polypyrrole, eventually the polymer would reach a perpetually doped state at which point it would serve as a low overpotential surface for the reduction of oxygen which would increase the corrosion rate. However, in the case of the PPY composite pigment, it is suggested, from the coupling current results, that the aluminum flake would act as the electron source for oxygen reduction in lieu of the aluminum 2024 thereby sustaining the oxygen scavenging behavior of the pigment until the Al flake is consumed. It was also observed that the dopant ions present in the composite pigment had a large effect on the coupling behavior between the coating and the aluminum 2024 substrate. In the case of the molybdate doped sample, the opposite behavior of the sulfate doped sample was observed. The molybdate doped sample exhibited a large amount of coupling with the substrate in air and very little coupling in a nitrogen atmosphere.

SVET measurements indicated that the sulfate and phosphate doped samples were not inhibiting corrosion in defect areas while the molybdate doped and vanadate doped

samples did exhibit corrosion inhibition in defect areas. Since similar behavior was observed in defect areas for both the as received flake sample and the sulfate doped sample, it is suggested that the dopant ion is what is responsible for inhibition in defects and no the presence of polypyrrole. This may be due to ion release from the PPY composite pigment.

ASTM B117 exposure of the sulfate doped samples indicated that while corrosion was taking place in the scribe area, it was not taking place underneath the coating. This behavior continued until the panel turned white in color at which point corrosion was present over the entire surface of the coating. Also, EIS measurements during exposure indicated that the corrosion protection that was afforded by the PPY composite coating was not due to the barrier properties of the coating. This supports the hypothesis from the coupling current measurements that the pigment is acting both as a sacrificial anode and possibly an oxygen scavenger with the aluminum flake being the electron source for both processes. Once the aluminum flake is consumed, which may be evident from the white color of the coating due to the corrosion products of the flake, the coating is no longer able to protect the underlying substrate and corrosion proceeds over the entire surface of the coating. A top coat drastically improved the performance of the coating system as it imparted some barrier properties to the system. This would delay the ingress of electrolyte into the system as well as slowing the diffusion of ions to the surface of the substrate. This served to reduce the rate at which the flake is consumed via corrosion. When samples that were pigment with the vanadate doped pigment were exposed to B117 salt spray, the scribed areas on the panels turned green in color indicating the presence of vanadium (III) and therefore the release of the dopant from the composite coating.

## 5.2. Future Work

While many different pigments were synthesized using different phenolic compounds to aid in the attachment of polypyrrole to the aluminum flake, only the pigment synthesized using catechol was investigated for its ability to inhibit corrosion as well as the effect of different dopants on its performance and morphology. A similar study should be done on the pigment synthesized using other phenolic compounds to determine if they also are able to inhibit corrosion.

Furthermore, while this study determined the electrochemical interactions between the pigment and the substrate via coupling current measurements, this same technique could be used to determine the interaction taking place between the polypyrrole and the aluminum flake. This could be done simply by replacing the aluminum 2024 substrates with pure aluminum in the experiment and synthesizing the polypyrrole used in the experiment sans aluminum flake.

Another experiment which could yield valuable information would be a coupled SVET experiment to determine the effect that coupling between the coating and the aluminum 2024 substrate would have on the anodic and cathodic behavior within a coating defect. This could be done by connecting a coated sample of aluminum 2024 that has been placed into a sealed, nitrogen purged electrolyte with an uncoated sample of aluminum 2024. SVET measurements would then be taken from the uncoated sample to determine what effect coupling would have on the corrosion behavior of the sample.

Also, the scanning ion-selective electrode technique (SIET) could be used in conjunction with a potentiostat to observe ion release from theses coating as a result of coating reduction. The coated sample of aluminum 2024 would be connected to the

potentiostat as the working electrode with a platinum wire counter electrode and a reference electrode. A reducing potential could then be applied to the sample while the current flowing through the sample would be monitored. Simultaneously, the concentration of the dopant could be monitored using the SIET. It could then be determine if an increase in the dopant ion concentration in the electrolyte coincided with the reduction of the coating thereby confirming the ion release mechanism.